Published in final edited form as:
Prog Retin Eye Res. 2009 November ; 28(6): 452–482. doi:10.1016/j.preteyeres.2009.06.003.

The Neurovascular Retina in Retinopathy of Prematurity

Anne B. Fulton, **Ronald M. Hansen**, **Anne Moskowitz**, and **James D. Akula**
Department of Ophthalmology, Children's Hospital and Harvard Medical School, 300 Longwood Ave., Boston, MA 02115-5737, USA

Abstract

The continuing worldwide epidemic of retinopathy of prematurity (ROP), a leading cause of childhood visual impairment, strongly motivates further research into mechanisms of the disease. Although the hallmark of ROP is abnormal retinal vasculature, a growing body of evidence supports a critical role for the neural retina in the ROP disease process. The age of onset of ROP coincides with the rapid developmental increase in rod photoreceptor outer segment length and rhodopsin content of the retina with escalation of energy demands. Using a combination of non-invasive electroretinographic (ERG), psychophysical, and image analysis procedures, the neural retina and its vasculature have been studied in prematurely born human subjects, both with and without ROP, and in rats that model the key vascular and neural parameters found in human ROP subjects. These data are compared to comprehensive numeric summaries of the neural and vascular features in normally developing human and rat retina. In rats, biochemical, anatomical, and molecular biological investigations are paired with the non-invasive assessments. ROP, even if mild, primarily and persistently alters the structure and function of photoreceptors. Post-receptor neurons and retinal vasculature, which are intimately related, are also affected by ROP; conspicuous neurovascular abnormalities disappear, but subtle structural anomalies and functional deficits may persist years after clinical ROP resolves. The data from human subjects and rat models identify photoreceptor and post-receptor targets for interventions that promise improved outcomes for children at risk for ROP.

Keywords

Electroretinogram; Retinopathy of prematurity; Infant visual psychophysics; Retinal development; Animal models; rats

1. Introduction

1.1. Preterm birth and retinopathy of prematurity (ROP)

Preterm birth introduces a tiny infant into an extrauterine world for which the infant's tissues and organs are incompletely prepared. In this external environment, the immature neurovascular tissues of the visual system, the retina and the brain, are particularly susceptible to injury (Volpe, 2009). The earlier the preterm birth, the greater the risk for damage to the retina and visual pathways. The clinical entity involving the retina is called retinopathy of prematurity (ROP); abnormalities of the retinal vasculature are the clinical hallmark of ROP. A growing body of evidence, however, demonstrates that the neural retina is critically involved

Corresponding author: Anne Fulton, Tel.: +1-617-355-5685, Fax: +1-617-507-7999, anne.fulton@childrens.harvard.edu.

in the ROP disease process. The onset of ROP is at approximately 32 weeks gestational age (term ≅40 weeks) regardless of the gestation at birth (Palmer et al., 1991). Interestingly, this coincides with the rapid developmental elongation of the rod outer segments and increase in retinal rhodopsin content (Fig. 1). As this rapid maturation occurs, putative energy demands of the rod escalate due to increase in turnover of outer segment material and the rod's circulating current.

Our studies of ROP are dedicated to delineating the closely allied neural and vascular components of the disease and the resulting retinal and visual dysfunction. Such an approach can identify targets for interventions that will give children with ROP the best possible visual outcome. The increasing number of children with ROP motivates the quest for further knowledge about neurovascular processes upon which improved management, and eventually prevention, of ROP will be based.

Due to advances in neonatal care, infants born as early as 22 to 24 weeks gestation survive. Each year in the United States, an estimated 10,000 infants are born prematurely (Penn et al., 2008). Of those born extremely prematurely (gestational age <31 weeks or birth weight <1,250 grams), approximately half develop ROP. In the majority, the disease is mild and resolves spontaneously. Nonetheless, ROP remains a leading cause of permanent, bilateral visual impairment in developed countries (Steinkuller et al., 1999). An estimated 1,100 to 1,500 each year have severe ROP that requires treatment, and approximately 500 of these infants are blinded by ROP (www.nei.nih.gov/health/rop/). Worldwide, a hundred times that number are blind from ROP (Gilbert, 2008). The risk of ROP blindness is particularly high in middle income countries where premature infants survive but screening programs for ROP or management of ROP are not well established (Gilbert, 2008). Although in countries with advanced neonatal care and established screening programs, the rates of retinal detachment and blindness due to ROP are quite low, even mild ROP causes residual retinal and visual dysfunction (Reisner et al., 1997; Hansen and Fulton, 2000b; Fulton et al., 2001; O'Connor et al., 2002a; Barnaby et al., 2007; Hammer et al., 2008).

1.2. Clinical issues in ROP

The primary concern of those caring for preterm infants is identification of acute ROP. At-risk infants have serial ophthalmoscopic examinations at preterm ages to evaluate the retina for blood vessels that are characteristic of ROP (Section on Ophthalmology American Academy of Pediatrics et al., 2006; Wilkinson et al., 2008). Infants are followed until ROP resolves spontaneously or requires treatment, or if no ROP develops, until the retinal blood vessels reach the ora serrata, the clinical definition of vascular maturity. The results of the multicenter Early Treatment of ROP study provide practical clinical criteria by which infants with ROP at high risk for dangerous worsening are selected for treatment (Early Treatment for Retinopathy of Prematurity Cooperative Group, 2003). Standard treatment for ROP is laser ablation of the peripheral avascular retina. Cryotherapy continues to be used on occasion in severe cases. Fewer treated infants suffer retinal detachment and blindness; this indicates beneficial effects on both retinal structure and visual acuity. Fortunately, most ROP does not reach the criteria for treatment but rather spontaneously resolves by approximately term (Repka et al., 2000). Despite clinical resolution of the vascular abnormalities, there are numerous examples of persistent retinal and visual dysfunction as a consequence of ROP (Dobson et al., 1994; Cryotherapy for Retinopathy of Prematurity Cooperative Group, 2001; Fulton et al., 2001, 2005; Barnaby et al., 2007; Hammer et al., 2008).

1.3. Clinical sequelae of ROP

The cells of the retina, starting with the photoreceptors, participate in the first steps of visual processing and mediate a wide range of visual functions. The retina is also a controller of eye

growth and refractive development (Troilo, 1992; Wallman, 1993). Thus, it is not surprising that prematurity and ROP are associated with both altered visual function and altered eye growth. In addition to clinical abnormalities of the retina, infants born prematurely are at risk for developing a range of structural and functional ophthalmic sequelae, including impaired ocular growth; increased incidence and magnitude of refractive error, particularly myopia; acuity deficits; field defects; and strabismus.

Ocular structures become identifiable early in embryonic development and continue to grow and develop throughout gestation into the early post-term years. Early departure from the protective intrauterine environment is associated with increased corneal curvature, increased lens power, and shallower anterior chamber depth, each of which can contribute to myopia (see below). Although it is these anterior segment features that are often taken as evidence that preterm birth arrests development of the ocular structures, we note that whether born preterm (regardless of ROP status) or at term, the ratio of anterior to posterior segment depth is approximately 0.6 in infants and approximately 0.45 in children. Axial length is typically shorter in preterm than in full term eyes. Because this is offset by the higher refractive power of the anterior segment, the magnitude of myopia in former preterms is greater than would be expected based on axial length. Nonetheless, among former preterms, axial length is greater in myopic than in emmetropic eyes. (Mann, 1964; Fledelius, 1976, 1981, 1982a, b, 1992, 1996a, b; Fielder et al., 1986; Gordon and Donzis, 1986; Gallo and Fagerholm, 1993; Fielder and Quinn, 1997; Choi et al., 2000; Kent et al., 2000; O'Connor et al., 2002a, 2006a; Cook et al., 2003, 2008; Jirasek, 2004; Snir et al., 2004; Mutti et al., 2005; Baker and Tasman, 2008; Mactier et al., 2008)

Term born infants are typically hyperopic and many have astigmatism in infancy (Mohindra et al., 1978; Atkinson et al., 1980; Fulton et al., 1980; Howland and Sayles, 1984; Saunders, 1995; Mayer et al., 2001; Mutti et al., 2005). For example, until age 4 months, the mean spherical equivalent is ≥2 diopters and cylindrical errors (≥0.75 diopter) occur in 25 to 40%. Normally, coordinated growth of the eye's refractive components during the first postnatal years causes refractive error to approach zero; this developmental process is called emmetropization (Troilo, 1992; Wallman, 1993).

Infants born prematurely, either with or without ROP, are on average less hyperopic than term born infants. However, the incidence of all types of refractive conditions - myopia, high hyperopia, astigmatism, and anisometropia - is higher than in the full term population. Thus, the normal, exquisite regulation of ocular growth appears to be diminished following preterm birth. (Saunders et al., 2002; Cook et al., 2003, 2008; Snir et al., 2004)

Myopia, the most common refractive error in preterms, typically develops in infancy and persists thereafter. In addition to ROP, low birth weight and gestational age may be independent risk factors for myopia. Both the prevalence and the magnitude of myopia increase with increasing severity of ROP and are greater in treated than in untreated eyes. Two large, multi-center, randomized ROP treatment trials, the Cryotherapy for ROP (CRYO-ROP) study and the Early Treatment for ROP (ETROP) study, concluded that treatment itself does not influence refractive status in eyes with severe ROP. Whether treatment is done for threshold or for high-risk pre-threshold ROP, the refractive outcome is the same. (Fletcher and Brandon, 1955; Zacharias et al., 1962; Fledelius, 1976, 1981, 1996a; Scharf et al., 1978; Dobson et al., 1981; Nissenkorn et al., 1983; Gallo and Lennerstrand, 1991; Kim et al., 1992; Quinn et al., 1992, 1998, 2001, 2008; Page et al., 1993; Robinson and O'Keefe, 1993; Lue et al., 1995; Pennefather et al., 1997; M. Holmstrom et al., 1998; Ricci, 1999; Choi et al., 2000; Kent et al., 2000; O'Connor et al., 2002a, 2006a, b; Saunders et al., 2002; Cook et al., 2003, 2008; Snir et al., 2004; Davitt et al., 2005; G. Holmstrom and Larsson, 2005; Sahni et al., 2005)

Acuity, the most commonly measured visual function, is usually reported to be lower in preterm than in term born infants and children. Acuity deficits range from subtle to severe, with the magnitude of the deficit related to the severity of ROP. (Birch and Spencer, 1991; Robinson and O'Keefe, 1993; Dobson et al., 1994; O'Connor et al., 2004; Palmer et al., 2005; Spencer, 2006)

Eyes with a history of ROP show visual field constriction compared to those of preterms with no ROP. Eyes with no ROP have fields similar to term born eyes. Comparison of fields in treated versus untreated eyes with severe ROP show that the former are slightly more constricted. The small field reduction due to treatment is considered to be of little or no functional significance and is outweighed by the benefit of preventing retinal detachment. (Quinn et al., 1996; Myers et al., 1999; Cryotherapy for Retinopathy of Prematurity Cooperative Group, 2001)

The prevalence of strabismus is higher in the preterm than in the term born population and increases with increasing ROP severity. Strabismus in preterms, as in other children, may be associated with anisometropia and amblyopia but also with other sequelae of preterm birth including encephalopathy of prematurity. (Graham, 1974; Roberts and Rowland, 1978; Friedmann et al., 1980; Kushner, 1982; Snir et al., 1988; Gallo et al., 1991; Laws et al., 1992; Page et al., 1993; Robinson and O'Keefe, 1993; Tuppurainen et al., 1993; Bremer et al., 1998; G. Holmstrom et al., 1999, 2006; Pennefather et al., 1999; Pott et al., 1999; Ricci, 1999; O'Connor et al., 2002b; Sahni et al., 2005; VanderVeen et al., 2006a; Volpe, 2009)

1.4. Retinal development and ROP

At the preterm ages during which clinical ROP becomes active, both the neural retina and the retinal vasculature are immature (Hendrickson, 1994; Provis et al., 1997; Provis, 2001). The choroidal vasculature, which directly supplies the adjacent photoreceptors, develops in advance of the retinal vasculature (Gogat et al., 2004). Over the ages during which rod outer segments are maturing, all other retinal cell types have differentiated, and all retinal laminae are identifiable. The rod outer segments are the last retinal structures to reach maturity (Grun, 1982). During developmental elongation of the rod outer segments, the rhodopsin content of the retina increases along a logistic growth curve (Fig. 1). Infants at age 5 weeks (95% confidence interval, CI: 0 to 10 weeks) and rats at age 18.7 days (95% CI: 18.2 to 19.2 days) are estimated to have half the rhodopsin content of adults (Bonting et al., 1961; Fulton et al., 1991a, 1998a, 1999a; Hendrickson, 1994). By term, the number of retinal cells present in the primate retina is approximately the same as in adults (Packer et al., 1990). As the eye grows, the same number of cells pave a larger retinal area (Robb, 1982). Thus, the spatial distribution of cells varies with age but the same number of cells is available to respond to full-field flashes of light such as those used in electroretinography (ERG). In primate extramacular retina, cones reach maturity before rods (Hendrickson and Drucker, 1992; Hendrickson, 1994). In the macula, the maturation of those cones that are destined to become foveal cones and the maturation of the parafoveal rods lag that of the more peripheral photoreceptors (Dorn et al., 1995; Fulton et al., 1996; Timmers et al., 1999). During normal foveal development, there is an interplay of neural and vascular elements (Provis et al., 2000; Springer and Hendrickson, 2004a, b, 2005).

ROP has effects on the function of the photoreceptors and post-receptor retina that persist even after its active phase (Sections 2 and 3). The late-maturing central retina appears to be particularly vulnerable to these effects. ROP, even if mild, affects the development of the central retina (Barnaby et al., 2007). Residual effects on the structure and function of the central retina are detectable years after ROP was active (Reisner et al., 1997; Hansen and Fulton, 2000b; Fulton et al., 2005; Hammer et al., 2008). Subtle deficits also occur in peripheral retinal

function and persist into adolescence and early adulthood (Reisner et al., 1997; Hansen and Fulton, 2000b; Fulton et al., 2001; Moskowitz et al., 2005a).

1.5. Our approach to investigation of ROP

Our investigations include human subjects (Section 2) and rat models of ROP (Section 3). A two-way bridge of information is built by investigations of these two classes of subjects, with each motivating the other.

1.5.1. Studies in human subjects—In our quest to understand the neurovascular components in ROP, we study human subjects using non-invasive measures of retinal function and structure. Analysis of function depends on electroretinographic and psychophysical measures. Structure is investigated using image analysis of the retinal vasculature displayed in digital fundus photographs and ultra-high resolution adaptive optics imaging of the retinal laminae and intra-retinal vasculature. We pair these measures with clinical history and assessments. In this report, results are mainly from infants and children tested at post-term ages, weeks to years after ROP was an active clinical issue. Of course, studies at post-term ages examine the consequence of a disease that is no longer active. It is from these post-term results, coupled with clinical history from the days in the newborn intensive care unit onward, that we draw inferences about the acute disease processes that were active at preterm ages. Data from rat models of ROP studied before and after the peak of acute disease also aid in interpretation of results from human subjects.

Former preterms who are subjects in our studies had ***Severe ROP*** that was successfully treated, ***Mild ROP***, or ***No ROP*** (Table 1). Thus, the subjects whose data are reported herein have been free of the mechanical effects of retinal detachment that have secondary effects on retinal neurons and blood vessels. The subjects were monitored in the nursery at preterm ages by serial examinations using indirect ophthalmoscopy, and clinical data were collected for each subject from infancy onward. The schedule of examinations in the nursery was modeled on those used in the Cryotherapy for ROP (CRYO-ROP) and Early Treatment for ROP (ETROP) multicenter treatment trials (Cryotherapy for Retinopathy of Prematurity Cooperative Group, 1988;Hardy et al., 2004). Those whom we categorized as ***Severe*** had ROP that reached criteria for treatment. Using the International Classification of ROP (ICROP), the maximum severity was stage 3; some had plus disease (International Committee for the Classification of Retinopathy of Prematurity, 2005). Those whom we categorized as ***Mild*** had ROP that did not reach criteria for treatment (Cryotherapy for Retinopathy of Prematurity Cooperative Group, 1988;Early Treatment for Retinopathy of Prematurity Cooperative Group, 2003). In these subjects, the ROP resolved by term and left no detectable retinal residua on clinical examination. According to ICROP, the maximum severity of their ROP was stage 1 or 2 in zone 2 or 3 (International Committee for the Classification of Retinopathy of Prematurity, 2005). Also included in our studies are former preterms who had serial examinations at preterm ages and never had ROP; these are termed ***No ROP***. For brevity, we designate all former preterms subjects as ROP subjects and categorize them as ***None, Mild***, or ***Severe*** (Table 1). We exclude from this report those who progressed to retinal detachment that could confound the main effects of ROP on retinal function. We also tested healthy, term born infants, children, and adults as control subjects.

Throughout this paper, we report age as corrected age in weeks post-term. Corrected age equals postnatal age minus the difference between term (40 weeks) and gestational age at birth [Corrected Age = Postnatal Age − (Term − Gestational Age)]. For instance, the corrected age of an infant born at 26 weeks gestation and tested at postnatal age 24 weeks is 10 weeks: 24 − (40 − 26) = 10.

1.5.2. Studies in rat models of ROP—We also study rat models of ROP. Controlled exposure of rats with immature retinal vasculature and neurons to ambient oxygen levels above or below those encountered in room air induces retinopathy. Two oxygen exposure protocols produce retinopathy that spans the gamut of severity of the ROP included in our human studies (Penn et al., 1995; Liu et al., 2006a; Akula et al., 2007a). Similar effects on key neural and vascular parameters are found in these rat models and human subjects (Fulton et al., 2009). ERG and image analyses of the retinal vasculature plus anatomic, biochemical, and molecular studies of the neurovascular elements have been performed in rats during the active phase as well as during the resolution of the ROP disease process. The rat results provide a conceptual framework for understanding the neurovascular elements not only in the rats, but also in the human subjects.

2. Human ROP: the neural retina and its vasculature

2.1. Stimulus specification

Troland values specify the retinal illuminance produced by a stimulus of 1 cd/m^2 viewed through a 1 mm^2 pupil (Pugh, 1988). Infants' eyes and pupils are smaller and their ocular media less dense than adults'. The retinal illuminance (E) produced by the stimulus (L, cd/m^2) varies directly with pupil area (A, mm^2) and transmissivity (τ_λ) of the ocular media (Section 2.5.1.2), and inversely with the square of the posterior nodal distance of the eye (d, mm) (Pugh, 1988):

$$E=(A/d^2)\tau_\lambda L \quad \text{(Eq. 1)}$$

Thus, age related variation in eye size and media density are taken into account.

In practice, direct measurement of the diameter of the subject's dilated pupil, previously determined measures of the ocular media density (Werner, 1982; Hansen and Fulton, 1989) and published ocular dimensions (Larsen, 1971; Mutti et al., 2005) are used. Typically, the dilated pupillary diameter in a dark adapted 10 week old infant is approximately 5 mm (Hansen and Fulton, 1993), although a combination of cycloplegic and mydriatic agents may produce larger diameters (Mactier et al., 2008). In 2 to 3 month old infants, posterior nodal distance is approximately 11.2 mm, or two thirds (0.67) of the adult value (16.7 mm) (Hamer and Schneck, 1984; Brown et al., 1987). These values are consistent with ultrasonographic measures of vitreous chamber depth (Larsen, 1971; Laws et al., 1994; Bron et al., 1997; Mactier et al., 2008).

Using Eq. 1 and assuming a dilated pupillary diameter of 5 mm in 2-3 month old infants, the ratio of E in infants to E in adults is approximately 1.25. In these conditions, equal intensity stimuli produce approximately equal retinal illuminance in young infants and adults (Brown et al., 1987;Hansen and Fulton, 1993;Malcolm et al., 2003). In other words, infant and adult troland values are about equal. If pupillary diameter is larger or axial length shorter, this equality breaks down, and in preterm infants with shorter axial length, retinal illuminance may be underestimated (Mactier et al., 2008). If we have underestimated retinal illuminance, the differences between ROP infants and controls would be even larger than the significant deficits reported in our ERG and psychophysical studies.

For ROP subjects, corrected age was used for calculation of troland value. For instance, for a former preterm infant tested at corrected age 10 weeks, troland value was calculated as for a term born 10 week old infant.

2.2. Full-field electroretinogram

2.2.1. Rod and rod-driven responses

2.2.1.1. Rod photoreceptor activation: The maturation of normal rod photoreceptor and rod-driven post-receptor retinal processes are demonstrated by analysis of the ERG a- and b-wave responses to full-field, brief flashes that span a several log unit range of stimulus intensities. Maturation of the photoreceptors and post-receptor neurons underlie the developmental changes in the ERG responses. This is most clearly shown in the rod photoreceptor responses, which are interpretable in terms of molecular events in the developing rods. Representative responses from an infant and an adult are shown in Fig. 2A.

The initial portion of the a-wave depends on the photocurrent in the rods (Lamb and Pugh, 1992, 2006; Pugh and Lamb, 1993; Hood and Birch, 1994; Friedburg et al., 2004). The Hood and Birch (Hood and Birch, 1994) modification of the Lamb and Pugh model (Lamb and Pugh, 1992; Pugh and Lamb, 1993) of the biochemical processes involved in the activation of rod phototransduction is summarized as

$$R(I,t) = R_{ROD}\,[1 - \exp(-0.5\, I\, S_{ROD}\, (t - t_d)^2)] \quad \text{(Eq. 2)}$$

This model was fit to the a-waves (Fig. 2B). The main parameters of the model are S_{ROD} and R_{ROD}. S_{ROD} is related to the amplification constant in the molecular model and summarizes the kinetics of a series of processes initiated by photoisomerization of rhodopsin and ending with closure of the channels in the photoreceptor (Lamb and Pugh, 1992). The saturated amplitude of the response, R_{ROD}, depends on the number of channels in the outer segment membrane that are available for closure by light. In Eq. 2, I is the flash intensity and t_d a brief delay.

Both S_{ROD} and R_{ROD} were significantly smaller in infants than in adults (Fig. 3, left panels). For example, at 10 weeks (0.2 years), these parameters were approximately half of the adult value. In dark adapted, immature human retina, as in the immature rat retina, both S_{ROD} and R_{ROD} are proportional to the rhodopsin content of the retina (Fulton et al., 1995;Fulton and Hansen, 2000). A logistic growth curve of the form

$$Y/Y_{MAX} = \mathrm{Age}^n/(\mathrm{Age}^n + \mathrm{Age}_{50}{}^n) \quad \text{(Eq. 3)}$$

summarizes normal development of S_{ROD} and R_{ROD}. In this model, Y_{MAX} is the adult value of the parameter and Age_{50} the age at which the parameter is half the adult value; the exponent *n* indicates the steepness of the curve.

Development of the rod photoresponse in ROP subjects has also been studied (Fulton et al., 2001). Results from 68 subjects with ***Severe, Mild***, or ***No ROP*** are plotted as a function of age in Fig. 3 (right panels). In the majority of the ROP subjects, S_{ROD} and R_{ROD} were below the normal mean (solid curves), and most subjects with ***Severe ROP*** (7 of 10) had S_{ROD} at or below the 95% prediction limit for normal (lower dashed curves). Those with ***No ROP*** were distributed about the normal mean and did not differ significantly from age-matched term born controls. Thus, ROP attenuates both S_{ROD} and R_{ROD}, and the severity of the attenuation varies significantly with the severity of ROP (ANOVA S_{ROD}: $F = 13.25$; $df = 2, 65$; $p < 0.01$; R_{ROD}: $F = 6.07$; $df = 2, 65$; $p < 0.01$), as was the case for the subset (N = 21) previously reported by Fulton et al. (2001). We argue that cellular dysfunction underlies these deficits rather than

loss of cells. Based on data from rats (Fulton et al., 1999b), we suspect that impaired mobility of the proteins in the transduction cascade account for the deficit in S_{ROD} and R_{ROD}.

2.2.1.2. Rod deactivation: Following activation of the rod's response to light, the photoreceptor must recover, that is, deactivate, in preparation for its response to the next flash of light. In healthy, term born infants and young adults (Hansen and Fulton, 2005b), a paired flash paradigm (Lyubarsky and Pugh, 1996; Birch et al., 1995; Pepperberg et al., 1996) was used to study recovery of rod photoreceptor response (Fig. 4). A probe flash was presented 2 to 120 s after a test flash of equal intensity. The amplitude of the a-wave to a photopically matched flash was subtracted from the response to the probe flash to yield the rod-isolated response. The amplitude of the a-wave was measured at a short, fixed time (8 ms) after the flash to minimize contamination by post-receptor response components. The amplitude of the a-wave response to the probe, which provides a measure of the rod's circulating current (Friedburg et al., 2001), was expressed as proportion of the amplitude of the a-wave response to the test flash alone (R/R_{MAX}). The time, t_{50}, at which a-wave amplitude was half the maximum a-wave amplitude, was determined by linear interpolation (Lyubarsky and Pugh, 1996).

Recovery time (t_{50}) decreased significantly with age from ~11 s in infants to ~5 s in adults (Fig. 4D). There was a significant correlation between S_{ROD}, the activation parameter, and t_{50}, the deactivation parameter (Hansen and Fulton, 2005b); higher values of S_{ROD} were associated with shorter values of t_{50}. This has also been shown in infant rats in a wider range of conditions (Fulton and Hansen, 2003) (Section 3.1.2).

Since t_{50} is correlated with S_{ROD}, which is scaled by the rhodopsin content of the infant retina, the kinetics of recovery during development may be determined by the probability of encounters of activated rhodopsin with the proteins involved in deactivation (rhodopsin kinase, arrestin, recoverin). In rats, the mRNAs of the deactivation proteins follow developmental courses similar to that of opsin. Therefore, it seems likely that the deactivation proteins are available to participate in recovery of the infant's rod response (Ho et al., 1986; Broekhuyse and Kuhlmann, 1989; Stepanik et al., 1993).

The same ERG procedure was used to assess deactivation in ROP subjects (Fulton and Hansen, 2004). As in the study of term born subjects (Hansen and Fulton, 2005b), the amplitude of the rod isolated a-wave response in subjects with ***Mild ROP*** and ***No ROP*** was expressed as a proportion of the amplitude of the response to the test flash alone, and the inter-stimulus interval at which a-wave amplitude was 50% of the test flash response was determined. In some older ***Mild ROP*** subjects, t_{50} was significantly prolonged, whereas t_{50} was normal in infants with ***Mild ROP*** and in the ***No ROP*** subjects at all ages. As in normal subjects, S_{ROD} and t_{50} were correlated. The t_{50} results in the older ***Mild ROP*** subjects are concerning because the possibility of progressive compromise of rod function between infancy and adolescence cannot be excluded. As in the studies of the activation of phototransduction in ROP rods, the prolonged t_{50} values obtained in the deactivation studies may be due to impaired mobility of transduction cascade proteins in the disc membranes.

2.2.1.3. Rod-driven post-receptor function: The rod-driven b-wave is due to activity of ON-bipolar and other second and third order retinal neurons (Aleman et al., 2001; Wurziger et al., 2001). Post-receptor function undergoes developmental changes (Fig. 5).

The scotopic b-wave amplitude was fit (Fig. 2C) by

$$V=V_{MAX}\,[I/(I+\sigma)] \quad \text{(Eq. 4)}$$

In this equation, V is the b-wave amplitude produced by a flash of intensity I, V_{MAX} the saturated b-wave amplitude, and σ the flash intensity producing a half maximum (semi-saturated) b-wave response (Fulton and Rushton, 1978).

The development of post-receptor response parameters is summarized by logistic growth curves (Fig. 5, left panels) (Fulton and Hansen, 2000). As shown, in healthy, dark adapted, young infants, the flash intensity needed to produce a half maximum b-wave amplitude (log σ) is higher and the saturated amplitude (V_{MAX}) lower than in adults. Deficits in log σ and V_{MAX} are accounted for by immaturities in the rod photoreceptor parameters, S_{ROD} and R_{ROD} (Fig. 6A).

Rod-driven b-wave response parameters log σ and V_{MAX} in ROP subjects (Fig. 5, right panels) show that the majority of points are below the normal mean for age, the solid curves in Fig. 5. In the ROP subjects (Fig. 6B), deficits in post-receptor sensitivity (log σ) are greater than deficits in rod sensitivity (S_{ROD}) and, thus, contrast with normal development, in which the immaturity in photoreceptor parameters predicts post-receptor immaturity. The post-receptor deficit is greater in older than in younger ROP subjects (Section 2.2.1.4).

2.2.1.4. Long term effects of ROP on the rod and rod-driven ERG: To evaluate long term effects of ROP on rod photoreceptor (ERG a-wave) and post-receptor (ERG b-wave) retinal function, the photoreceptor parameters (S_{ROD} and R_{ROD}) and rod-driven post-receptor b-wave parameters (log σ and V_{MAX}) of ROP subjects tested at young ages (2 to 8 months post-term) were compared to those of others tested at older ages (5 to 23 years) (Harris et al., 2009). Effects of both age and ROP severity (***Severe, Mild***, or ***None***) on S_{ROD} and log σ were significant. In both age groups, amplitude parameters were smallest in those with ***Severe ROP***. In those with ***Severe ROP***, post-receptor sensitivity (log σ) was relatively lower in the older than in the younger group. These data raise the concern that older subjects with ***Severe ROP*** have had progressive compromise of neural retinal function. From a practical perspective, long term follow up of patients with ***Severe ROP*** is indicated, even those whose ERG parameters fall within normal limits during infancy.

2.2.1.5. Early myopia and rod photoreceptor function in ROP: As previously mentioned (Section 1.3.2), early ametropia, particularly myopia, is frequent in children born prematurely. The retina is a controller of eye growth and refractive development (Troilo, 1992; Wallman, 1993). Because ROP affects the developing retina, we hypothesized that the ametropia associated with ROP is due to altered rod photoreceptor and post-receptor activity. In a study of 40 ROP subjects, rod photoreceptor sensitivity, S_{ROD}, was significantly lower in subjects born prematurely who developed early myopia, defined as spherical equivalent below the prediction limit for normal (Mayer et al., 2001) before age 2 years (Moskowitz et al., 2005a). In infants, the deficits in S_{ROD} antedated development of myopia and, thus, may be regarded as predictive of myopia. Children who were myopic many years before the ERG tests also had deficits in S_{ROD}. The other ERG parameters (R_{ROD}, log σ, and V_{MAX}) also showed deficits in the ROP myopes. Healthy myopic subjects (-4.75 to −11.00 diopters) who had no history of preterm birth had normal values of the ERG parameters. Thus, myopia alone does not account for the deficits. These results suggest that the regulatory mechanisms underlying refractive development in ROP subjects may involve rod and rod-driven activity.

2.2.2. Cone and cone-driven responses—To study development of normal cone and cone mediated function, full-field ERG responses to a 1.8 log unit range of red (λ > 610 nm)

stimuli presented on a steady, rod-saturating background were recorded from healthy, term born infants and adults. Cone photoresponse parameters were derived from the a-wave, and b-wave stimulus-response functions were analyzed (Fig. 7A, B). Prior to the cone ERG test, dark adapted rod responses were recorded from the same subjects in the same session (Section 2.2.1.1).

The cone photoresponse parameters were calculated by fit of a modification of the Lamb and Pugh (Lamb and Pugh, 1992; Pugh and Lamb, 1993) model of the activation of cone phototransduction to the ERG a-wave. The model was fit to only the first 10.8 ms of the a-wave to minimize the contribution of post-receptor activity (Hood and Birch, 1993, 1995). The model incorporates a cascaded RC (resistance-capacitance) filter to model the capacitance of the cone membrane (Hood and Birch, 1995). The equation is

$$R(I,t)=[(1-\exp\{-0.5\, I\, S_{CONE}\,(t-t_d)^2\})\, R_{CONE}] * \exp(-t/\tau) \quad \text{(Eq. 5)}$$

where R_{CONE} is the saturated response amplitude, S_{CONE} the gain parameter, t_d a brief delay, and τ the time constant of the RC filter. The symbol * represents the convolution operation (Hood and Birch, 1995).

In infants, both S_{CONE} and R_{CONE} were significantly smaller than in adults but at 4 to 10 weeks, both S_{CONE} and R_{CONE} were already 60-70% of the adult value (Hansen and Fulton, 2005a). This contrasts with the rod photoreceptor sensitivity (S_{ROD}) and saturated amplitude (R_{ROD}) parameters, which in the same subjects were only approximately 40% of the adult values (Hansen and Fulton, 2005a). For rods and for cones, the relative immaturity of both the sensitivity and the saturated amplitude parameters were similar.

Consistent with the photoreceptor response parameters, anatomic data show relatively greater maturity of peripheral cone than rod outer segment lengths. At age 1 week, peripheral cone outer segment length is 91% and rod outer segment length 42% compared to mature outer segments (Hendrickson, 1994). The early maturation of peripheral cones sharply contrasts the protracted course of development of the foveal cones (Hendrickson and Yuodelis, 1984; Yuodelis and Hendrickson, 1986; Hendrickson, 1994).

Cone b-wave stimulus-response functions show that in adults, the stimulus-response relationship shows a photopic hill (Fig. 8A). That is, amplitude of the b-wave increases with flash intensity to a maximum and then decreases with further increases in stimulus intensity (Peachey et al., 1992;Wali and Leguire, 1992;Lachapelle et al., 2001;Rufiange et al., 2002, 2003;Ueno et al., 2004;Hansen and Fulton, 2005a). Infants do not have a photopic hill even though they have responses to the same range of stimulus intensities as adults and the maximum b-wave amplitude in infants and adults is similar (Hansen and Fulton, 2005a). The cone pathway includes both ON- and OFF-bipolar cells that make contributions to the b-wave. A decrease in the positive amplitude of the ON-bipolar cell response and delay in the peak of the OFF response with increasing stimulus intensity is thought to account for the photopic hill in the cone-mediated ERG (Ueno et al., 2004). Possibly, the lack of a photopic hill in infants results from immaturities in the relative strength and/or timing of these ON- and OFF-bipolar cell contributions to the b-wave.

In ROP subjects, cone and cone-driven ERG responses from infants (N = 19) and older subjects (N = 23) were recorded and analyzed as described above (Fulton et al., 2008). S_{CONE} was only minimally reduced in those with ***Mild ROP*** but was below the normal mean in all with ***Severe ROP*** (Fig. 7C). The ***No ROP*** subjects had cone activation parameters (S_{CONE}, R_{CONE}) indistinguishable from those in controls. The cone photoreceptor results are evidence of lower

vulnerability of cones than rods to ROP. Earlier maturation may protect the cones. Compared to rods, cones, with twice as many mitochondria and greater aerobic ATP production, may be protected against hypoxia (Perkins et al., 2003). Cones may also be protected against the adverse effects of hypoxia and attendant hypoglycemia through their capability (in contrast to rods) for using endogenous glucogen (Nihira et al., 1995). As with rod and rod-driven ERG responses to full-field stimuli, we argue that cellular dysfunction rather than loss of cells underlies the cone and cone-driven deficits (Fulton et al., 2008).

In ROP subjects, whether infants or adults, the shapes of the b-wave stimulus-response functions are similar to those of age similar term born controls (Fig. 8B, C). Thus, the neurovascular disease ROP appears not to discriminate ON from OFF circuitry of the cone-driven pathways. Amplitude of the b-wave responses to full-field stimuli is mildly attenuated in the ROP subjects, as is the case for the multifocal ERG (Fulton et al., 2005) (Section 2.2). In rat models of ROP (Section 3.2.1), neural changes accompany abnormal retinal vascularization (Akula et al., 2007a; Downie et al., 2007). We suspect that a similar neurovascular abnormality has a role in attenuating the post-receptor activity that is represented in the cone ERG b-wave.

2.2.3. Oscillatory potentials—The oscillatory potentials (OPs), high frequency, low amplitude wavelets on the rising phase of the b-wave, represent neural activity distinct from that of the a- and b-waves (Brown, 1968; Ogden, 1973). Early OPs have been associated with photoreceptors and bipolar cells of the distal retina and later OPs with the amacrine, interplexiform, and ganglion cells of the proximal retina (Heynen et al., 1985; Wachtmeister, 1998, 2001; Rangaswamy et al., 2003; Dong et al., 2004). The OPs are affected by ROP (Fulton and Hansen, 1996; Akula et al., 2007b) and other ocular conditions in which abnormal retinal blood vessels are the primary clinical sign (Wachtmeister, 1998).

The normal course of OP development may be consequent to maturation and refinements of inner retinal circuitry that include feedback pathways and ON and OFF activity (Heynen et al., 1985; Pugh et al., 1998; Dong et al., 2004; Hancock and Kraft, 2004; Akula et al., 2007b). In 10 week old term born infants, OPs were significantly smaller than in adults and significantly less mature than photoreceptor responses (Moskowitz et al., 2005b). In infant ROP subjects (Fig. 9A), OP energy was higher than in control infants (Akula et al., 2007b). While we have no explanation for this unexpected result, we take it as one sign that post-receptor circuitry remodels in ROP and is intimately related to the vascular abnormalities (Akula et al., 2008b). In older ROP subjects (Fig. 9A), OP energy was lower than in age-similar controls (Akula et al., 2007b). Among the older ROP subjects, OP energy varied with spherical equivalent; energy was lowest in those with high myopia (Fig. 9B).

2.3 Multifocal electroretinogram (mfERG)

The structure of the fovea and central rod-free retina does not reach maturity until well into childhood (Hendrickson and Yuodelis, 1984). The low acuity of infants is attributed to immaturity of the central retina. The mfERG allows direct assessment of central retinal function in young infants. Through analysis of focal responses from a large number of small, discrete retinal regions, the mfERG provides information about the functional topography of the central retina (Sutter and Tran, 1992; Hood, 2000). Cone initiated activity in the bipolar cells is the main contributor to the mfERG response (Hood et al., 2002). In young infants, immaturity of ON- and OFF-bipolar cell activity is suspected because of the absence of a photopic hill in the full-field ERG (Hansen and Fulton, 2005a).

In healthy, term born 10 week olds, mfERG responses to 61 equal size (unscaled) hexagons in a 43° diameter region centered on the fovea were recorded (Hansen et al., 2009). Fixation was monitored continuously during recording. The waveform of the first order kernel of the mfERG

was similar in term born infants and adults (Fig. 10A). Responses from the individual stimulus elements were combined into five concentric rings, with ring 1 the central hexagon and ring 5 the most peripheral ring.

The results for the positive peak of the waveform, P_1, illustrate the principal features of the infant response: reduced amplitude, increased implicit time, and little variation with eccentricity (Fig. 10B). The large central peak in the adults' mfERG responses was not found in the infants'. The amplitude difference between infants and adults was significant for the central hexagon but not for the most peripheral ring. Control experiments indicated that small changes in fixation could not account for these results (Hansen et al., 2009). Rather, immaturity of the macula holds the explanation.

While cones are packed tightly in the adult fovea (~200,000 cones/mm^2) and less densely in the parafovea (11,300 cones/mm^2 at 10°) (Hendrickson and Yuodelis, 1984; Yuodelis and Hendrickson, 1986; Hendrickson, 1994), infants have a relatively even distribution of cones in the central retina (fovea: 15,000 cones/mm^2; 10° eccentric: 12,500 cones/mm^2) (Candy et al., 1998). If the relative density of bipolar cells is similar to that of cones, as it is in simian retina, (Calkins et al., 1994; Wassle et al., 1994; Martin and Grunert, 1999; Chan et al., 2001), the amplitude of the infants' mfERG response would vary little with eccentricity, accounting for our results.

Our preliminary analysis of mfERG data recorded from former preterm infants using the 61 hexagon unscaled array shows that at corrected age 10 weeks, ***No ROP*** subjects have mfERG responses similar to those of term born 10 week olds, indicating that premature birth alone does not alter the responses. However, preterm infants who had ***Mild ROP*** had smaller responses. Similarly, in a separate study, mfERG responses from ROP subjects tested at older ages (11 to 23 years) using an array of 103 hexagons scaled with eccentricity to produce equal response amplitude in normal adults, showed that the components of the first order kernel (Fig. 11A) had significantly smaller amplitudes and longer implicit times in ***Mild ROP*** subjects than in healthy controls (Fulton et al., 2005). The difference between ROP and control subjects was greatest for central ring 1 and became smaller with increasing eccentricity (Fig. 11B). Compared to term born infants with a flat distribution of mfERG responses, these older ROP subjects had a central peak, suggesting that even in ROP, the central retina develops, albeit in an abnormal fashion. We hypothesized that ROP alters the developmental re-distribution of retinal cells in this region and predicted specifically that the density of bipolar cells, the main contributors to the mfERG response, is different in the central retina of ROP subjects. Consistent with this hypothesis, OCT results (Hammer et al., 2008) in these same ROP subjects who had participated in the 103 hexagon mfERG study (Fulton et al., 2005) showed that the inner nuclear layer is thicker in ROP subjects than in controls (Section 2.4).

2.4. Imaging studies of the neural retina and retinal vasculature

Optical coherence tomography (OCT) has demonstrated subtle abnormalities of the ROP macula. A study that used conventional OCT measured the thickness of the laminae in the central retina of children with a range of ROP severity (Ecsedy et al., 2007). The main findings were that, compared to age similar, term born controls, the foveal and parafoveal retina were thicker and the thickness increased with greater severity of ROP.

Hammer and colleagues (2008; 2009) used ultra-high resolution adaptive optics imaging to study the central retina of the same ***Mild ROP*** subjects in whom mfERG responses were studied (Fulton et al., 2005). As predicted by the mfERG results (Fulton et al., 2005), the OCT images showed that the bipolar cell layer (inner nuclear layer, INL indicated in Fig. 12A) was thickened in the fovea of ROP subjects (Fig. 12B). A broader and shallower foveal pit was found in ROP subjects than in controls. An avascular zone was present in all control subjects, while in the

Mild ROP subjects, intraretinal capillaries at the level of both the inner and outer plexiform layers overlaid the fovea (Fig. 13). To have blood vessels overlying the fovea is abnormal at any age; even at preterm ages, there is a foveal avascular zone (Provis and Hendrickson, 2008). The diameter of the capillaries in the ROP macula was significantly smaller than in the control macula (Hammer et al., 2008). The photoreceptor layer thickness did not differ between ROP and control subjects. The significant structural abnormalities in the fovea of ***Mild ROP*** subjects are thought to be a consequence of perturbations of neurovascular development.

In preliminary scanning laser ophthalmoscopy (SLO) images, photoreceptors could be resolved and counted at eccentricities of <1° in control subjects and in some ROP subjects (Hammer et al., 2009). In other ROP subjects, the photoreceptors could not be resolved, even with adaptive optics compensation. Because the OCT studies (Hammer et al., 2008) had found no difference in the thickness of the photoreceptor layer between ROP and control subjects, the photoreceptor counts, or lack thereof, may be indicative of some disorder of the photoreceptor arrangement in the ROP eye. This may contribute to the slight visual acuity deficit in some ***Mild ROP*** subjects (Reisner et al., 1997; Fulton et al., 2005).

At preterm ages, the retinal vasculature in ROP subjects has been studied. Digital fundus photographs were obtained from 12 ROP eyes that had plus disease and from 20 without plus disease (Gelman et al., 2005). Plus disease, a clinical definition, is characterized by dilated venules and tortuous arterioles and often heralds worsening ROP. Calculations done using image analysis software (Martinez-Perez et al., 2002) indicated that integrated curvature (the sum of angles along the vessel), diameter, and tortuosity of the retinal vasculature, both arterioles and venules, were significantly greater in eyes with plus disease than in eyes without plus disease (Gelman et al., 2005). The sensitivity and specificity of each parameter (integrated curvature, diameter, tortuosity) were evaluated. The area under the resulting ROC curve was greatest for integrated curvature of arterioles. This suggests that for preterm infants, assessment of integrated arteriolar curvature could aid in diagnosis of plus disease. Vessel diameter in preterm infants was difficult to analyze because of the relatively low contrast and resolution of the retinal images afforded by the camera used in the newborn intensive care unit. Modern digital cameras in regular use in the clinic for older subjects provide images with higher resolution (Fig. 14), which facilitates analysis of the vascular features, including accurate assessment of arteriolar diameter (Hansen et al., 2008). Nonetheless, abnormal perifoveal vasculature deep to the retinal surface is not visible in these fundus photographs or on clinical examination, even with highly magnified views of the macula. Thus, ultra-high resolution assessment of the deep capillaries (Hammer et al., 2008) appears to be an essential step toward understanding the neurovascular relation and, thus, the ROP disease process.

2.5. Psychophysics

Psychophysical methods allow evaluation of function in selected, small retinal areas, whereas the full-field ERG tests the retina as a whole and the multi-focal ERG tests a relatively large region of posterior retina. Results of psychophysical studies provide the foundation for inferences about mechanisms underlying retinal sensitivity and adaptation and so, allow characterization of immaturities in these fundamental retinal functions. Furthermore, from a practical perspective, the rigorous visual psychophysical tests afford an approach to the retina in virtually all young children, some of whom are not readily testable using the ERG procedures described in Section 2.2. In psychophysical procedures, as in electroretinography, the subject's response is under stimulus control, and the stimulus is specified in exact physical terms.

In this section, psychophysical procedures and biophysical considerations that pertain to both term born and ROP subjects are outlined. The specification of retinal stimulus in the infant eye with smaller axial length, smaller pupil, and highly transmissive media, including the calculation of retinal illuminance, are detailed in Section 2.1. The results of psychophysical

studies in infants and children with a history of preterm birth, both with and without ROP, are compared to those in healthy term born subjects.

2.5.1. Scotopic thresholds

2.5.1.1. Measuring scotopic visual thresholds in pediatric subjects: Infants' thresholds are estimated using a two-alternative, forced-choice, preferential-looking method (Teller, 1979) that incorporates a “fix and flash” procedure (Schneck et al., 1984; Hansen et al., 1986). After 30 minutes of dark adaptation, the infant is held in front of a rear projection screen. A small, red LED fixation target attracts the infant's gaze to the center of the screen. An adult observer uses an infrared viewer to watch the infant. When the observer reports that the infant is alert and looking at the fixation target, the experimenter extinguishes it and presents a test flash. The observer, unaware of the position of the test flash, reports stimulus location, right or left, based on the infant's head and eye movements. The observer receives feedback from the experimenter on every trial. Child and adult subjects point or report verbally the right-left position of the test spot. Thus, the basic method is applicable from infancy through adulthood.

Thresholds are determined using a transformed up-down staircase that efficiently estimates the 70.7% correct point of the psychometric function (Wetherill and Levitt, 1965). There is good agreement between thresholds estimated using this rapid staircase and using the method of constant stimuli (Hansen et al., 1986; Fulton et al., 1991b). Stimulus parameters (size, duration, spectral composition, and eccentricity) are chosen based on the experiment at hand. Large (109° diameter), steady background fields are added to control adaptation level.

2.5.1.2. Ocular media density: The estimated density of the ocular media increases significantly with age (Pokorny et al., 1987). Werner reported a continuous increase in media density between 4.5 months and 66 years (Werner, 1982). The media density in 2 month old infants is significantly lower than in adults (Powers et al., 1981; Werner, 1982; Hansen and Fulton, 1989). At any given age, the range of media density is approximately 1 log unit (Werner, 1982; Pokorny et al., 1987).

To determine ocular media density, thresholds for detecting 401 nm and 560 nm stimuli were measured in 10 week old infants and young adults using the method of constant stimuli (Hansen and Fulton, 1989). Although rhodopsin absorbs quanta equally at 401 nm and 560 nm (Bowmaker and Dartnall, 1980), the ocular media strongly absorbs 401 nm light but absorption at 560 nm is negligible (Norren and Vos, 1974; Wyszecki and Stiles, 1982). Thus, differences in threshold between the two wavelengths are attributable to absorption by the ocular media. In 10 week old infants, we take the media density (401 nm) to be 0.75 log unit compared to 1.46 log units in young adults (Hansen and Fulton, 1989). Correction for light losses in individual subjects can be made using this method (Norren and Vos, 1974).

2.5.1.3. Scotopic threshold development: In dark adapted peripheral retina (~20° eccentric), thresholds in healthy, young, term born infants are significantly higher (sensitivity lower) than those in adults (Hansen and Fulton, 1981; Powers et al., 1981; Hamer and Schneck, 1984; Schneck et al., 1984; Brown, 1986). Cross-sectional data (Fig. 15A) show that thresholds at 4 weeks are, on average, 1.4 log units higher; at 10 weeks, 1.1 log units higher; and at 18 weeks, 0.65 log unit higher than in adults (Hansen et al., 1986).

Spectral sensitivity functions were needed to demonstrate that the higher thresholds in dark adapted infants were, indeed, rod mediated rather than contaminated by cone activity. The spectral sensitivity functions of dark adapted infants (Fig. 15B) are well described by the scotopic luminous efficiency function (Wyszecki and Stiles, 1982;Hansen and Fulton, 1993). This is evidence that the thresholds in infants are rod mediated (Powers et al., 1981;Clavadetscher et al., 1988;Hansen and Fulton, 1993). As previously demonstrated for rat

rod b-wave spectral sensitivity functions (Alpern et al., 1987), when the psychophysical spectral sensitivity functions in infants were compared to the absorption spectrum of rhodopsin, the infants' functions were narrower than the adults' (Hansen and Fulton, 1993). This result is consistent with lower axial density of rhodopsin in the immature rod and lower total rhodopsin content in the immature retina (Fulton et al., 1999a).

During the course of eye growth and retinal cell development, regional variation in the maturation of rod photoreceptors occurs. Anatomic studies have shown that developmental elongation of the parafoveal rod photoreceptor outer segments is delayed relative to that in the peripheral retina (Hendrickson and Drucker, 1992; Hendrickson, 1994; Dorn et al., 1995; Fulton et al., 1996). We hypothesized, therefore, that threshold development at a parafoveal site would lag that at a peripheral site (Fulton et al., 1996). In a study of 10 week old infants, stimuli that produce thresholds of equal troland values at 10° (parafoveal) and 30° (peripheral) eccentricities in healthy, dark adapted adults were presented (Hansen and Fulton, 1995). The infants' thresholds were higher than those of adults at both sites. Additionally, the infants' parafoveal thresholds were 0.5 log unit higher than those in peripheral retina. The infants' data are explained by reduced quantum catch and consequent proportionate elevation of parafoveal relative to peripheral thresholds in healthy young infants (Hansen and Fulton, 1995, 1999; Fulton et al., 1996).

Results of a longitudinal study indicated that infants' thresholds decreased at both sites (10° and 30°) and reached the adult level by age six months (Fig. 16A, B). The difference between parafoveal and peripheral thresholds ($\Delta_{10\text{-}30}$) was 0.5 log unit at 10 weeks and zero by age six months (Fig. 16C), as it is in adults (Hansen and Fulton, 1995).

In ROP subjects, as well as in rat models of ROP, full-field ERG studies have documented abnormalities in rod and rod-driven function (Reynaud et al., 1995; Fulton et al., 2001; Liu et al., 2006a; Akula et al., 2007a). Studies of the rods in a rat model of ROP have shown that the outer segments are disorganized with a broad distribution of transverse rhodopsin absorbances, although rhodopsin content of model and control retinas did not differ (Fulton et al., 1999b).

Using the above described $\Delta_{10\text{-}30}$ procedure, we tested the hypothesis that in ROP infants, the rods in the late maturing parafoveal retina are more vulnerable to the effects of ROP than earlier maturing rods in the peripheral retina (Barnaby et al., 2007). The specific prediction was that the parafoveal threshold would be relatively more elevated than the peripheral in ROP infants. The parafoveal site (10° eccentric) is within zone I and the peripheral site (30° eccentric) is within zone II, as defined by ICROP (International Committee for the Classification of Retinopathy of Prematurity, 2005). In the preterm infant, active ROP in zone I is associated with high risk of poor outcome (Early Treatment for Retinopathy of Prematurity Cooperative Group, 2003). The results of our study of the former preterms with ***Mild ROP*** and those with ***No ROP*** are summarized in Fig. 17.

In those with ***Mild ROP***, threshold development, particularly at the parafoveal site, lagged normal development. The dashed lines in Fig. 17 indicate the 99% prediction interval for normal. Analysis of the course of individuals using a linear model indicated that the course in ***Mild ROP*** subjects is significantly slower than in those with ***No ROP*** whose course was the same as that in term born controls (Barnaby et al., 2007).

There are a number of possible explanations for the slow course of threshold development in ROP subjects. Possibly, rod outer segments elongate more slowly in the ROP infants, or ROP affects the packing density (rods per unit area) of parafoveal rods with age. Redistribution of rod and cone photoreceptors in the parafovea occurs during simian development (Packer et al., 1990). Ordinarily, as the foveal pit develops, cone photoreceptors pack together. Development of the foveal pit is delayed in infants with ROP (Isenberg, 1986). Perhaps the packing of nearby

parafoveal rods and cones is also delayed or disordered (Hammer et al., 2009). A third possibility is that disorganized rod outer segments, as have been found in an infant rat model of ROP (Fulton et al., 1999b), decrease the efficiency of photon capture. If there were rod outer segment abnormalities in the ***Mild ROP*** subjects, they must have resolved sufficiently for the detection threshold to have become normal by approximately 12 months corrected age.

The prolonged course of scotopic threshold development is a sign that even mild ROP affects development of the neural retina. The slower course at the parafoveal site is evidence that the late maturing parafoveal rods are particularly vulnerable to the ROP disease process, whereas the peripheral rods are less affected. While the underlying mechanisms remain to be defined, in experiments on rat models of ROP (Section 3), injury to the immature rods and also the role of growth factors in determining the fate of the photoreceptors and organization of the post-receptor retina in ROP continue to be studied (Akula et al., 2007a, b, 2008b; Fulton et al., 2008).

2.5.2. Background adaptation—The development of adaptation to steady background lights in healthy infants was studied using psychophysical and ERG procedures (Hansen and Fulton, 1981, 1986, 1991, 2000a, b). Increment threshold functions, which plot log threshold as a function of log background intensity, provide the classic display of background adaptation data (Fig. 18A). Models of the increment threshold function (Hood and Greenstein, 1990) can be used to make inferences about the effect of disease or immaturity on the photoreceptors and post-receptor neural retina. Immaturity of the rod photoreceptors is predicted to shift the increment threshold function diagonally, by equal amounts along both axes; this would be due to reduced catch of quanta from both the background and test stimuli. A post-receptor immaturity is predicted to elevate thresholds, that is, shift the function vertically but not shift the function horizontally (Hansen and Fulton, 2000a).

The increment threshold function is summarized by

$$\log T = \log T_{DA} + \log [(A_o + I)/A_o] \quad \text{(Eq. 6)}$$

where T is the threshold measured at background intensity I. T_{DA} is the dark adapted threshold and A_o the *eigengrau*, or dark light. The background that elevates threshold 0.3 log unit above the dark adapted level produces an equal number of thermal and photoisomerizations and is designated the *eigengrau* (Brown, 1986). The *eigengrau*, thus, is an estimate of noise produced in the retina by the thermal isomerization of rhodopsin and other sources. At more intense backgrounds, log threshold increases linearly with log background intensity until saturation is reached (Aguilar and Stiles, 1954).

Rod mediated increment threshold functions measured at parafoveal (10° eccentric) and peripheral (30° eccentric) sites in a 10 week old infant and a mature control subject are shown in Fig. 18B and D (Hansen and Fulton, 2000a). In all conditions, the infant's thresholds are higher. At the peripheral site, there were approximately equal horizontal and vertical shifts of the increment threshold functions (~0.8 log unit) relative to the adult values. This is consistent with a receptor immaturity (Hood and Greenstein, 1990). At the parafoveal site, the relative shift in the dark adapted threshold (~1.3 log units) was larger than the than shift in the *eigengrau* (~0.4 log unit). Thus, the results suggest that in addition to a photoreceptor immaturity, a post-receptor immaturity must also contribute to the parafoveal threshold elevation. In mature subjects (Fig. 18D), parafoveal and peripheral increment thresholds were superimposed (Hansen and Fulton, 2000a).

In individual infants, the parafoveal function had elevated dark adapted threshold but lower *eigengrau* relative to these parameters for the peripheral increment threshold function. These results are consistent with shorter rod outer segments with proportionately lower rhodopsin content and fewer thermal isomerizations in the parafoveal retina. In adult control subjects, parafoveal and peripheral increment threshold functions were superimposed; dark adapted thresholds and *eigengrau* values are within the range that have been previously reported (Sharpe et al., 1992).

Increment threshold functions were studied in four subjects with ***Mild ROP*** (Hansen and Fulton, 2000b). The dark adapted thresholds of all were elevated relative to those in term born controls (Fig. 18C). In two of the ROP subjects, parafoveal thresholds were elevated 0.2 to 0.4 log unit above the peripheral threshold. Higher e*igengrau* values, and thus higher intrinsic noise in the rods, of these two subjects may be a consequence of disorganized rod outer segments, similar to those seen in a rat model of ROP (Fulton et al., 1999b), or irregular rod to rod spacing within the patch of retina tested (Hammer et al., 2009). Interestingly, these two subjects were high myopes (-8.00 to -9.00 diopters). The parafoveal threshold of other myopic, ***Mild ROP*** subjects who were tested only in the dark adapted condition was also elevated (Reisner et al., 1997).

The other two ROP subjects, who were not myopic, did not show a relative shift of the parafoveal and peripheral increment threshold functions. The *eigengrau* values were shifted toward dimmer backgrounds by ~0.2 log unit, an amount equal to their dark adapted threshold elevation. These results suggest reduced quantum catch and lower intrinsic photoreceptor noise. A parsimonious explanation for these results is short rod outer segments. The saturated amplitude of the ERG rod photoresponse (R_{ROD}), which depends on the number of channels available for closure by light and is proportional to rod outer segment length, is also low in ROP subjects (Fulton et al., 2001); see also Fig. 3D.

2.5.3. Spatial summation—Spatial summation functions demonstrate integration of information over retinal area (Hood and Finkelstein, 1986). As stimulus diameter increases, threshold decreases up to a critical diameter beyond which threshold changes little with further increases in diameter. The effect of stimulus diameter on dark adapted threshold at ~20° eccentricity has been measured in term born 4 week old (Hamer and Schneck, 1984; Schneck et al., 1984) and 10 to 11 week old infants (Hamer and Schneck, 1984; Hansen et al., 1992). The critical diameter for complete spatial summation in infants at 4 weeks (~ 9 - 17°) and at 10 to 11 weeks (6°) is significantly larger than critical diameter in adults (~2.3°) (Hamer and Schneck, 1984; Schneck et al., 1984; Hansen et al., 1992). This is evidence that scotopic receptive fields become smaller with age. Even in the presence of dim scotopic adapting fields, critical diameters for complete summation in term born 10 week old infants remain about four times larger than in adults (Hansen et al., 1992). The adapting field is thought to activate inhibitory center surround mechanisms that lead to a reduction in the area of complete summation (Barlow, 1972; Hood and Finkelstein, 1986). The properties of this interaction were studied in 10 week old infants using the preferential looking procedure described in Section 2.5.1.1. The center-surround stimuli were modified from those used in Westheimer's classic experiments in adults (Westheimer, 1965). Thresholds for small probe flashes (Fig. 19) were determined on backgrounds of varying diameters (Hansen and Fulton, 1994). Increasing the background diameter causes elevation of the threshold (desensitization), followed by a decrease in threshold (sensitization) as the background diameter increases further. The diameter of the background that causes the maximum threshold elevation is thought to indicate the extent of the central excitatory region of the receptive field.

Evidence of a balanced center-surround organization was found in young infants, but the central excitatory region was, on average, about four times greater than that in adults (Hansen and

Fulton, 1994). This is in excellent agreement with the estimates of receptive field size obtained in the study of light adapted spatial summation (Hansen et al., 1992). Reorganization of the post-receptor neural circuitry may underlie the narrowing of the Westheimer function with development.

In an adolescent with ***Mild ROP***, the critical diameter for complete summation in the parafoveal retina (10° eccentric) was 2.7°, nearly three times the expected value (Scholtes and Bouman, 1977) but was normal (2.1°) in the peripheral retina (30° eccentric). This is another example of lasting dysfunction in parafoveal ROP retina that suggests abnormal organization of post-receptor neurons. Further high resolution imaging studies paired with psychophysical evaluation of additional ROP subjects are needed to elucidate this subtle but important consequence of ROP.

3. Rat models of ROP

Models of ROP have been created in a variety of mammals (Madan and Penn, 2003). Oxygen exposures delivered at ages during which the neural retina and its vasculature are immature induce a retinopathy that models ROP. Several rat models of ROP have been created (Penn et al., 1994; Reynaud et al., 1995; Fulton et al., 1999b; Lachapelle et al., 1999; Dembinska et al., 2001; Liu et al., 2006a, b; Akula et al., 2007a, b). We have studied the model originated by Penn (Penn et al., 1995) as well as others (Reynaud et al., 1995; Liu et al., 2006a, b; Akula et al., 2007a, b). In addition to abnormalities of the retinal vasculature, subtle abnormalities of the structure of photoreceptor and post-receptor retina have been documented (Fulton et al., 1999b; Dembinska et al., 2001; Favazza et al., 2009). The combination of these models spans the gamut of severity represented in our human ROP subjects. Key neural (rod sensitivity, S_{ROD}) and vascular (arteriolar integrated curvature, IC_A) parameters are similar in rat models and human ROP subjects (Fig. 20) (Fulton et al., 2009). The rat models facilitate our aim to understand the cellular and molecular basis for the neurovascular interplay in ROP and to obtain data throughout the course of evolution and resolution of ROP. As in the human infants, we studied normal rat retinal development before studying rat models of ROP disease.

3.1 Normal rat retinal development

3.1.1. Structure of neural retina and its vasculature—Not only are the photoreceptors the last retinal cells to differentiate, but the photoreceptor outer segments are the last retinal structures to appear (Grun, 1982). In the rat, rod outer segments first appear at approximately postnatal day six (P6). At P13, rod outer segments (ROS) are half the length of those in adults (Fig. 21A), and by P19 approach adult length (Bonting et al., 1961; Fulton et al., 1995). Rhodopsin content of the whole retina reaches half the adult value at P19 (Bonting et al., 1961; Fulton et al., 1995). In the immature ROS, there is a gradient of rhodopsin absorbance, with the lowest density at the tip and the highest at the base where newly formed discs are added (Fig. 21B). As detailed by Dodge et al. (1996), this gradient accounts for the discrepancy in ROS and rhodopsin growth curves. Rhodopsin concentration, expressed as weight of rhodopsin per dry weight of retina, increases with ROS length (Fox and Rubinstein, 1989; Timmers et al., 1999). The three principal proteins involved in the activation of phototransduction (opsin, transducin, and phosphodiesterase) appear to be available to the developing ROS (Fulton et al., 1995). In addition to phototransduction and maintenance of the circulating current, one of the most energy demanding activities of the rod photoreceptors is renewal of outer segment material with disposal of old discs to the pigment epithelium. During development, the number of large phagasomes in the pigment epithelial cells increases following the rhodopsin growth curve (Tamai and Chader, 1979; Fulton et al., 1995). Thus, with the developmental increase in rhodopsin content, there is a sharp increase in essential rod activities (phototransduction; maintenance of circulating current; turnover of outer segments) that are known to require high levels of aerobic energy to operate properly (Steinberg, 1987).

In addition to photoreceptor development, post-receptor neurons and retinal vessels also undergo developmental changes after birth. Throughout development, post-receptor neurons reorganize (Xu and Tian, 2004, 2007, 2008). Normal rat retinal vasculature grows centripetally to reach the ora at approximately P14 (Reynaud and Dorey, 1994). These developmental changes in neurons and blood vessels are under cooperative molecular control (Gariano et al., 2006).

3.1.2. Full-field ERG—As in normal infants, to study developmental changes non-invasively, ERG responses to ~5 log unit intensity range of full-field, white strobe flashes were recorded from dark adapted Sprague-Dawley albino rats. Rod photoreceptor and post-receptor ERG response components (Fig. 22) differed between the immature and the mature rat retina (Fulton et al., 1995). Control experiments demonstrated that responses are rod dominated in both infant and adult rats (Fulton et al., 1995).

A-wave responses were analyzed using the Hood and Birch modification of the Lamb and Pugh model of the activation of phototransduction (Section 2.2.1.1, Eq. 2). Post-receptor b-wave responses were analyzed using the Naka-Rushton equation (Fulton and Rushton, 1978) (Section 2.2.1.3, Eq. 4). Under these conditions, the b-wave represents the activity of ON-bipolar cells and other second and third order neurons (Aleman et al., 2001;Wurziger et al., 2001).

As with human rod and rod-driven ERG response parameters, a logistic growth curve [(Fulton et al., 1995); Section 2.2.1.1., Eq. 3] was used to summarize the developmental course for each parameter of rod photoreceptor (a-wave) activation (S_{ROD} and R_{ROD}) and post-receptor (b-wave) activity ($\log \sigma$ and V_{MAX}). Rod photoreceptor sensitivity, S_{ROD}, increased significantly with age. Specifically, Age_{50} for S_{ROD} is P17.9 (95% Cl: 16.2 to 19.6), similar to Age_{50} for rhodopsin content (P18.7; 95% CI: 18.2 to 19.2) (Dodge et al., 1996; Fulton et al., 1995). In infants, low rhodopsin content limits quantum catch; throughout development, photon capture appears to constrain the activation of phototransduction. The mobility of the transduction proteins in the immature disc membrane may be the same as in adults (Fulton and Hansen, 2003).

Post-receptor b-wave $\log \sigma$ is also half the adult value at P18. The developmental course for $\log \sigma$ is indistinguishable from that for S_{ROD} and rhodopsin. As in human development, deficits in rod photoreceptor (a-wave) sensitivity, S_{ROD}, predict deficits in post-receptor (b-wave) sensitivity, $\log \sigma$.

The mean saturated amplitude of the rod photoresponse, R_{ROD}, doubles between age P18 and P30, as does post-receptor saturated amplitude, V_{MAX}. R_{ROD} represents the rod's circulating current and thus the number of channels in the outer segment available for closure by light. Increases in V_{MAX} were significantly correlated with increases in R_{ROD}. Furthermore, the ratio of R_{ROD} to S_{ROD} was invariant with age (Fulton and Hansen, 2003). The stability of this ratio is consistent with a fixed number of channels per disc during normal development.

Following activation of the rod's response to light, the photoreceptor must recover (deactivate) in preparation for its response to the next flash of light. Deactivation depends on events in the disc membrane and cytosol of the ROS, specifically, deactivation of rhodopsin, transducin, and phosphodiesterase and restoration of the circulating current (Pugh and Lamb, 2000). The developmental increase in several deactivation components, including arrestin (Broekhuyse and Kuhlmann, 1989), kinase (Ho et al., 1986), recoverin (Stepanik et al., 1993), and cGMP (Colombaioni and Strettoi, 1993; Johnson et al., 2001), is concurrent with ROS elongation. Thus, we suspect that the biochemical underpinnings of deactivation are similar in infants and adults.

To investigate deactivation in immature rat rods, we studied the kinetics of recovery of the circulating current as represented in the ERG a-wave (Fulton and Hansen, 2003). Infant (P18-19) and adult (P60-90) Sprague-Dawley albino rats were studied. Deactivation was evaluated using a paired flash paradigm (Lyubarsky and Pugh, 1996) in which equal intensity test and probe flashes were presented at selected inter-flash intervals (2 to 120 s), as described in Section 2.2.1.2. Recovery was studied using six intensities spanning a 2.4 log unit range.

The amplitude of the a-wave response to the test flash as a function of ISI for an infant and an adult rat is plotted in Fig. 23A. We equated the estimated proportion of rhodopsin molecules isomerized by the stimulus (Fig. 23B) and found that the t_{50} values of the infants and adults are coincident over the ~2 log unit range of stimuli (Fulton and Hansen, 2003). This suggests that the molecular processes controlling the recovery of the rod photoreceptor response are the same in immature and mature rods. Thus, the kinetics of recovery may be set by the possibility of encounters of activated rhodopsin with the proteins involved in deactivation.

The oscillatory potentials (OPs), which signal retinal activity distinct from that represented in the a- and b-waves, were studied in dark adapted rats (Akula et al., 2007b). The ERG records were digitally filtered (100 – 380 Hz) and the trough-to-peak amplitude and implicit time of OP wavelets measured (Liu et al., 2006b). Summed OP amplitude increased and implicit time decreased with increasing stimulus intensity. In general, OPs in infants were smaller and slower than those in adults. In the frequency domain, by using discrete Fourier transform to produce a power spectrum, the peak frequency and energy of the OPs were determined. Peak frequency was ~95 Hz and did not vary with age. The total energy decreased between infancy and childhood. Refinements in inner retinal circuitry that include feedback pathways and interplay of ON and OFF activity (Heynen et al., 1985; Pugh et al., 1998; Dong et al., 2004; Hancock and Kraft, 2004; Xu and Tian, 2004, 2007, 2008) may account for the decrease in total OP energy between infancy and adulthood (Akula et al., 2007b).

3.2. Oxygen induced retinopathy

Selected alternating exposures to hypoxia and hyperoxia reliably produce models of ROP (Penn et al., 1994; Reynaud et al., 1995; Fulton et al., 1999b; Lachapelle et al., 1999; Dembinska et al., 2001; Liu et al., 2006a, b; Akula et al., 2007a, b). We have used two oxygen exposure schedules (Fig. 24), chosen to produce a range of ROP severity similar to that observed in our human ROP subjects. In the first, developed by Penn et al. (1995), rats are exposed to alternating 24 hour periods of 50% or 10% oxygen levels for the first 14 days after birth and then returned to room air (21% oxygen). In the second, the rats are kept in room air from birth to P7, then placed in constant 75% oxygen from P7 to P14, and then returned to room air. The animals are kept in a 12 hour dark/12 hour light cycle with low average luminance (~10 lux) throughout the experiment. Herein, we designate the rats as 50/10 model, 75 model, or controls that were maintained in room air.

3.2.1. Full-field ERG and retinal vasculature—Akula et al. (2007a) conducted a longitudinal study of rod-driven ERG responses and retinal vascular abnormalities in the 50/10 and 75 models and in controls (Fig. 25). Test ages were P20, P30, and P60. Parameters of the dark-adapted ERG a-wave (S_{ROD}, R_{ROD}) and b-wave (log σ, V_{MAX}) were determined as described above (Section 2.2.1.1 and 2.2.1.3). Computer assisted analysis of the superficial retinal vasculature displayed in wide field digital fundus photographs, obtained from the same animals, yielded quantitative estimates of the vascular tortuosity and caliber of the retinal vessels. Integrated curvature of the retinal arterioles, defined as the sum of angles along a vessel divided by its length, was the most accurate diagnostic measure and demonstrated several significant relationships with parameters of the ERG. The ERG parameters and arteriolar integrated curvature were analyzed for significant variations among the ROP models (50/10,

75) and controls and for changes with age (P20, P30, P60). Significant attenuation in sensitivity and amplitude parameters of receptor and also post-receptor retina occurred in both the 50/10 and 75 models. The arterioles were also significantly more tortuous (integrated curvature higher) than in controls. With increasing age, these signs of neurovascular abnormality diminish spontaneously just as most human ROP resolves without intervention. Nonetheless some functional deficits persisted in the 60 day old rats just as in some older children and adolescents with ***Mild*** and ***Severe ROP*** (Section 2).

The most provocative relationship of ERG responses to retinal vasculature was that of rod photoreceptor sensitivity, S_{ROD}, to arteriolar integrated curvature at P60, IC_A. In Fig. 26, for each rat, S_{ROD} at P20 and IC_A at P60 are shown relative to the normal mean for age. Rod photoreceptor sensitivity at a young age (P20) predicted, in the same animals, vascular outcome in adulthood (P60). This temporal priority of rod dysfunction was consistent with a causal role for the rod photoreceptors in producing the retinal vascular abnormality.

As the natural course of rat ROP continued, the vascular abnormalities resolved and the function of the post-receptor retina in both the 50/10 and 75 models improved, even though S_{ROD} remained low in the 75 model (Akula et al., 2007a). Specifically, b-wave log σ shifted to dimmer intensities in parallel with decrease in IC_A (Fig. 27). This suggests that the post-receptor retina re-organized as the vascular abnormality resolved, despite low S_{ROD}. The improvement in log σ is not unlike the recovery of post-receptor (b-wave) and visual functions that occurred in a patient whose rods had irreversible, stable dysfunction due to medication (Lu et al., 2007).

3.2.2. Growth factors—In a follow-up study, Akula and colleagues (2008b) investigated whether receptor and post-receptor function were related to the expression of growth factors known to mediate both vascular development and neural remodeling. Such growth factors are candidate mediators of the neurovascular interplay documented in ROP. ERGs and fundus images were obtained prior to harvest of retinal material at P15-16, P18-19, or P25-26. Vascular endothelial growth factor (VEGF) and semaphorin were selected because VEGF is essential for physiologic vascular development (Saint-Geniez et al., 2006) and has been implicated in pathologic vascularization such as found in ROP (Pierce et al., 1995; Dorey et al., 1996; Stone et al., 1996). Semaphorin acts as an axon growth cone guidance molecule (He et al., 2002) involved in plasticity and stabilization during post-receptor retinal development (de Winter et al., 2004). VEGF and semaphorin are expressed in temporally and spatially overlapping domains during retinal development (He et al., 2002; de Winter et al., 2004) and share a receptor: neuropilin. Neuropilin receptors are found both on vascular endothelial cells and in retinal neurons (Bielenberg et al., 2006), including progenitors of photoreceptors (Amato et al., 2005). Neuropilin, therefore, sits at a nexus of vascular and neural development by competitively binding two disparate ligand families (VEGF and semaphorin), a fact supporting the hypothesis that retinal neurogenesis and angiogenesis are inseparably linked. Assessment of mRNA expression, evaluated in retinal lysates by reverse-transcriptase polymerase chain reaction (rt-PCR), revealed that VEGF and semaphorin were elevated immediately following the induction of retinopathy (P15-16), in both 50/10 and 75 models, relative to controls. Retinal levels of both VEGF and semaphorin plummeted as vascular abnormalities resolved and ERG parameters improved (Akula et al., 2008b).

Lower rod sensitivity was correlated with more severe vascular abnormality. Low post-receptor sensitivity was strongly associated with tortuous retinal vasculature (Akula et al., 2008b). Furthermore, retinal sensitivity was also negatively correlated with VEGF and semaphorin expression. The post-receptor neural retina is supplied by the retinal vasculature and, therefore, is ideally situated to mediate the rod-vascular relationship (Akula et al., 2007a). Thus, there are at least two explanations for these results: 1) abnormal retinal vessels presumably offer

subnormal circulation to post-receptor retina, while more normal vasculature provides an environment favorable to post-receptor function; 2) the distressed post-receptor neural retina might trigger vascular genesis by up-regulating mRNA of proangiogenic growth factors such as VEGF or semaphorin, and an excess of these signals might induce vascular tortuosity.

These data suggest that intervention at two novel retinal targets at critical times in the pathogenesis of retinopathy could disrupt or even prevent the untoward vascular outcomes. Both the molecular crosstalk between post-receptor neurons and retinal vasculature and the immature rod photoreceptors are potential sites for pharmacological intervention. Protection of the immature rods might be achieved, for instance, by modulating the energy-demanding visual cycle of the rods. A preclinical trial of this approach was conducted and did result in improved rod-mediated retinal function in ROP rats (Akula et al., 2008a).

4. Future directions

4.1. Structure–function relationships

As detailed in Sections 2 and 3, a number of neurovascular structure–function relationships have already been demonstrated in human ROP and rat models of ROP. Further delineation of these relationships is needed to advance our understanding of the disease process and its consequences. Improved management of ROP can be built on this foundation.

To date, studies of structure and function have provided evidence that the rods are injured in ROP. The proximal cause of the injury remains unknown. Both hyperoxia and hypoxia, which are injurious to the immature photoreceptors (Fulton et al., 1999b; Wellard et al., 2005), are encountered during the course of clinical management of the preterm infant or in the creation of rat models of ROP (Cunningham et al., 1995; Penn et al., 1995; Liu et al., 2006a; Akula et al., 2007a). The retinal vasculature has been studied extensively in ROP, but less is known about the role of the choroid. The choroid supplies oxygen to the photoreceptors. The swiftly flowing choroid, with oxygen diffusing freely through its fenestrated vessels, may allow local oxygen to reach levels that damage the immature rods. If this is the case, the molecular crosstalk between choroid and pigment epithelium would be altered in the ROP eye (Gogat et al., 2004; Saint-Geniez et al., 2006). Molecular hypotheses based on this idea are testable in animal models of ROP.

In human subjects, additional quantitative information about the microscopic structure of the macula is urgently needed in three specific areas: 1) the array of the cone photoreceptors in the macula, 2) the relationship between these cones and the pigment epithelium, and 3) the neural laminae in the central retina. Currently, it is not clear if altered cone and cone bipolar distributions are the basis for the altered mfERG topography, altered visual acuity, and color vision deficits in ROP. This can be elucidated using a combination of adaptive optics ultra-high resolution imaging, multifocal electroretinography, and visual psychophysics in children.

Understanding of the ROP disease process and its lasting consequences, both in children and in rat models of ROP, also calls for further investigation of the cellular and molecular basis for dysfunction in the post-receptor ROP retina. It is the superficial retinal vasculature on which the criteria for clinical diagnosis of ROP at preterm ages is based. More complete information about the deep retinal vasculature is needed to understand the neurovascular interplay in ROP. As detailed in Section 2.4, in older subjects, the locus and characteristics of the deep capillaries are abnormal years after acute ROP has resolved (Hammer et al., 2008). And in rat models of ROP (Section 3.2.1), an intimate association of the vascular and neural characteristics have been demonstrated through analysis of post-receptor retinal activity and anatomic and molecular biological data, not only after the peak of the acute ROP rat disease but also during its evolution (Akula et al., 2008b; Favazza et al., 2009).

In rat models, the proteins (growth factors) that share in the regulation of development of the post-receptor neurons and the retinal vasculature, both superficial and deep, will be studied in animals with well characterized retinal and vascular function and morphology. This will advance our understanding of the intra-laminar reorganization of the post-receptor retina (Jones et al., 2003; Xu and Tian, 2004, 2007, 2008) during the evolution and resolution of ROP. In human ROP subjects, the structure and function of post-receptor central retina will be studied using adaptive optics imaging (Hammer et al., 2008, 2009) and by analyzing higher order signals in the mfERG (Hood, 2000; Bearse et al., 2006). Rod-driven post-receptor function will be further studied using psychophysical assessments of adaptation and spatial processing. In some retinal regions, oximetry (Pournaras et al., 2008) is expected to yield further insights into the neurovascular function of the ROP retina and its relation to vision.

4.2. Eye growth and refractive development

The frequent occurrence of significant refractive errors in ROP subjects is well established (Section 1.3). However, the mechanisms that alter eye growth and lead to the refractive errors remain to be defined. As mentioned above, the choroid-pigment epithelial-photoreceptor complex may be disturbed in acute ROP. The retinal pigment epithelium, which is thought to play a role in the control of eye growth (Rymer and Wildsoet, 2005), may be critical in the regulation of the growth and refractive development of the ROP eye. Explicit hypotheses will be developed and tested using cellular and molecular biological techniques in animal models of ROP. As has been our approach to studies of normal development, following the animal work, streamlined hypotheses and efficient, non-invasive tests can then be devised to evaluate ROP children.

4.3. Therapeutic targets

Even in our current state of knowledge, it is clear that both photoreceptor and post-receptor retina are involved in the ROP disease process. Both are potential targets for intervention.

Persistent rod dysfunction is documented in human ROP subjects (Section 2). Structure and function of ROP rat rods are altered acutely and chronically (Section 3). ROP has its onset at the ages during which the developing rod outer segments elongate with consequent escalation of energy demands. Early ROP rat rod dysfunction predicts the severity of the retinal vascular outcome. Thus, interventions that target the rods are strongly motivated. Theoretically, interventions that support either the metabolic and nutritional needs of the immature rods or protect those rods from injurious exposures, or both, would reduce the neurovascular abnormalities of ROP. The photoreceptor's turnover of outer segment material, maintenance of the circulating current, and operation of the visual cycle demand a level of energy use that exceeds that of any other cell in the body (Steinberg, 1987). This extreme metabolic demand makes the photoreceptor vulnerable to injury. Interventions that could be safely administered very early in the clinical course of ROP, such as at the first detected sign of neurovascular disease, should be the most beneficial.

Light exposure modulates the turnover of outer segment material and suppresses the rods' circulating current and, accordingly, decreases the photoreceptor's energy requirement. Arden et al. (2005) have proposed light as a safe, effective treatment for ROP. Light level of the habitat in which infant rats are reared affects long term the ERG photoresponse parameters in both normal control and ROP rats (Fulton et al., 1998a, b). Thus, a pre-clinical test of the Arden hypothesis is feasible. Following a longitudinal design, with outcome measures being ERG receptor and post-receptor components and integrated curvature of the retinal arterioles, it can be determined if moderate, non-damaging light levels, rather than very dim light, improve the neurovascular outcome in rat models of ROP. For success, such a strategy must consider rod

photoreceptor development (Fig. 1), which was not necessarily the case in a clinical study of effects of light on ROP (Reynolds et al., 1998).

Control of ambient oxygen may be hypothesized to damp hyperoxia-hypoxia swings that damage the rods and to supply, via the choroid, optimal oxygen levels to cope with the rods' energy demands. Tight regulation of supplemental oxygen has reduced the frequency and severity of ROP in some studies. (Askie et al., 2003; Chow et al., 2003; Saugstad, 2006; Vanderveen et al., 2006b). Interestingly, Sears and colleagues reported lower oxygen saturation targets at less than 34 weeks (85% to 92%) and higher targets at greater than 34 weeks (92% to 97%) decrease the severity and incidence of ROP (Sears et al., 2009). Although the age for shift in oxygen management was not based on the rhodopsin growth curve, it appears well chosen (Fig. 1).

Based on this evidence, one can argue that extensions of current practice to evidence-based standardization of light and oxygen interventions, plus vigorous screening programs, are the components of a practicable, global program that will relegate ROP to the history books. However, to date, adjustments in light and oxygen and faithful adherence to screening and treatment guidelines do not prevent clinical ROP or residual visual deficits that occur even when ROP has been mild. Thus, consideration of additional approaches is warranted. We theorize that improved management, or better yet, prevention of ROP, may be achieved through timely pharmaceutical interventions.

Goals of pharmaceutical treatment of ROP rods include suppression of turnover of outer segment material and support of the circulating current. By following this line of reasoning, many possible pharmaceutical agents may hold realistic promise for treatments of ROP. A few are mentioned below.

Members of the family of carbonic anhydrase inhibitors (CAI) suppress conversion of carbon dioxide to bicarbonate and are commonly used to treat glaucoma by decreasing production of aqueous humor. CAIs, such as acetazolamide that is administered systemically, also alter circulating current of the rods (Donner et al., 1990; Findl et al., 1995). In a pilot study on mature rats, a topically administered CAI, dorzolamide (Trusopt, Merck), doubled the saturated amplitude of the rod photoresponse, R_{ROD}, derived from the ERG a-wave (Chang et al., 1997). Thus, dorzolamide is forecast to relieve the immature photoreceptor from one of its most energy demanding tasks (generation of the circulating current) and to reduce injury to the photoreceptor and hypoxia in the post-receptor ROP retina. We also note in our recent ROP rat experiments (Section 3), a visual cycle modulator that at early ages increased the saturated amplitude of the rod photoresponse (R_{ROD}) improved both rod sensitivity (S_{ROD}) and integrated curvature (IC_A) of the arterioles at older ages (Akula et al., 2008a).

Another likely mechanism of injury to the rod includes generation of reactive oxygen species, or free radicals. Oxidative stress increases the production of reactive oxygen species that can damage intracellular lipids, proteins, and DNA, including mtDNA (Corral-Debrinski et al., 1991; Cadenas and Davies, 2000). In the retina, 90% of the mitochondria are in the photoreceptor inner segments. Damage to mitochondria reduces their ability to produce cellular energy, which exacerbates oxidative stress and eventually activates the apoptotic cascade. Activation of the apoptotic cascade leads to death of photoreceptors in retinal degenerative disorders (Delyfer et al., 2004). Because antioxidants scavenge free radicals, shrewdly compounded antioxidants administered in a timely fashion to at-risk infants may protect the mitochondria and the rod itself from oxidative damage (Penn et al., 1997; Liu and Ames, 2005; Dorfman et al., 2006; Ates et al., 2009) and thus prevent initiation of the apoptotic pathway and attendant cell damage. Although this intervention targets the photoreceptor with

abundant mitochondria, it is also anticipated to reduce expression of VEGF and have beneficial effects on post-receptor neural retina and the retinal vasculature.

In addition to the secondary benefits that may arise from treatments targeting the photoreceptors, interventions that target primarily the retinal vasculature and post-receptor neurons, which are intimately associated, both in normal development and in ROP, also warrant consideration for treatment of ROP (Akula et al., 2008b). VEGF is critical to angiogenesis and neurogenesis (Provis et al., 1997; Sandercoe et al., 2003; Gariano et al., 2006). Thus, lowering VEGF is touted as a promising treatment for neovascular diseases of the retina. It is tempting to inhibit the actions of VEGF as early as possible, thereby preventing the occurrence of ROP altogether (Gariano et al., 2006). However, timing such treatment of the developing retina poses a number of concerns because neural dysfunction (receptor and post-receptor) antedates the vascular abnormalities and survives their resolution. Thus, it seems unlikely that anti-VEGF treatment holds much hope of restoring good vision to patients with milder forms of ROP (Fulton et al., 2009). In the mature retina, VEGF is a survival factor for many retinal cells including the photoreceptors (Saint-Geniez et al., 2008). Considerable concern about treatment of ROP with anti-VEGF pharmaceuticals has already been expressed due to the potential for adverse effects on developing neurons and possible adverse system effects in the growing child (Aiello, 1997; Yourey et al., 2000; Hashimoto et al., 2006).

5. Summary

The retina offers an accessible tissue for studies of neurovascular disease in the developing visual system. Our systems approach considers physically and temporally congruent neural and vascular components and demonstrates quantitative neurovascular relationships. Through a combination of non-invasive and molecular biological techniques, fundamental ROP disease processes are delineated in rat models. The information so gained is then translated to the human condition using efficient but rigorous non-invasive procedures. We anticipate that further development of this strategy will lead to new knowledge about neurovascular disease in general and the determinants of ROP eye growth and vision in particular. This will lead to improved outcomes for all children at risk for ROP.

Acknowledgments

This work was supported by grants from the National Eye Institute (EY10597), the Massachusetts Lions Eye Research Fund, the March of Dimes Birth Defects Foundation, the Pearle Vision Foundation, the William Randolph Hearst Foundation, Knights Templar, and Fight for Sight. The authors gratefully acknowledge past and present research fellows, students, and assistants. We especially thank Susie Eklund for thorough and astute critique of this paper.

References

Aguilar M, Stiles WS. Saturation of the rod mechanism of the retina at high levels of stimulation. Optica Acta 1954;1:59–65.

Aiello LP. Vascular endothelial growth factor and the eye: biochemical mechanisms of action and implications for novel therapies. Ophthalmic Res 1997;29:354–362. [PubMed: 9323726]

Akula JD, Hansen RM, Martinez-Perez ME, Fulton AB. Rod photoreceptor function predicts blood vessel abnormality in retinopathy of prematurity. Invest Ophthalmol Vis Sci 2007a;48:4351–4359. [PubMed: 17724227]

Akula JD, Mocko JA, Moskowitz A, Hansen RM, Fulton AB. The oscillatory potentials of the dark-adapted electroretinogram in retinopathy of prematurity. Invest Ophthalmol Vis Sci 2007b;48:5788–5797. [PubMed: 18055833]

Akula JD, Kutoba R, Hansen RM, Tzekov R, McGee D, Fulton AB. Effects of a vitamin-A derivative (AG-787-14-2) on retinal function in oxygen-induced retinopathy. Investigative Ophthalmology and Visual Science 2008a;49ARVO E-Abstract 2629

Akula JD, Mocko JA, Benador IY, Hansen RM, Favazza TL, Vyhovsky TC, Fulton AB. The neurovascular relation in oxygen-induced retinopathy. Mol Vis 2008b;14:2499–2508. [PubMed: 19112532]

Aleman TS, LaVail MM, Montemayor R, Ying G, Maguire MM, Laties AM, Jacobson SG, Cideciyan AV. Augmented rod bipolar cell function in partial receptor loss: an ERG study in P23H rhodopsin transgenic and aging normal rats. Vision Res 2001;41:2779–2797. [PubMed: 11587727]

Alpern M, Fulton AB, Baker BN. “Self-screening” of rhodopsin in rod outer segments. Vision Res 1987;27:1459–1470. [PubMed: 3445480]

Amato MA, Boy S, Arnault E, Girard M, Della Puppa A, Sharif A, Perron M. Comparison of the expression patterns of five neural RNA binding proteins in the Xenopus retina. J Comp Neurol 2005;481:331–339. [PubMed: 15593335]

Arden GB, Sidman RL, Arap W, Schlingemann RO. Spare the rod and spoil the eye. Br J Ophthalmol 2005;89:764–769. [PubMed: 15923516]

Askie LM, Henderson-Smart DJ, Irwig L, Simpson JM. Oxygen-saturation targets and outcomes in extremely preterm infants. N Engl J Med 2003;349:959–967. [PubMed: 12954744]

Ates O, Alp HH, Caner I, Yildirim A, Tastekin A, Kocer I, Baykal O. Oxidative DNA damage in retinopathy of prematurity. Eur J Ophthalmol 2009;19:80–85. [PubMed: 19123153]

Atkinson J, Braddick O, French J. Infant astigmatism: its disappearance with age. Vision Res 1980;20:891–893. [PubMed: 7210516]

Baker PS, Tasman W. Myopia in adults with retinopathy of prematurity. Am J Ophthalmol 2008;145:1090–1094. [PubMed: 18374298]

Barlow, HB. Dark and light adaptation. In: Jameson, D.; Hurvich, LM., editors. Visual psychophysics. Vol. VII. Springer Verlag; New York: 1972. p. 1-27.

Barnaby AM, Hansen RM, Moskowitz A, Fulton AB. Development of scotopic visual thresholds in retinopathy of prematurity. Invest Ophthalmol Vis Sci 2007;48:4854–4860. [PubMed: 17898313]

Bearse MA Jr, Adams AJ, Han Y, Schneck ME, Ng J, Bronson-Castain K, Barez S. A multifocal electroretinogram model predicting the development of diabetic retinopathy. Prog Retin Eye Res 2006;25:425–448. [PubMed: 16949855]

Bielenberg DR, Pettaway CA, Takashima S, Klagsbrun M. Neuropilins in neoplasms: expression, regulation, and function. Exp Cell Res 2006;312:584–593. [PubMed: 16445911]

Birch DG, Hood DC, Nusinowitz S, Pepperberg DR. Abnormal activation and inactivation mechanisms of rod transduction in patients with autosomal dominant retinitis pigmentosa and the pro-23-his mutation. Invest Ophthalmol Vis Sci 1995;36:1603–1614. [PubMed: 7601641]

Birch EE, Spencer R. Visual outcome in infants with cicatricial retinopathy of prematurity. Invest Ophthalmol Vis Sci 1991;32:410–415. [PubMed: 1993593]

Bonting SL, Caravaggio LL, Gouras P. The rhodopsin cycle in the developing vertebrate retina. I. Relation of rhodopsin content, electroretinogram and rod structure in the rat. Exp Eye Res 1961;1:14–24. [PubMed: 13871106]

Bowmaker JK, Dartnall HJ. Visual pigments of rods and cones in a human retina. J Physiol 1980;298:501–511. [PubMed: 7359434]

Bremer DL, Palmer EA, Fellows RR, Baker JD, Hardy RJ, Tung B, Rogers GL. Strabismus in premature infants in the first year of life. Cryotherapy for Retinopathy of Prematurity Cooperative Group. Arch Ophthalmol 1998;116:329–333. [PubMed: 9514486]

Broekhuyse RM, Kuhlmann ED. Assay of S-antigen immunoreactivity in mammalian retinas in relation to age, ocular dimension and retinal degeneration. Jpn J Ophthalmol 1989;33:243–250. [PubMed: 2761118]

Bron, AJ.; Tripathi, RC.; Tripathi, BJ. Wolff's Anatomy of the Eye and Orbit. Vol. 8th. Chapman & Hall; London: 1997. The eyeball and its dimensions; p. 211-232.

Brown AM. Scotopic sensitivity of the two-month-old human infant. Vision Res 1986;26:707–710. [PubMed: 3750850]

Brown AM, Dobson V, Maier J. Visual acuity of human infants at scotopic, mesopic and photopic luminances. Vision Res 1987;27:1845–1858. [PubMed: 3445474]

Brown KT. The electroretinogram: its components and their origins. Vision Res 1968;8:633–677. [PubMed: 4978009]

Cadenas E, Davies KJ. Mitochondrial free radical generation, oxidative stress, and aging. Free Radic Biol Med 2000;29:222–230. [PubMed: 11035250]

Calkins DJ, Schein SJ, Tsukamoto Y, Sterling P. M and L cones in macaque fovea connect to midget ganglion cells by different numbers of excitatory synapses. Nature 1994;371:70–72. [PubMed: 8072528]

Candy TR, Crowell JA, Banks MS. Optical, receptoral, and retinal constraints on foveal and peripheral vision in the human neonate. Vision Res 1998;38:3857–3870. [PubMed: 10211379]

Chan TL, Martin PR, Clunas N, Grunert U. Bipolar cell diversity in the primate retina: morphologic and immunocytochemical analysis of a new world monkey, the marmoset Callithrix jacchus. J Comp Neurol 2001;437:219–239. [PubMed: 11494253]

Chang J, Fulton AB, Hansen RM. The effects of dorzolamide on the rod photoreceptors. Investigative Ophthalmology and Visual Science 1997;38ARVO abstract #2864

Choi MY, Park IK, Yu YS. Long term refractive outcome in eyes of preterm infants with and without retinopathy of prematurity: comparison of keratometric value, axial length, anterior chamber depth, and lens thickness. Br J Ophthalmol 2000;84:138–143. [PubMed: 10655187]

Chow LC, Wright KW, Sola A. Can changes in clinical practice decrease the incidence of severe retinopathy of prematurity in very low birth weight infants? Pediatrics 2003;111:339–345. [PubMed: 12563061]

Clavadetscher JE, Brown AM, Ankrum C, Teller DY. Spectral sensitivity and chromatic discriminations in 3- and 7-week-old human infants. J Opt Soc Am A 1988;5:2093–2105. [PubMed: 3230478]

Colombaioni L, Strettoi E. Appearance of cGMP-phosphodiesterase immunoreactivity parallels the morphological differentiation of photoreceptor outer segments in the rat retina. Vis Neurosci 1993;10:395–402. [PubMed: 8388244]

Cook A, White S, Batterbury M, Clark D. Ocular growth and refractive error development in premature infants without retinopathy of prematurity. Invest Ophthalmol Vis Sci 2003;44:953–960. [PubMed: 12601014]

Cook A, White S, Batterbury M, Clark D. Ocular growth and refractive error development in premature infants with or without retinopathy of prematurity. Invest Ophthalmol Vis Sci 2008;49:5199–5207. [PubMed: 19036998]

Corral-Debrinski M, Stepien G, Shoffner JM, Lott MT, Kanter K, Wallace DC. Hypoxemia is associated with mitochondrial DNA damage and gene induction. Implications for cardiac disease. Jama 1991;266:1812–1816. [PubMed: 1890710]

Cryotherapy for Retinopathy of Prematurity Cooperative Group. Multicenter trial of cryotherapy for retinopathy of prematurity. Preliminary results. Arch Ophthalmol 1988;106:471–479. [PubMed: 2895630]

Cryotherapy for Retinopathy of Prematurity Cooperative Group. Effect of retinal ablative therapy for threshold retinopathy of prematurity: results of Goldmann perimetry at the age of 10 years. Arch Ophthalmol 2001;119:1120–1125. [PubMed: 11483077]

Cunningham S, Fleck BW, Elton RA, McIntosh N. Transcutaneous oxygen levels in retinopathy of prematurity. Lancet 1995;346:1464–1465. [PubMed: 7490994]

Davitt BV, Dobson V, Good WV, Hardy RJ, Quinn GE, Siatkowski RM, Summers CG, Tung B. Prevalence of myopia at 9 months in infants with high-risk prethreshold retinopathy of prematurity. Ophthalmology 2005;112:1564–1568. [PubMed: 16023214]

de Winter F, Cui Q, Symons N, Verhaagen J, Harvey AR. Expression of class-3 semaphorins and their receptors in the neonatal and adult rat retina. Invest Ophthalmol Vis Sci 2004;45:4554–4562. [PubMed: 15557467]

Delyfer MN, Leveillard T, Mohand-Said S, Hicks D, Picaud S, Sahel JA. Inherited retinal degenerations: therapeutic prospects. Biol Cell 2004;96:261–269. [PubMed: 15145530]

Dembinska O, Rojas LM, Varma DR, Chemtob S, Lachapelle P. Graded contribution of retinal maturation to the development of oxygen-induced retinopathy in rats. Invest Ophthalmol Vis Sci 2001;42:1111–1118. [PubMed: 11274093]

Dobson V, Fulton AB, Manning K, Salem D, Petersen RA. Cycloplegic refractions of premature infants. Am J Ophthalmol 1981;91:490–495. [PubMed: 7223822]

Dobson V, Quinn GE, Summers CG, Saunders RA, Phelps DL, Tung B, Palmer EA. Effect of acute-phase retinopathy of prematurity on grating acuity development in the very low birth weight infant. The Cryotherapy for Retinopathy of Prematurity Cooperative Group. Invest Ophthalmol Vis Sci 1994;35:4236–4244. [PubMed: 8002243]

Dodge J, Fulton AB, Parker C, Hansen RM, Williams TP. Rhodopsin in immature rod outer segments. Invest Ophthalmol Vis Sci 1996;37:1951–1956. [PubMed: 8814134]

Dong CJ, Agey P, Hare WA. Origins of the electroretinogram oscillatory potentials in the rabbit retina. Vis Neurosci 2004;21:533–543. [PubMed: 15579219]

Donner K, Hemila S, Kalamkarov G, Koskelainen A, Shevchenko T. Rod phototransduction modulated by bicarbonate in the frog retina: roles of carbonic anhydrase and bicarbonate exchange. J Physiol 1990;426:297–316. [PubMed: 2172515]

Dorey CK, Aouididi S, Reynaud X, Dvorak HF, Brown LF. Correlation of vascular permeability factor/vascular endothelial growth factor with extraretinal neovascularization in the rat. Arch Ophthalmol 1996;114:1210–1217. [PubMed: 8859080]

Dorfman AL, Dembinska O, Chemtob S, Lachapelle P. Structural and functional consequences of trolox C treatment in the rat model of postnatal hyperoxia. Invest Ophthalmol Vis Sci 2006;47:1101–1108. [PubMed: 16505047]

Dorn EM, Hendrickson L, Hendrickson AE. The appearance of rod opsin during monkey retinal development. Invest Ophthalmol Vis Sci 1995;36:2634–2651. [PubMed: 7499086]

Downie LE, Pianta MJ, Vingrys AJ, Wilkinson-Berka JL, Fletcher EL. Neuronal and glial cell changes are determined by retinal vascularization in retinopathy of prematurity. J Comp Neurol 2007;504:404–417. [PubMed: 17663451]

Early Treatment for Retinopathy of Prematurity Cooperative Group. Revised indications for the treatment of retinopathy of prematurity: results of the early treatment for retinopathy of prematurity randomized trial. Arch Ophthalmol 2003;121:1684–1694. [PubMed: 14662586]

Ecsedy M, Szamosi A, Karko C, Zubovics L, Varsanyi B, Nemeth J, Recsan Z. A comparison of macular structure imaged by optical coherence tomography in preterm and full-term children. Invest Ophthalmol Vis Sci 2007;48:5207–5211. [PubMed: 17962475]

Favazza T, Benador IY, Mocko JA, Vyhovsky TC, Hansen RM, Fulton AB, Akula JD. Anatomic and histologic features in rat models of retinopathy of prematurity (ROP). Investigative Ophthalmology and Visual Science 2009;50ARVO E-Abstract 3125

Fielder AR, Levene MI, Russell-Eggitt IM, Weale RA. Temperature--a factor in ocular development? Dev Med Child Neurol 1986;28:279–284. [PubMed: 3721069]

Fielder AR, Quinn GE. Myopia of prematurity: nature, nurture, or disease? Br J Ophthalmol 1997;81:2–3. [PubMed: 9135397]

Findl O, Hansen RM, Fulton AB. The effects of acetazolamide on the electroretinographic responses in rats. Invest Ophthalmol Vis Sci 1995;36:1019–1026. [PubMed: 7730011]

Fledelius HC. Prematurity and the eye. Ophthalmic 10-year follow-up of children of low and normal birth weight. Acta Ophthalmol Suppl 1976;128:3–245. [PubMed: 183455]

Fledelius HC. Ophthalmic changes from age of 10 to 18 years. A longitudinal study of sequels to low birth weight. II. Visual acuity. Acta Ophthalmol (Copenh) 1981;59:64–70. [PubMed: 7211284]

Fledelius HC. Inhibited growth and development as permanent features of low birth weight. A longitudinal study of eye size, height, head circumference, interpupillary distance and exophthalmometry, as measured at age of 10 and 18 years. Acta Paediatr Scand 1982a;71:645–650. [PubMed: 7136682]

Fledelius HC. Ophthalmic changes from age of 10 to 18 years. A longitudinal study of sequels to low birth weight. III. Ultrasound oculometry and keratometry of anterior eye segment. Acta Ophthalmol (Copenh) 1982b;60:393–402. [PubMed: 7136551]

Fledelius HC. Pre-term delivery and the growth of the eye. An oculometric study of eye size around term-time. Acta Ophthalmol Suppl 1992:10–15. [PubMed: 1332382]

Fledelius HC. Pre-term delivery and subsequent ocular development. A 7-10 year follow-up of children screened 1982-84 for ROP. 3) Refraction. Myopia of prematurity. Acta Ophthalmol Scand 1996a; 74:297–300. [PubMed: 8828731]

Fledelius HC. Pre-term delivery and subsequent ocular development. A 7-10 year follow-up of children screened 1982-84 for ROP. 4) Oculometric - and other metric considerations. Acta Ophthalmol Scand 1996b;74:301–305. [PubMed: 8828732]

Fletcher MC, Brandon S. Myopia of prematurity. Am J Ophthalmol 1955;40:474–481. [PubMed: 13258727]

Fox DA, Rubinstein SD. Age-related changes in retinal sensitivity, rhodopsin content and rod outer segment length in hooded rats following low-level lead exposure during development. Exp Eye Res 1989;48:237–249. [PubMed: 2924811]

Friedburg C, Thomas MM, Lamb TD. Time course of the flash response of dark- and light-adapted human rod photoreceptors derived from the electroretinogram. J Physiol 2001;534:217–242. [PubMed: 11433004]

Friedburg C, Allen CP, Mason PJ, Lamb TD. Contribution of cone photoreceptors and post-receptoral mechanisms to the human photopic electroretinogram. J Physiol 2004;556:819–834. [PubMed: 14990682]

Friedmann L, Biedner B, David R, Sachs U. Screening for refractive errors, strabismus and other ocular anomalies from ages 6 months to 3 years. J Pediatr Ophthalmol Strabismus 1980;17:315–317. [PubMed: 7441442]

Fulton AB, Rushton WA. The human rod ERG: correlation with psychophysical responses in light and dark adaptation. Vision Res 1978;18:793–800. [PubMed: 676087]

Fulton AB, Dobson V, Salem D, Mar C, Petersen RA, Hansen RM. Cycloplegic refractions in infants and young children. Am J Ophthalmol 1980;90:239–247. [PubMed: 7425037]

Fulton AB, Dodge J, Hansen RM, Schremser JL, Williams TP. The quantity of rhodopsin in young human eyes. Curr Eye Res 1991a;10:977–982. [PubMed: 1959384]

Fulton AB, Hansen RM, Yeh YL, Tyler CW. Temporal summation in dark-adapted 10-week old infants. Vision Res 1991b;31:1259–1269. [PubMed: 1891817]

Fulton AB, Hansen RM, Findl O. The development of the rod photoresponse from dark-adapted rats. Invest Ophthalmol Vis Sci 1995;36:1038–1045. [PubMed: 7730013]

Fulton AB, Hansen RM. Photoreceptor function in infants and children with a history of mild retinopathy of prematurity. J Opt Soc Am A Opt Image Sci Vis 1996;13:566–571. [PubMed: 8627413]

Fulton, AB.; Hansen, RM.; Dorn, E.; Hendrickson, AE. Development of primate rod structure and function. In: Vital-Durand, F.; Atkinson, J.; Braddick, O., editors. Infant Vision. Oxford University Press; Oxford, UK: 1996. p. 33-49.

Fulton, AB.; Hansen, RM.; Dodge, J.; Williams, TP. Photoreceptor development and photostasis. In: Williams, TP.; Thistle, A., editors. Photostasis and Related Phenomena. Plenum Press; New York: 1998a. p. 189-198.

Fulton AB, Hansen RM, Roberto K, Penn JS. Persistent retinal dysfunction in a rat model of ROP. Investigative Ophthalmology and Visual Science 1998b;39ARVO Abstract #3799

Fulton AB, Dodge J, Hansen RM, Williams TP. The rhodopsin content of human eyes. Invest Ophthalmol Vis Sci 1999a;40:1878–1883. [PubMed: 10393065]

Fulton AB, Reynaud X, Hansen RM, Lemere CA, Parker C, Williams TP. Rod photoreceptors in infant rats with a history of oxygen exposure. Invest Ophthalmol Vis Sci 1999b;40:168–174. [PubMed: 9888440]

Fulton AB, Hansen RM. The development of scotopic sensitivity. Invest Ophthalmol Vis Sci 2000;41:1588–1596. [PubMed: 10798680]

Fulton AB, Hansen RM, Petersen RA, Vanderveen DK. The rod photoreceptors in retinopathy of prematurity: an electroretinographic study. Arch Ophthalmol 2001;119:499–505. [PubMed: 11296015]

Fulton AB, Hansen RM. Recovery of the rod photoresponse in infant rats. Vision Res 2003;43:3081–3085. [PubMed: 14611945]

Fulton AB, Hansen RM. Recovery of the rod photoresponse in retinopathy of prematurity (ROP). Investigative Ophthalmology and Visual Science 2004;45ARVO E-Abstract 1353

Fulton AB, Hansen RM, Moskowitz A, Barnaby AM. Multifocal ERG in subjects with a history of retinopathy of prematurity. Doc Ophthalmol 2005;111:7–13. [PubMed: 16502302]

Fulton AB, Hansen R. Rod photoreceptor function in ROP. Mol Vis 2006;12:548–549.

Fulton AB, Hansen RM, Moskowitz A. The cone electroretinogram in retinopathy of prematurity. Invest Ophthalmol Vis Sci 2008;49:814–819. [PubMed: 18235032]

Fulton AB, Akula JD, Mocko JA, Hansen RM, Benador IY, Beck SC, Fahl E, Seeliger MW, Moskowitz A, Harris ME. Retinal degenerative and hypoxic ischemic disease. Doc Ophthalmol 2009;118:55–61. [PubMed: 18483822]

Gallo JE, Holmstrom G, Kugelberg U, Hedquist B, Lennerstrand G. Regressed retinopathy of prematurity and its sequelae in children aged 5-10 years. Br J Ophthalmol 1991;75:527–531. [PubMed: 1911653]

Gallo JE, Lennerstrand G. A population-based study of ocular abnormalities in premature children aged 5 to 10 years. Am J Ophthalmol 1991;111:539–547. [PubMed: 2021159]

Gallo JE, Fagerholm P. Low-grade myopia in children with regressed retinopathy of prematurity. Acta Ophthalmol (Copenh) 1993;71:519–523. [PubMed: 8249585]

Gariano RF, Hu D, Helms J. Expression of angiogenesis-related genes during retinal development. Gene Expr Patterns 2006;6:187–192. [PubMed: 16330258]

Gelman R, Martinez-Perez ME, Vanderveen DK, Moskowitz A, Fulton AB. Diagnosis of plus disease in retinopathy of prematurity using Retinal Image multiScale Analysis. Invest Ophthalmol Vis Sci 2005;46:4734–4738. [PubMed: 16303973]

Gilbert C. Retinopathy of prematurity: a global perspective of the epidemics, population of babies at risk and implications for control. Early Hum Dev 2008;84:77–82. [PubMed: 18234457]

Gogat K, Le Gat L, Van Den Berghe L, Marchant D, Kobetz A, Gadin S, Gasser B, Quere I, Abitbol M, Menasche M. VEGF and KDR gene expression during human embryonic and fetal eye development. Invest Ophthalmol Vis Sci 2004;45:7–14. [PubMed: 14691147]

Gordon RA, Donzis PB. Myopia associated with retinopathy of prematurity. Ophthalmology 1986;93:1593–1598. [PubMed: 3808618]

Graham PA. Epidemiology of strabismus. Br J Ophthalmol 1974;58:224–231. [PubMed: 4834596]

Grun G. The development of the vertebrate retina: a comparative survey. Adv Anat Embryol Cell Biol 1982;78:1–85. [PubMed: 7158472]

Hamer RD, Schneck ME. Spatial summation in dark-adapted human infants. Vision Res 1984;24:77–85. [PubMed: 6695510]

Hammer DX, Iftimia NV, Ferguson RD, Bigelow CE, Ustun TE, Barnaby AM, Fulton AB. Foveal fine structure in retinopathy of prematurity: an adaptive optics Fourier domain optical coherence tomography study. Invest Ophthalmol Vis Sci 2008;49:2061–2070. [PubMed: 18223243]

Hammer DX, Mujat M, Ferguson RD, Iftimia NV, Harris ME, Eklund SE, Fulton AB. Retinopathy of prematurity (ROP) imaged with adaptive optics scanning laser ophthalmoscopy. Investigative Ophthalmology and Visual Science 2009;50ARVO E-Abstract 3152

Hancock HA, Kraft TW. Oscillatory potential analysis and ERGs of normal and diabetic rats. Invest Ophthalmol Vis Sci 2004;45:1002–1008. [PubMed: 14985323]

Hansen RM, Fulton AB. Behavioral measurement of background adaptation in infants. Invest Ophthalmol Vis Sci 1981;21:625–629. [PubMed: 7287353]

Hansen RM, Fulton AB, Harris SJ. Background adaptation in human infants. Vision Res 1986;26:771–779. [PubMed: 3750858]

Hansen RM, Fulton AB. Psychophysical estimates of ocular media density of human infants. Vision Res 1989;29:687–690. [PubMed: 2626826]

Hansen RM, Fulton AB. Electroretinographic assessment of background adaptation in 10-week-old human infants. Vision Res 1991;31:1501–1507. [PubMed: 1949619]

Hansen RM, Hamer RD, Fulton AB. The effect of light adaptation on scotopic spatial summation in 10-week-old infants. Vision Res 1992;32:387–392. [PubMed: 1574853]

Hansen, RM.; Fulton, AB. Development of scotopic retinal sensitivity. In: Simons, K., editor. Early visual development, normal and abnormal. Oxford University Press; New York: 1993. p. 130-142.

Hansen RM, Fulton AB. Scotopic center surround organization in 10-week-old infants. Vision Res 1994;34:621–624. [PubMed: 8160381]

Hansen RM, Fulton AB. Dark-adapted thresholds at 10- and 30-deg eccentricities in 10-week-old infants. Vis Neurosci 1995;12:509–512. [PubMed: 7654607]

Hansen RM, Fulton AB. The course of maturation of rod-mediated visual thresholds in infants. Invest Ophthalmol Vis Sci 1999;40:1883–1886. [PubMed: 10393066]

Hansen RM, Fulton AB. Rod-mediated increment threshold functions in infants. Invest Ophthalmol Vis Sci 2000a;41:4347–4352. [PubMed: 11095637]

Hansen RM, Fulton AB. Background adaptation in children with a history of mild retinopathy of prematurity. Invest Ophthalmol Vis Sci 2000b;41:320–324. [PubMed: 10634637]

Hansen RM, Fulton AB. Development of the cone ERG in infants. Invest Ophthalmol Vis Sci 2005a; 46:3458–3462. [PubMed: 16123452]

Hansen RM, Fulton AB. Recovery of the rod photoresponse in infants. Invest Ophthalmol Vis Sci 2005b; 46:764–768. [PubMed: 15671311]

Hansen RM, Eklund SE, Benador IY, Mocko JA, Akula JD, Liu Y, Martinez-Perez ME, Fulton AB. Retinal degeneration in children: dark adapted visual threshold and arteriolar diameter. Vision Res 2008;48:325–331. [PubMed: 17765282]

Hansen RM, Moskowitz A, Fulton AB. Multifocal ERG responses in infants. Invest Ophthalmol Vis Sci 2009;50:470–475. [PubMed: 18719077]

Hardy RJ, Good WV, Dobson V, Palmer EA, Phelps DL, Quintos M, Tung B. Multicenter trial of early treatment for retinopathy of prematurity: study design. Control Clin Trials 2004;25:311–325. [PubMed: 15157731]

Harris ME, Hansen RM, Moskowitz A, Fulton AB. Long term effects of retinopathy of prematurity (ROP) on rod and rod-driven function. Investigative Ophthalmology and Visual Science 2009;50ARVO E-Abstract 5310

Hashimoto T, Zhang XM, Chen BY, Yang XJ. VEGF activates divergent intracellular signaling components to regulate retinal progenitor cell proliferation and neuronal differentiation. Development 2006;133:2201–2210. [PubMed: 16672338]

He Z, Wang KC, Koprivica V, Ming G, Song HJ. Knowing how to navigate: mechanisms of semaphorin signaling in the nervous system. Sci STKE 2002;2002:RE1. [PubMed: 11842242]

Hendrickson AE, Yuodelis C. The morphological development of the human fovea. Ophthalmology 1984;91:603–612. [PubMed: 6462623]

Hendrickson AE, Drucker D. The development of parafoveal and mid-peripheral human retina. Behav Brain Res 1992;49:21–31. [PubMed: 1388798]

Hendrickson, AE. The morphologic development of human and monkey retina. In: Albert, DM.; Jakobiec, FA., editors. Principles and Practice of Ophthalmology: Basic Sciences. WB Saunders; Philadelphia: 1994. p. 561-577.

Heynen H, Wachtmeister L, van Norren D. Origin of the oscillatory potentials in the primate retina. Vision Res 1985;25:1365–1373. [PubMed: 4090272]

Ho AK, Somers RL, Klein DC. Development and regulation of rhodopsin kinase in rat pineal and retina. J Neurochem 1986;46:1176–1179. [PubMed: 3950623]

Holmstrom G, el Azazi M, Kugelberg U. Ophthalmological follow up of preterm infants: a population based, prospective study of visual acuity and strabismus. Br J Ophthalmol 1999;83:143–150. [PubMed: 10396188]

Holmstrom G, Larsson EK. Development of spherical equivalent refraction in prematurely born children during the first 10 years of life: a population-based study. Arch Ophthalmol 2005;123:1404–1411. [PubMed: 16219732]

Holmstrom G, Rydberg A, Larsson E. Prevalence and development of strabismus in 10-year-old premature children: a population-based study. J Pediatr Ophthalmol Strabismus 2006;43:346–352. [PubMed: 17162971]

Holmstrom M, el Azazi M, Kugelberg U. Ophthalmological long-term follow up of preterm infants: a population based, prospective study of the refraction and its development. Br J Ophthalmol 1998;82:1265–1271. [PubMed: 9924330]

Hood, DC.; Finkelstein, MA. Sensitivity to light. In: Boff, KR.; Kaufman, L.; Thomas, J., editors. Handbook of perception, vol 1, sensory processes and perception. Wiley; New York: 1986. p. 5-16.p. 15-22.

Hood DC, Greenstein V. Models of the normal and abnormal rod system. Vision Res 1990;30:51–68. [PubMed: 2321366]

Hood DC, Birch DG. Human cone receptor activity: the leading edge of the a-wave and models of receptor activity. Vis Neurosci 1993;10:857–871. [PubMed: 8217936]

Hood DC, Birch DG. Rod phototransduction in retinitis pigmentosa: estimation and interpretation of parameters derived from the rod a-wave. Invest Ophthalmol Vis Sci 1994;35:2948–2961. [PubMed: 8206712]

Hood DC, Birch DG. Phototransduction in human cones measured using the alpha-wave of the ERG. Vision Res 1995;35:2801–2810. [PubMed: 8533321]

Hood DC. Assessing retinal function with the multifocal technique. Prog Retin Eye Res 2000;19:607–646. [PubMed: 10925245]

Hood DC, Frishman LJ, Saszik S, Viswanathan S. Retinal origins of the primate multifocal ERG: implications for the human response. Invest Ophthalmol Vis Sci 2002;43:1673–1685. [PubMed: 11980890]

Howland HC, Sayles N. Photorefractive measurements of astigmatism in infants and young children. Invest Ophthalmol Vis Sci 1984;25:93–102. [PubMed: 6698735]

International Committee for the Classification of Retinopathy of Prematurity. The International Classification of Retinopathy of Prematurity revisited. Arch Ophthalmol 2005;123:991–999. [PubMed: 16009843]

Isenberg SJ. Macular development in the premature infant. Am J Ophthalmol 1986;101:74–80. [PubMed: 3753633]

Jirasek, JE. Anatomy and Staging. New York: Informa Healthcare; 2004. An Atlas of Human Prenatal Developmental Mechanics; p. 298

Johnson PT, Williams RR, Reese BE. Developmental patterns of protein expression in photoreceptors implicate distinct environmental versus cell-intrinsic mechanisms. Vis Neurosci 2001;18:157–168. [PubMed: 11347813]

Jones BW, Watt CB, Frederick JM, Baehr W, Chen CK, Levine EM, Milam AH, Lavail MM, Marc RE. Retinal remodeling triggered by photoreceptor degenerations. J Comp Neurol 2003;464:1–16. [PubMed: 12866125]

Kent D, Pennie F, Laws D, White S, Clark D. The influence of retinopathy of prematurity on ocular growth. Eye 2000;14(Pt 1):23–29. [PubMed: 10755095]

Kim JY, Kwak SI, Yu YS. Myopia in premature infants at the age of 6 months. Korean J Ophthalmol 1992;6:44–49. [PubMed: 1434045]

Kushner BJ. Strabismus and amblyopia associated with regressed retinopathy of prematurity. Arch Ophthalmol 1982;100:256–261. [PubMed: 6895993]

Lachapelle P, Dembinska O, Rojas LM, Benoit J, Almazan G, Chemtob S. Persistent functional and structural retinal anomalies in newborn rats exposed to hyperoxia. Can J Physiol Pharmacol 1999;77:48–55. [PubMed: 10535666]

Lachapelle P, Rufiange M, Dembinska O. A physiological basis for definition of the ISCEV ERG standard flash (SF) based on the photopic hill. Doc Ophthalmol 2001;102:157–162. [PubMed: 11518458]

Lamb TD, Pugh EN Jr. A quantitative account of the activation steps involved in phototransduction in amphibian photoreceptors. J Physiol 1992;449:719–758. [PubMed: 1326052]

Lamb TD, Pugh EN Jr. Phototransduction, dark adaptation, and rhodopsin regeneration the proctor lecture. Invest Ophthalmol Vis Sci 2006;47:5137–5152. [PubMed: 17122096]

Larsen JS. The sagittal growth of the eye. 1. Ultrasonic measurement of the depth of the anterior chamber from birth to puberty. Acta Ophthalmol (Copenh) 1971;49:239–262. [PubMed: 5109787]

Laws D, Shaw DE, Robinson J, Jones HS, Ng YK, Fielder AR. Retinopathy of prematurity: a prospective study. Review at six months. Eye 1992;6(Pt 5):477–483. [PubMed: 1286710]

Laws D, Haslett R, Ashby D, O'Brien C, Clark D. Axial length biometry in infants with retinopathy of prematurity. Eye 1994;8(Pt 4):427–430. [PubMed: 7821466]

Liu J, Ames BN. Reducing mitochondrial decay with mitochondrial nutrients to delay and treat cognitive dysfunction, Alzheimer's disease, and Parkinson's disease. Nutr Neurosci 2005;8:67–89. [PubMed: 16053240]

Liu K, Akula JD, Falk C, Hansen RM, Fulton AB. The retinal vasculature and function of the neural retina in a rat model of retinopathy of prematurity. Invest Ophthalmol Vis Sci 2006a;47:2639–2647. [PubMed: 16723481]

Liu K, Akula JD, Hansen RM, Moskowitz A, Kleinman MS, Fulton AB. Development of the electroretinographic oscillatory potentials in normal and ROP rats. Invest Ophthalmol Vis Sci 2006b;47:5447–5452. [PubMed: 17122135]

Lu M, Hansen RM, Cunningham MJ, Eklund SE, Fulton AB. Effects of desferoxamine on retinal and visual function. Arch Ophthalmol 2007;125:1581–1582. [PubMed: 17998528]

Lue CL, Hansen RM, Reisner DS, Findl O, Petersen RA, Fulton AB. The course of myopia in children with mild retinopathy of prematurity. Vision Res 1995;35:1329–1335. [PubMed: 7610594]

Lyubarsky AL, Pugh EN Jr. Recovery phase of the murine rod photoresponse reconstructed from electroretinographic recordings. J Neurosci 1996;16:563–571. [PubMed: 8551340]

Mactier H, Maroo S, Bradnam M, Hamilton R. Ocular biometry in preterm infants: implications for estimation of retinal illuminance. Invest Ophthalmol Vis Sci 2008;49:453–457. [PubMed: 18172125]

Madan A, Penn JS. Animal models of oxygen-induced retinopathy. Front Biosci 2003;8:d1030–1043. [PubMed: 12700061]

Malcolm CA, Hamilton R, McCulloch DL, Montgomery C, Weaver LT. Scotopic electroretinogram in term infants born of mothers supplemented with docosahexaenoic acid during pregnancy. Invest Ophthalmol Vis Sci 2003;44:3685–3691. [PubMed: 12882824]

Mann, I. The Development of the Human Eye. New York: Grune & Stratton, Inc; 1964.

Martin PR, Grunert U. Analysis of the short wavelength-sensitive (“blue”) cone mosaic in the primate retina: comparison of New World and Old World monkeys. J Comp Neurol 1999;406:1–14. [PubMed: 10100889]

Martinez-Perez ME, Hughes AD, Stanton AV, Thom SA, Chapman N, Bharath AA, Parker KH. Retinal vascular tree morphology: a semi-automatic quantification. IEEE Trans Biomed Eng 2002;49:912–917. [PubMed: 12148830]

Mayer DL, Hansen RM, Moore BD, Kim S, Fulton AB. Cycloplegic refractions in healthy children aged 1 through 48 months. Arch Ophthalmol 2001;119:1625–1628. [PubMed: 11709012]

Mohindra I, Held R, Gwiazda J, Brill J. Astigmatism in infants. Science 1978;202:329–331. [PubMed: 694539]

Moskowitz A, Hansen RM, Fulton AB. Early ametropia and rod photoreceptor function in retinopathy of prematurity. Optom Vis Sci 2005a;82:307–317. [PubMed: 15829858]

Moskowitz A, Hansen RM, Fulton AB. ERG oscillatory potentials in infants. Doc Ophthalmol 2005b; 110:265–270. [PubMed: 16328935]

Mutti DO, Mitchell GL, Jones LA, Friedman NE, Frane SL, Lin WK, Moeschberger ML, Zadnik K. Axial growth and changes in lenticular and corneal power during emmetropization in infants. Invest Ophthalmol Vis Sci 2005;46:3074–3080. [PubMed: 16123404]

Myers VS, Gidlewski N, Quinn GE, Miller D, Dobson V. Distance and near visual acuity, contrast sensitivity, and visual fields of 10-year-old children. Arch Ophthalmol 1999;117:94–99. [PubMed: 9930166]

Nihira M, Anderson K, Gorin FA, Burns MS. Primate rod and cone photoreceptors may differ in glucose accessibility. Invest Ophthalmol Vis Sci 1995;36:1259–1270. [PubMed: 7775103]

Nissenkorn I, Yassur Y, Mashkowski D, Sherf I, Ben-Sira I. Myopia in premature babies with and without retinopathy of prematurity. Br J Ophthalmol 1983;67:170–173. [PubMed: 6687430]

Norren DV, Vos JJ. Spectral transmission of the human ocular media. Vision Res 1974;14:1237–1244. [PubMed: 4428632]

O'Connor AR, Stephenson T, Johnson A, Tobin MJ, Moseley MJ, Ratib S, Ng Y, Fielder AR. Long-term ophthalmic outcome of low birth weight children with and without retinopathy of prematurity. Pediatrics 2002a;109:12–18. [PubMed: 11773536]

O'Connor AR, Stephenson TJ, Johnson A, Tobin MJ, Ratib S, Fielder AR. Strabismus in children of birth weight less than 1701 g. Arch Ophthalmol 2002b;120:767–773. [PubMed: 12049582]

O'Connor AR, Stephenson TJ, Johnson A, Tobin MJ, Ratib S, Moseley M, Fielder AR. Visual function in low birthweight children. Br J Ophthalmol 2004;88:1149–1153. [PubMed: 15317706]

O'Connor AR, Stephenson TJ, Johnson A, Tobin MJ, Ratib S, Fielder AR. Change of refractive state and eye size in children of birth weight less than 1701 g. Br J Ophthalmol 2006a;90:456–460. [PubMed: 16547327]

O'Connor AR, Stewart CE, Singh J, Fielder AR. Do infants of birth weight less than 1500 g require additional long term ophthalmic follow up? Br J Ophthalmol 2006b;90:451–455. [PubMed: 16547326]

Ogden TE. The oscillatory waves of the primate electroretinogram. Vision Res 1973;13:1059–1074. [PubMed: 4197416]

Packer O, Hendrickson AE, Curcio CA. Development redistribution of photoreceptors across the Macaca nemestrina (pigtail macaque) retina. J Comp Neurol 1990;298:472–493. [PubMed: 2229476]

Page JM, Schneeweiss S, Whyte HE, Harvey P. Ocular sequelae in premature infants. Pediatrics 1993;92:787–790. [PubMed: 8233737]

Palmer EA, Flynn JT, Hardy RJ, Phelps DL, Phillips CL, Schaffer DB, Tung B. Incidence and early course of retinopathy of prematurity. The Cryotherapy for Retinopathy of Prematurity Cooperative Group. Ophthalmology 1991;98:1628–1640. [PubMed: 1800923]

Palmer EA, Hardy RJ, Dobson V, Phelps DL, Quinn GE, Summers CG, Krom CP, Tung B. 15-year outcomes following threshold retinopathy of prematurity: final results from the multicenter trial of cryotherapy for retinopathy of prematurity. Arch Ophthalmol 2005;123:311–318. [PubMed: 15767472]

Peachey NS, Alexander KR, Derlacki DJ, Fishman GA. Light adaptation and the luminance-response function of the cone electroretinogram. Doc Ophthalmol 1992;79:363–369. [PubMed: 1633746]

Penn JS, Henry MM, Tolman BL. Exposure to alternating hypoxia and hyperoxia causes severe proliferative retinopathy in the newborn rat. Pediatr Res 1994;36:724–731. [PubMed: 7898981]

Penn JS, Henry MM, Wall PT, Tolman BL. The range of PaO2 variation determines the severity of oxygen-induced retinopathy in newborn rats. Invest Ophthalmol Vis Sci 1995;36:2063–2070. [PubMed: 7657545]

Penn JS, Tolman BL, Bullard LE. Effect of a water-soluble vitamin E analog, trolox C, on retinal vascular development in an animal model of retinopathy of prematurity. Free Radic Biol Med 1997;22:977–984. [PubMed: 9034236]

Penn JS, Madan A, Caldwell RB, Bartoli M, Caldwell RW, Hartnett ME. Vascular endothelial growth factor in eye disease. Prog Retin Eye Res 2008;27:331–371. [PubMed: 18653375]

Pennefather PM, Tin W, Strong NP, Clarke MP, Dutton J, Cottrell DG. Refractive errors in children born before 32 weeks gestation. Eye 1997;11(Pt 5):736–743. [PubMed: 9474329]

Pennefather PM, Clarke MP, Strong NP, Cottrell DG, Dutton J, Tin W. Risk factors for strabismus in children born before 32 weeks' gestation. Br J Ophthalmol 1999;83:514–518. [PubMed: 10216046]

Pepperberg DR, Birch DG, Hofmann KP, Hood DC. Recovery kinetics of human rod phototransduction inferred from the two-branched alpha-wave saturation function. J Opt Soc Am A Opt Image Sci Vis 1996;13:586–600. [PubMed: 8627416]

Perkins GA, Ellisman MH, Fox DA. Three-dimensional analysis of mouse rod and cone mitochondrial cristae architecture: bioenergetic and functional implications. Mol Vis 2003;9:60–73. [PubMed: 12632036]

Pierce EA, Avery RL, Foley ED, Aiello LP, Smith LE. Vascular endothelial growth factor/vascular permeability factor expression in a mouse model of retinal neovascularization. Proc Natl Acad Sci U S A 1995;92:905–909. [PubMed: 7846076]

Pokorny J, Smith VC, Lutze M. Aging of the human lens. Applied Optics 1987;26:1437–1440.

Pott JW, Sprunger DT, Helveston EM. Infantile esotropia in very low birth weight (VLBW) children. Strabismus 1999;7:97–102. [PubMed: 10420214]

Pournaras CJ, Rungger-Brandle E, Riva CE, Hardarson SH, Stefansson E. Regulation of retinal blood flow in health and disease. Prog Retin Eye Res 2008;27:284–330. [PubMed: 18448380]

Powers MK, Schneck M, Teller DY. Spectral sensitivity of human infants at absolute visual threshold. Vision Res 1981;21:1005–1016. [PubMed: 7314480]

Provis JM, Leech J, Diaz CM, Penfold PL, Stone J, Keshet E. Development of the human retinal vasculature: cellular relations and VEGF expression. Exp Eye Res 1997;65:555–568. [PubMed: 9464188]

Provis JM, Sandercoe T, Hendrickson AE. Astrocytes and blood vessels define the foveal rim during primate retinal development. Invest Ophthalmol Vis Sci 2000;41:2827–2836. [PubMed: 10967034]

Provis JM. Development of the primate retinal vasculature. Prog Retin Eye Res 2001;20:799–821. [PubMed: 11587918]

Provis JM, Hendrickson AE. The foveal avascular region of developing human retina. Arch Ophthalmol 2008;126:507–511. [PubMed: 18413520]

Pugh, EN, Jr. Vision: Physical and retinal physiology. In: Atkinson, RC.; Herrnstein, RJ.; Lindzey, G.; Luce, RD., editors. Stevens Handbook of Experimental Psychology, Volume 1, Perception and Motivation. Vol. 2nd. Wiley; New York: 1988. p. 75-163.

Pugh EN Jr, Lamb TD. Amplification and kinetics of the activation steps in phototransduction. Biochim Biophys Acta 1993;1141:111–149. [PubMed: 8382952]

Pugh, EN., Jr; Falsini, B.; Lyubarsky, AL. The origins of the major rod- and cone-driven components of the rodent electroretinogram and the effect of age and light-rearing history on the magnitude of these components. In: Williams, TP.; Thistle, AB., editors. Photostasis and Related Phenomena. Plenum Press; New York: 1998. p. 93-128.

Pugh, EN., Jr; Lamb, TD. Phototransduction in vertebrate rods and cones: Molecular mechanisms of amplification, recovery and light adaptation. In: Stavenga, DG.; de Grip, WJ.; Pugh, EN., Jr, editors. Handbook of biological physics Molecular mechanisms of visual transduction. Vol. 3. Elsevier Science; 2000. p. 183-255.

Quinn GE, Dobson V, Repka MX, Reynolds J, Kivlin J, Davis B, Buckley E, Flynn JT, Palmer EA. Development of myopia in infants with birth weights less than 1251 grams. The Cryotherapy for Retinopathy of Prematurity Cooperative Group. Ophthalmology 1992;99:329–340. [PubMed: 1565444]

Quinn GE, Dobson V, Hardy RJ, Tung B, Phelps DL, Palmer EA. Visual fields measured with double-arc perimetry in eyes with threshold retinopathy of prematurity from the cryotherapy for retinopathy of prematurity trial. The CRYO-Retinopathy of Prematurity Cooperative Group. Ophthalmology 1996;103:1432–1437. [PubMed: 8841302]

Quinn GE, Dobson V, Kivlin J, Kaufman LM, Repka MX, Reynolds JD, Gordon RA, Hardy RJ, Tung B, Stone RA. Prevalence of myopia between 3 months and 5 1/2 years in preterm infants with and without retinopathy of prematurity. Cryotherapy for Retinopathy of Prematurity Cooperative Group. Ophthalmology 1998;105:1292–1300. [PubMed: 9663236]

Quinn GE, Dobson V, Siatkowski R, Hardy RJ, Kivlin J, Palmer EA, Phelps DL, Repka MX, Summers CG, Tung B, Chan W. Does cryotherapy affect refractive error? Results from treated versus control eyes in the cryotherapy for retinopathy of prematurity trial. Ophthalmology 2001;108:343–347. [PubMed: 11158812]

Quinn GE, Dobson V, Davitt BV, Hardy RJ, Tung B, Pedroza C, Good WV. Progression of myopia and high myopia in the early treatment for retinopathy of prematurity study: findings to 3 years of age. Ophthalmology 2008;115:1058–1064. e1051. [PubMed: 18423871]

Rangaswamy NV, Hood DC, Frishman LJ. Regional variations in local contributions to the primate photopic flash ERG: revealed using the slow-sequence mfERG. Invest Ophthalmol Vis Sci 2003;44:3233–3247. [PubMed: 12824276]

Reisner DS, Hansen RM, Findl O, Petersen RA, Fulton AB. Dark-adapted thresholds in children with histories of mild retinopathy of prematurity. Invest Ophthalmol Vis Sci 1997;38:1175–1183. [PubMed: 9152237]

Repka MX, Palmer EA, Tung B. Involution of retinopathy of prematurity. Cryotherapy for Retinopathy of Prematurity Cooperative Group. Arch Ophthalmol 2000;118:645–649. [PubMed: 10815156]

Reynaud X, Dorey CK. Extraretinal neovascularization induced by hypoxic episodes in the neonatal rat. Invest Ophthalmol Vis Sci 1994;35:3169–3177. [PubMed: 8045712]

Reynaud X, Hansen RM, Fulton AB. Effect of prior oxygen exposure on the electroretinographic responses of infant rats. Invest Ophthalmol Vis Sci 1995;36:2071–2079. [PubMed: 7657546]

Reynolds JD, Hardy RJ, Kennedy KA, Spencer R, van Heuven WA, Fielder AR. Lack of efficacy of light reduction in preventing retinopathy of prematurity. Light Reduction in Retinopathy of Prematurity (LIGHT-ROP) Cooperative Group. N Engl J Med 1998;338:1572–1576. [PubMed: 9603794]

Ricci B. Refractive errors and ocular motility disorders in preterm babies with and without retinopathy of prematurity. Ophthalmologica 1999;213:295–299. [PubMed: 10516517]

Robb RM. Increase in retinal surface area during infancy and childhood. J Pediatr Ophthalmol Strabismus 1982;19:16–20. [PubMed: 7108705]

Roberts J, Rowland M. Refractive status and motility defects of persons 4-74 years, United States 1971-1972. Journal. 1978

Robinson R, O'Keefe M. Follow-up study on premature infants with and without retinopathy of prematurity. Br J Ophthalmol 1993;77:91–94. [PubMed: 8435426]

Rufiange M, Rousseau S, Dembinska O, Lachapelle P. Cone-dominated ERG luminance-response function: the Photopic Hill revisited. Doc Ophthalmol 2002;104:231–248. [PubMed: 12076014]

Rufiange M, Dassa J, Dembinska O, Koenekoop RK, Little JM, Polomeno RC, Dumont M, Chemtob S, Lachapelle P. The photopic ERG luminance-response function (photopic hill): method of analysis and clinical application. Vision Res 2003;43:1405–1412. [PubMed: 12742110]

Rymer J, Wildsoet CF. The role of the retinal pigment epithelium in eye growth regulation and myopia: a review. Vis Neurosci 2005;22:251–261. [PubMed: 16079001]

Sahni J, Subhedar NV, Clark D. Treated threshold stage 3 versus spontaneously regressed subthreshold stage 3 retinopathy of prematurity: a study of motility, refractive, and anatomical outcomes at 6 months and 36 months. Br J Ophthalmol 2005;89:154–159. [PubMed: 15665344]

Saint-Geniez M, Maldonado AE, D'Amore PA. VEGF expression and receptor activation in the choroid during development and in the adult. Invest Ophthalmol Vis Sci 2006;47:3135–3142. [PubMed: 16799060]

Saint-Geniez M, Maharaj AS, Walshe TE, Tucker BA, Sekiyama E, Kurihara T, Darland DC, Young MJ, D'Amore PA. Endogenous VEGF is required for visual function: evidence for a survival role on muller cells and photoreceptors. PLoS ONE 2008;3:e3554. [PubMed: 18978936]

Sandercoe TM, Geller SF, Hendrickson AE, Stone J, Provis JM. VEGF expression by ganglion cells in central retina before formation of the foveal depression in monkey retina: evidence of developmental hypoxia. J Comp Neurol 2003;462:42–54. [PubMed: 12761823]

Saugstad OD. Oxygen and retinopathy of prematurity. J Perinatol 2006;26:S46–50. [PubMed: 16482198] discussion S63-44

Saunders KJ. Early refractive development in humans. Surv Ophthalmol 1995;40:207–216. [PubMed: 8599156]

Saunders KJ, McCulloch DL, Shepherd AJ, Wilkinson AG. Emmetropisation following preterm birth. Br J Ophthalmol 2002;86:1035–1040. [PubMed: 12185134]

Scharf J, Zonis S, Zeltzer M. Refraction in premature babies: a prospective study. J Pediatr Ophthalmol Strabismus 1978;15:48–50. [PubMed: 739329]

Schneck ME, Hamer RD, Packer OS, Teller DY. Area-threshold relations at controlled retinal locations in 1-month-old infants. Vision Res 1984;24:1753–1763. [PubMed: 6533998]

Scholtes AM, Bouman MA. Psychophysical experiments on spatial summation at threshold level of the human peripheral retina. Vision Res 1977;17:867–873. [PubMed: 898693]

Sears JE, Pietz J, Sonnie C, Dolcini D, Hoppe G. A change in oxygen supplementation can decrease the incidence of retinopathy of prematurity. Ophthalmology 2009;116:513–518. [PubMed: 19157560]

Section on Ophthalmology American Academy of Pediatrics, American Academy of Ophthalmology and American Association for Pediatric Ophthalmology and Strabismus. Screening examination of premature infants for retinopathy of prematurity. Pediatrics 2006;117:572–576. [PubMed: 16452383]Erratum in: Pediatrics. 2006 Sep;2118(2003):1324

Sharpe LT, Fach CC, Stockman A. The field adaptation of the human rod visual system. J Physiol 1992;445:319–343. [PubMed: 1501137]

Snir M, Nissenkorn I, Sherf I, Cohen S, Ben Sira I. Visual acuity, strabismus, and amblyopia in premature babies with and without retinopathy of prematurity. Ann Ophthalmol 1988;20:256–258. [PubMed: 3178079]

Snir M, Friling R, Weinberger D, Sherf I, Axer-Siegel R. Refraction and keratometry in 40 week old premature (corrected age) and term infants. Br J Ophthalmol 2004;88:900–904. [PubMed: 15205234]

Spencer R. Long-term visual outcomes in extremely low-birth-weight children (an American Ophthalmological Society thesis). Trans Am Ophthalmol Soc 2006;104:493–516. [PubMed: 17471358]

Springer AD, Hendrickson AE. Development of the primate area of high acuity. 1. Use of finite element analysis models to identify mechanical variables affecting pit formation. Vis Neurosci 2004a;21:53–62. [PubMed: 15137581]

Springer AD, Hendrickson AE. Development of the primate area of high acuity. 2. Quantitative morphological changes associated with retinal and pars plana growth. Vis Neurosci 2004b;21:775–790. [PubMed: 15683563]

Springer AD, Hendrickson AE. Development of the primate area of high acuity, 3: temporal relationships between pit formation, retinal elongation and cone packing. Vis Neurosci 2005;22:171–185. [PubMed: 15935110]

Steinberg RH. Monitoring communications between photoreceptors and pigment epithelial cells: effects of “mild” systemic hypoxia. Friedenwald lecture. Invest Ophthalmol Vis Sci 1987;28:1888–1904. [PubMed: 3316105]

Steinkuller PG, Du L, Gilbert C, Foster A, Collins ML, Coats DK. Childhood blindness. J Aapos 1999;3:26–32. [PubMed: 10071898]

Stepanik PL, Lerious V, McGinnis JF. Developmental appearance, species and tissue specificity of mouse 23-kDa, a retinal calcium-binding protein (recoverin). Exp Eye Res 1993;57:189–197. [PubMed: 8405185]

Stone J, Chan-Ling T, Pe'er J, Itin A, Gnessin H, Keshet E. Roles of vascular endothelial growth factor and astrocyte degeneration in the genesis of retinopathy of prematurity. Invest Ophthalmol Vis Sci 1996;37:290–299. [PubMed: 8603833]

Sutter EE, Tran D. The field topography of ERG components in man--I. The photopic luminance response. Vision Res 1992;32:433–446. [PubMed: 1604830]

Tamai M, Chader GJ. The early appearance of disc shedding in the rat retina. Invest Ophthalmol Vis Sci 1979;18:913–917. [PubMed: 478781]

Teller DY. The forced choice preferential looking method: a psychophysical technique for use with human infants. Infant Behavior and Development 1979;2:135–153.

Timmers AM, Fox DA, He L, Hansen RM, Fulton AB. Rod photoreceptor maturation does not vary with retinal eccentricity in mammalian retina. Curr Eye Res 1999;18:393–402. [PubMed: 10435825]

Troilo D. Neonatal eye growth and emmetropisation--a literature review. Eye 1992;6(Pt 2):154–160. [PubMed: 1624037]

Tuppurainen K, Herrgard E, Martikainen A, Mantyjarvi M. Ocular findings in prematurely born children at 5 years of age. Graefes Arch Clin Exp Ophthalmol 1993;231:261–266. [PubMed: 8319915]

Ueno S, Kondo M, Niwa Y, Terasaki H, Miyake Y. Luminance dependence of neural components that underlies the primate photopic electroretinogram. Invest Ophthalmol Vis Sci 2004;45:1033–1040. [PubMed: 14985327]

VanderVeen DK, Coats DK, Dobson V, Fredrick D, Gordon RA, Hardy RJ, Neely DE, Palmer EA, Steidl SM, Tung B, Good WV. Prevalence and course of strabismus in the first year of life for infants with prethreshold retinopathy of prematurity: findings from the Early Treatment for Retinopathy of Prematurity study. Arch Ophthalmol 2006a;124:766–773. [PubMed: 16769828]

Vanderveen DK, Mansfield TA, Eichenwald EC. Lower oxygen saturation alarm limits decrease the severity of retinopathy of prematurity. J Aapos 2006b;10:445–448. [PubMed: 17070480]

Volpe JJ. Brain injury in premature infants: a complex amalgam of destructive and developmental disturbances. Lancet Neurol 2009;8:110–124. [PubMed: 19081519]

Wachtmeister L. Oscillatory potentials in the retina: what do they reveal. Prog Retin Eye Res 1998;17:485–521. [PubMed: 9777648]

Wachtmeister L. Some aspects of the oscillatory response of the retina. Prog Brain Res 2001;131:465–474. [PubMed: 11420963]

Wali N, Leguire LE. The photopic hill: a new phenomenon of the light adapted electroretinogram. Doc Ophthalmol 1992;80:335–345. [PubMed: 1473449]

Wallman J. Retinal control of eye growth and refraction. Progress in Retinal Research 1993;12:133–153.

Wassle H, Grunert U, Martin PR, Boycott BB. Immunocytochemical characterization and spatial distribution of midget bipolar cells in the macaque monkey retina. Vision Res 1994;34:561–579. [PubMed: 8160377]

Wellard J, Lee D, Valter K, Stone J. Photoreceptors in the rat retina are specifically vulnerable to both hypoxia and hyperoxia. Vis Neurosci 2005;22:501–507. [PubMed: 16212707]

Werner JS. Development of scotopic sensitivity and the absorption spectrum of the human ocular media. J Opt Soc Am 1982;72:247–258. [PubMed: 7057292]

Westheimer G. Spatial interaction in the human retina during scotopic vision. J Physiol 1965;181:881–894. [PubMed: 5881260]

Wetherill GB, Levitt H. Sequential Estimation of Points on a Psychometric Function. Br J Math Stat Psychol 1965;18:1–10. [PubMed: 14324842]

Whitmore GA. Prediction limits for a univariate normal observation. Am Stat 1986;40:141–143.

Wilkinson AR, Haines L, Head K, Fielder AR. UK retinopathy of prematurity guideline. Early Hum Dev 2008;84:71–74. [PubMed: 18280404]

Wurziger K, Lichtenberger T, Hanitzsch R. On-bipolar cells and depolarising third-order neurons as the origin of the ERG-b-wave in the RCS rat. Vision Res 2001;41:1091–1101. [PubMed: 11301082]

Wyszecki, G.; Stiles, WS. Color Science: Concepts and Methods, Quantitative Data and Formulae. New York: Wiley; 1982.

Xu HP, Tian N. Pathway-specific maturation, visual deprivation, and development of retinal pathway. Neuroscientist 2004;10:337–346. [PubMed: 15271261]

Xu HP, Tian N. Retinal ganglion cell dendrites undergo a visual activity-dependent redistribution after eye opening. J Comp Neurol 2007;503:244–259. [PubMed: 17492624]

Xu HP, Tian N. Glycine receptor-mediated synaptic transmission regulates the maturation of ganglion cell synaptic connectivity. J Comp Neurol 2008;509:53–71. [PubMed: 18425804]

Yourey PA, Gohari S, Su JL, Alderson RF. Vascular endothelial cell growth factors promote the in vitro development of rat photoreceptor cells. J Neurosci 2000;20:6781–6788. [PubMed: 10995821]

Yuodelis C, Hendrickson A. A qualitative and quantitative analysis of the human fovea during development. Vision Res 1986;26:847–855. [PubMed: 3750868]

Zacharias L, Chisholm JF Jr, Chapman RB. Visual and ocular damage in retrolental fibroplasia. Am J Ophthalmol 1962;53:337–345. [PubMed: 14009515]

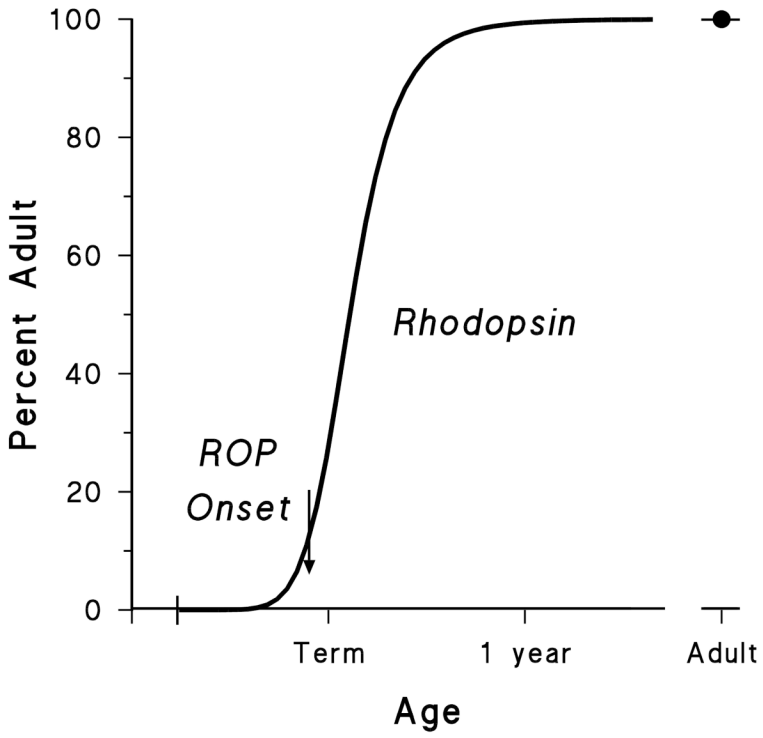

Fig. 1.

Human rhodopsin growth curve and ROP onset. The smooth curve is normalized to the median adult rhodopsin content, 7.19 nmols/retina (Fulton et al., 1999a). Rhodopsin content reached 50% of the adult value at 5 weeks post-term (95% confidence interval: 0 to 10 weeks). The arrow indicates the age of ROP onset (technically pre-threshold ROP) at 32 weeks gestational age (Palmer et al., 1991). ROP onset coincides with a period of rapid developmental increase in rhodopsin content.

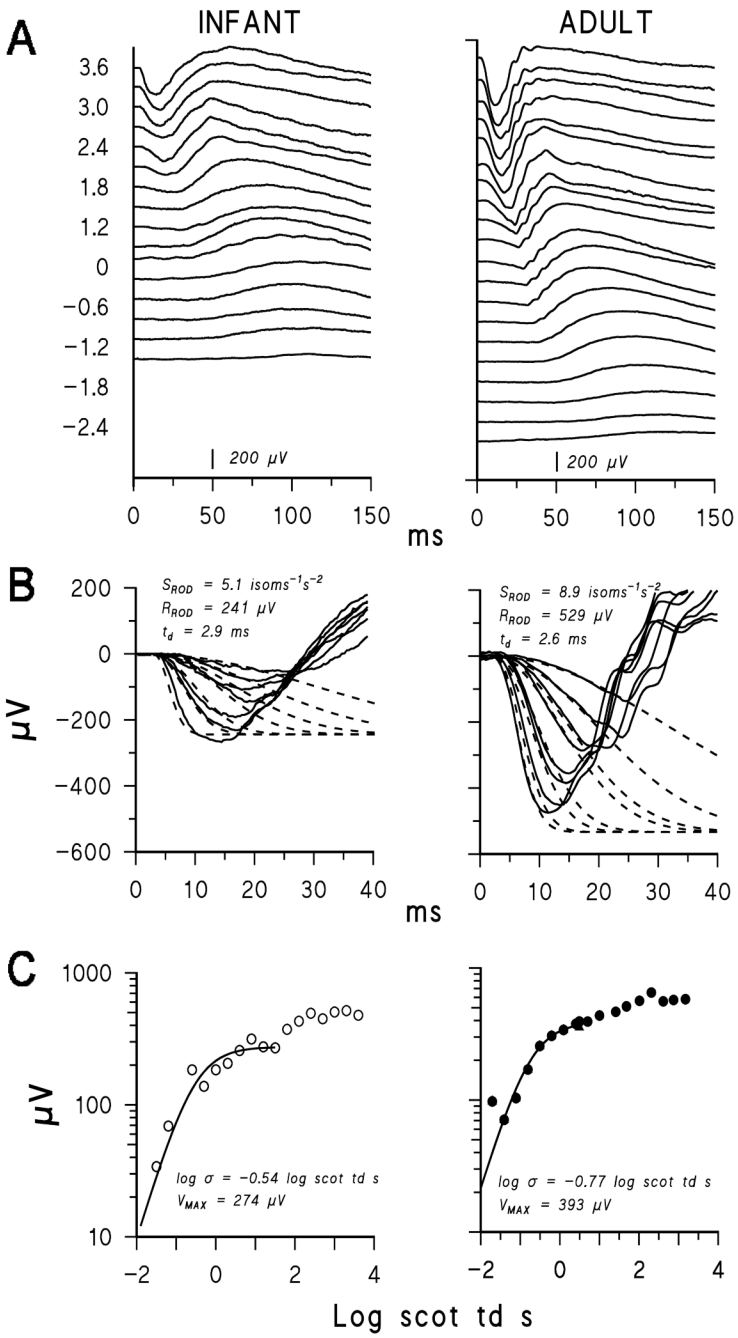

Fig. 2.

Rod mediated ERG records and model fits of a-wave and b-wave responses in a 10 week old infant (left) and an adult (right). (A) Dark adapted ERG responses to a series of short-wavelength flashes. Flash intensity in log scot td s is indicated to the right of the traces; for clarity, only alternate flashes are labeled. (B) Solid lines re-plot the first 40 ms of the response to the seven brightest flashes; dashed lines represent the Lamb and Pugh model (Eq. 2) fit to the a-waves. The parameters S_{ROD}, R_{ROD}, and t_d for these fits are indicated. (C) b-wave amplitude plotted as a function of stimulus intensity. The smooth curve represents Eq. 4 fit to the b-wave data; responses to higher intensities were not included in the curve fit. The parameters log σ and V_{MAX} are indicated.

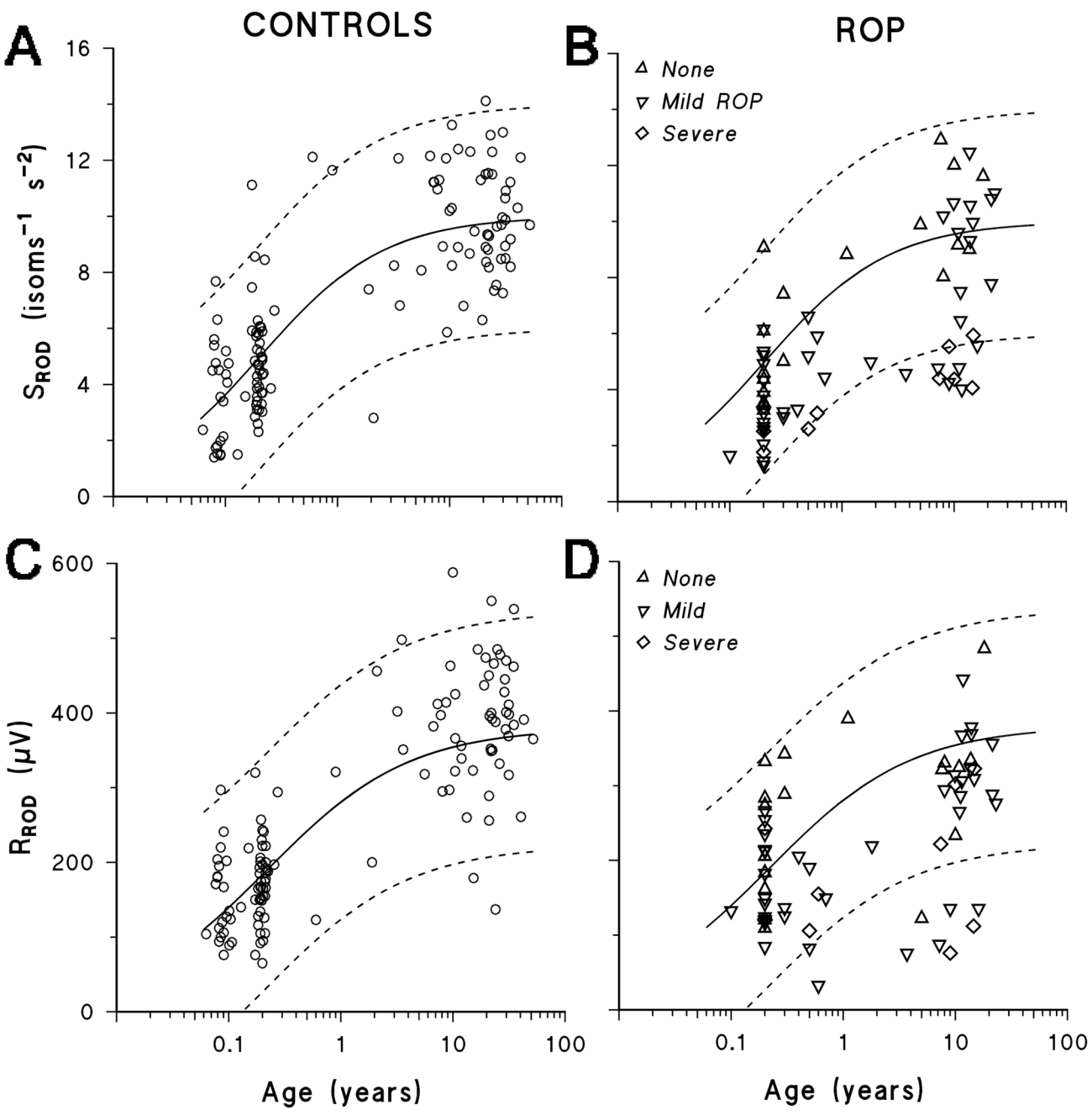

Fig. 3.

Growth curves for rod photoreceptor model parameters, S_{ROD} and R_{ROD}, in human subjects. In each panel, the smooth curve is Eq. 3 fit to the data. The dashed lines indicate the 5th and 95th prediction limits of normal (Whitmore, 1986). Left panels (A, C): Development of S_{ROD} and R_{ROD} plotted as a function of age for 126 term born subjects with normal eyes (age 23 days to 52 years). Infants were recruited for testing at 4 or 10 weeks of age. Age_{50} for S_{ROD} is 10.7 weeks (95% CI: 8.9 to 12.5) and for R_{ROD} is 11.2 weeks (95% CI: 9.4 to 13.0). Right panels (B, D): S_{ROD} and R_{ROD} for subjects with ***Severe ROP*** (N = 10), ***Mild ROP*** (N = 40), and ***No ROP*** (N = 18). Subsets of the data from both the term born (N = 71) and the preterm subjects (N = 21) were previously reported (Fulton and Hansen, 2000;Fulton et al., 2001).

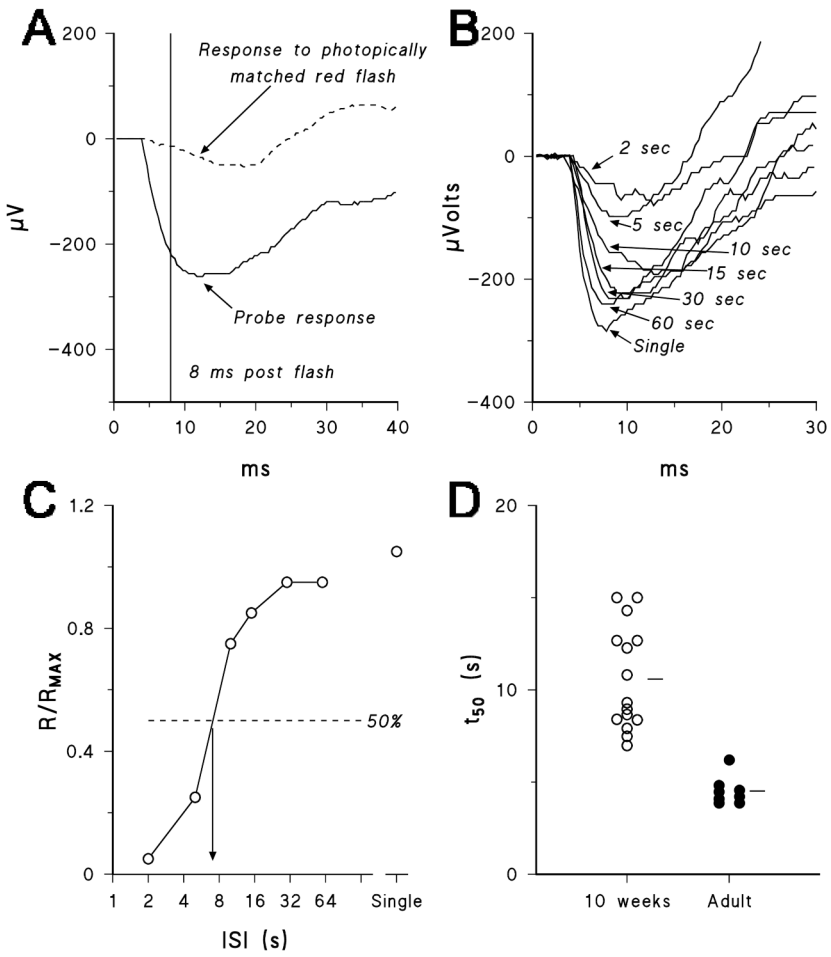

Fig. 4.

Deactivation of the rod photoresponse in term born subjects. (A) Rod isolation. A sample response in a 10 week old infant is shown. The amplitude of the a-wave response to a photopically matched red flash (dashed line) was subtracted from the a-wave response to the probe flash (solid line). The amplitude used in the analysis was measured 8 ms after the flash (vertical line). (B) Sample rod isolated a-wave responses from a 10 week old infant. The interval between probe and test flashes (ISI) is indicated for each response. (C) Deactivation in a 10 week old was summarized by t_{50}, the time to recover to half the amplitude of the a-wave to a single flash as determined by linear interpolation. R/R_{MAX} (see text) is plotted as a function of ISI. (D) The distribution of t_{50} values for term born 10 week old infants (N = 15) and adults (N = 8). The horizontal lines represent the mean for each group. Re-plotted from Hansen and Fulton, 2005b.

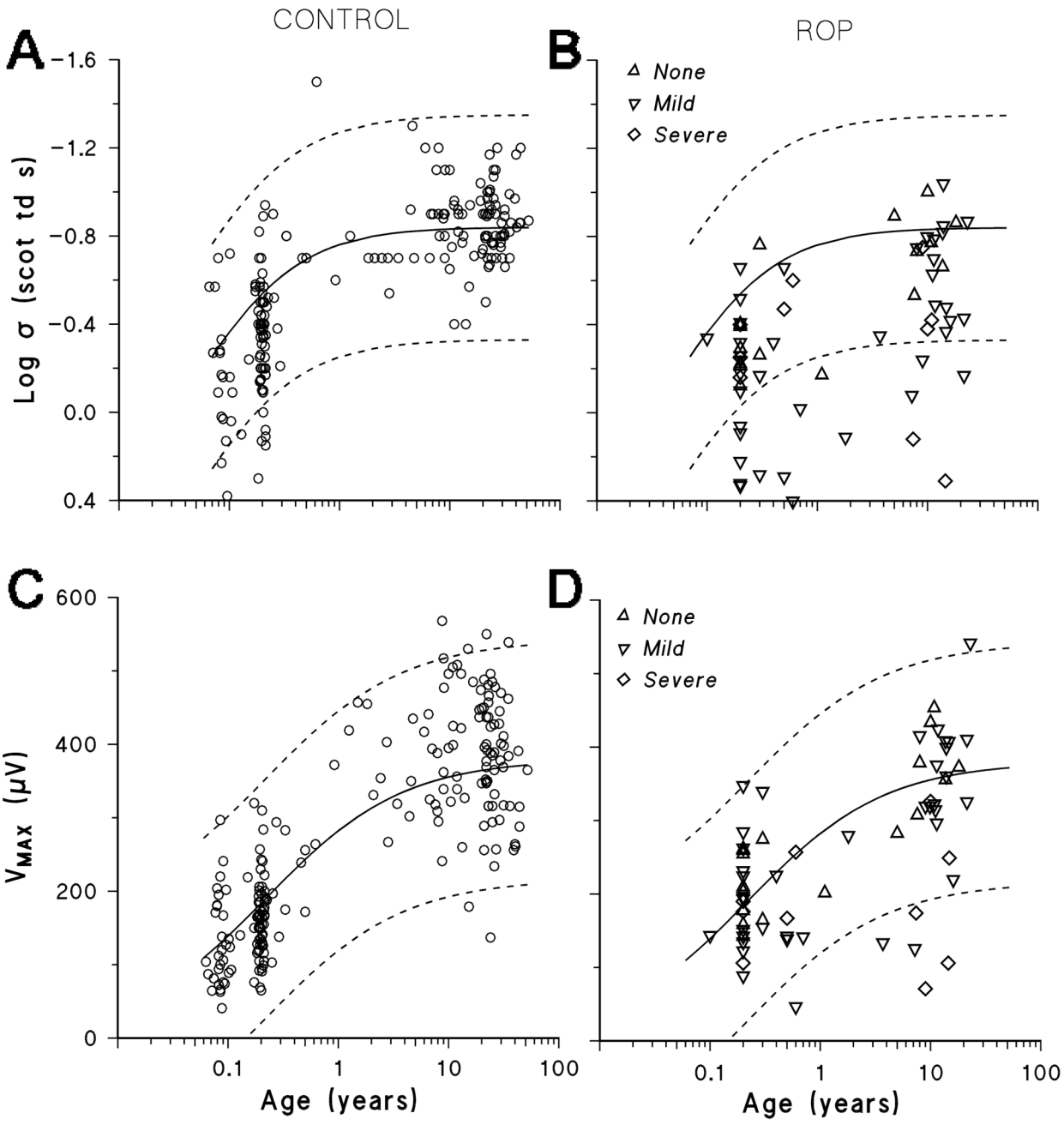

Fig. 5.

Growth curves for rod-driven post-receptor function, log σ and V_{MAX}, in human subjects. In each panel, the smooth curve is Eq. 3 fit to the data. The dashed lines indicate the 5th and 95th prediction limits of normal (Whitmore, 1986). Left panels (A, C): log σ and V_{MAX} plotted as a function of age for 211 subjects with normal eyes (age 23 days to 52 years). Age_{50} for log σ is 11.0 weeks (95% CI: 9.3 to 12.7) and for V_{MAX} is 10.0 weeks (95% CI: 8.3 to 11.7). Right panels (B, D): log σ and V_{MAX} for subjects with ***Severe ROP*** (N = 10), ***Mild ROP*** (N = 40), and ***No ROP*** (N = 18). Fifty-eight (85%) of the ROP subjects have log σ below the normal mean for age and 30 (44%) have V_{MAX} below the normal mean for age. Subsets of the data

from both the term born (N = 142) and the preterm subjects (N = 21) were previously reported (Fulton and Hansen, 2000;Fulton et al., 2001).

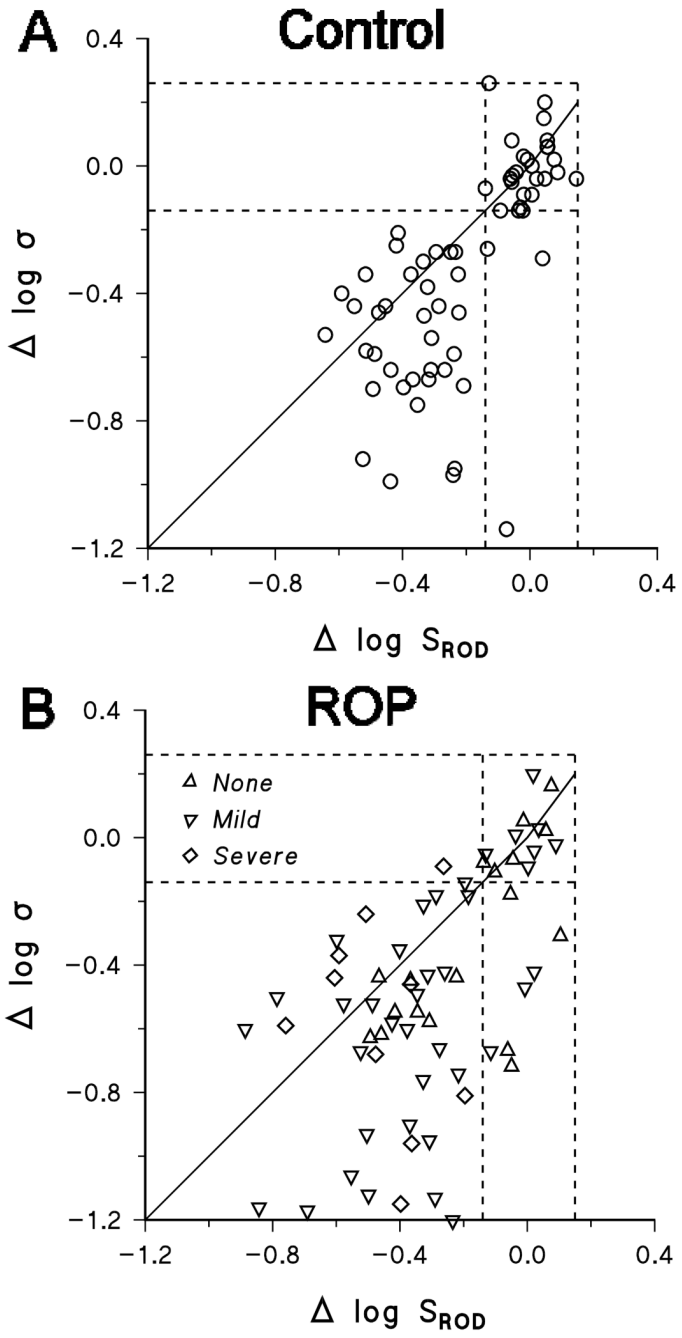

Fig. 6.

Relationship between rod photoreceptor sensitivity, S_{ROD}, and post-receptor b-wave log σ. Deficits in log σ are plotted as a function of deficits in S_{ROD}. The solid diagonal line has slope of 1; dashed lines represent the range of values for each parameter found in healthy, mature control subjects. (A) Results from term born 10 week olds and adults. During normal development, deficits in rod sensitivity (S_{ROD}) predict deficits in post-receptor b-wave log σ. That is, the points fall near the diagonal line. (B) Results from ROP subjects. Many ROP subjects have deficits in log σ that are greater than predicted by deficits in S_{ROd}. Subsets of the data from both the term born (N = 71) and the preterm subject (N = 21) were previously reported (Fulton and Hansen, 2000; Fulton et al., 2001).

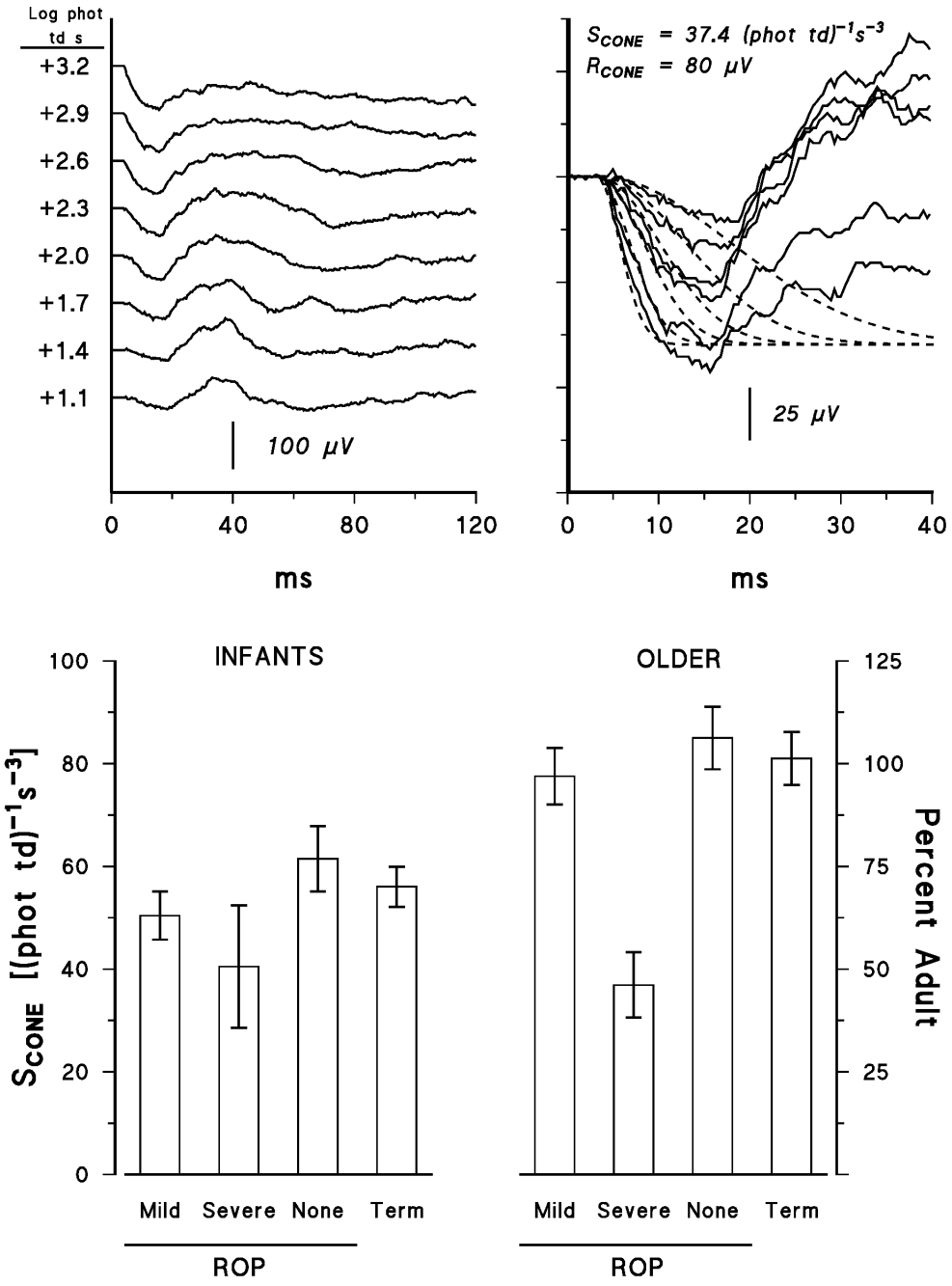

Fig. 7.

Cone ERG. (A) Sample responses from a 10 week old infant to a 2.1 log unit range of red stimuli (λ > 610 nm) presented on a steady, white, rod saturating background (~+3.0 log phot td). (B) Fit of the cone photoreceptor model to the infant's a-waves. The parameters S_{CONE} and R_{CONE} are indicated. In these fits, t_d was 3.0 ms and τ was 1.8 ms. (C) S_{CONE} [left axis: (phot td_{-1}) s_{-3}; right axis: percent adult] for infants and older subjects. Data from subjects with Severe ROP, Mild ROP, and No ROP are compared to data from term born 10 week olds and adults. The means (±SEM) are plotted. Data in panel C re-plotted from Hansen and Fulton, 2005a and Fulton et al., 2008.

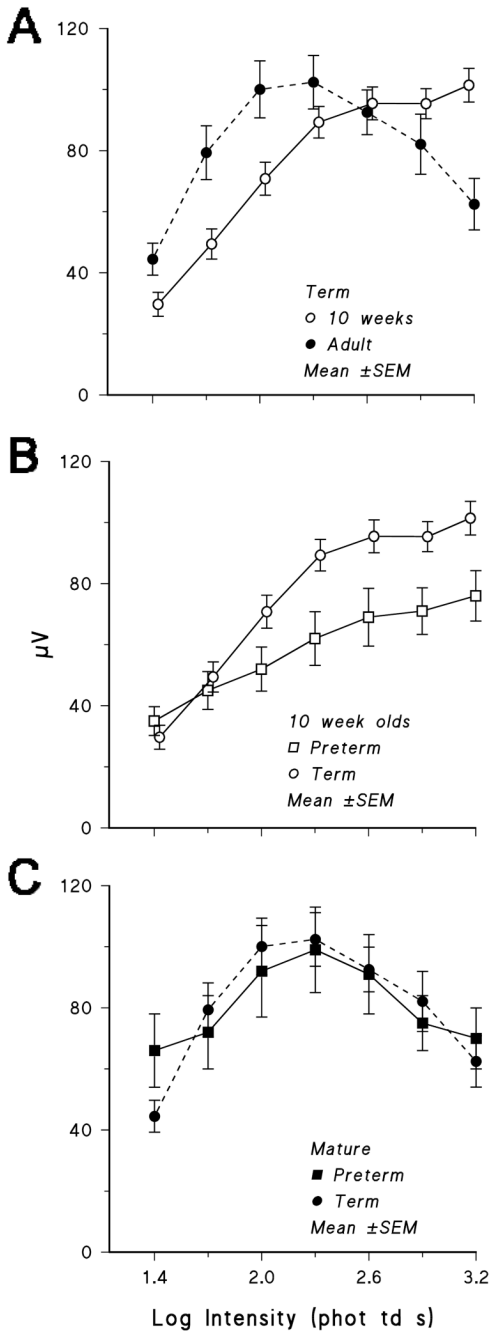

Fig. 8.

Cone-driven b-wave responses as a function of stimulus intensity. (A) Results from term born 10 week old infants (N = 28) and adults (N = 13). A photopic hill, which peaks at approximately +2.3 log phot td s, is apparent in the adults but not in the infants. (B) Results from ROP infants (***Severe, Mild, None***) tested at corrected age 10 weeks compared to results from term born infants. (C) Results from former pre-terms tested at older ages compared to results from adult controls. Re-plotted from Hansen and Fulton, 2005a and Fulton et al., 2008.

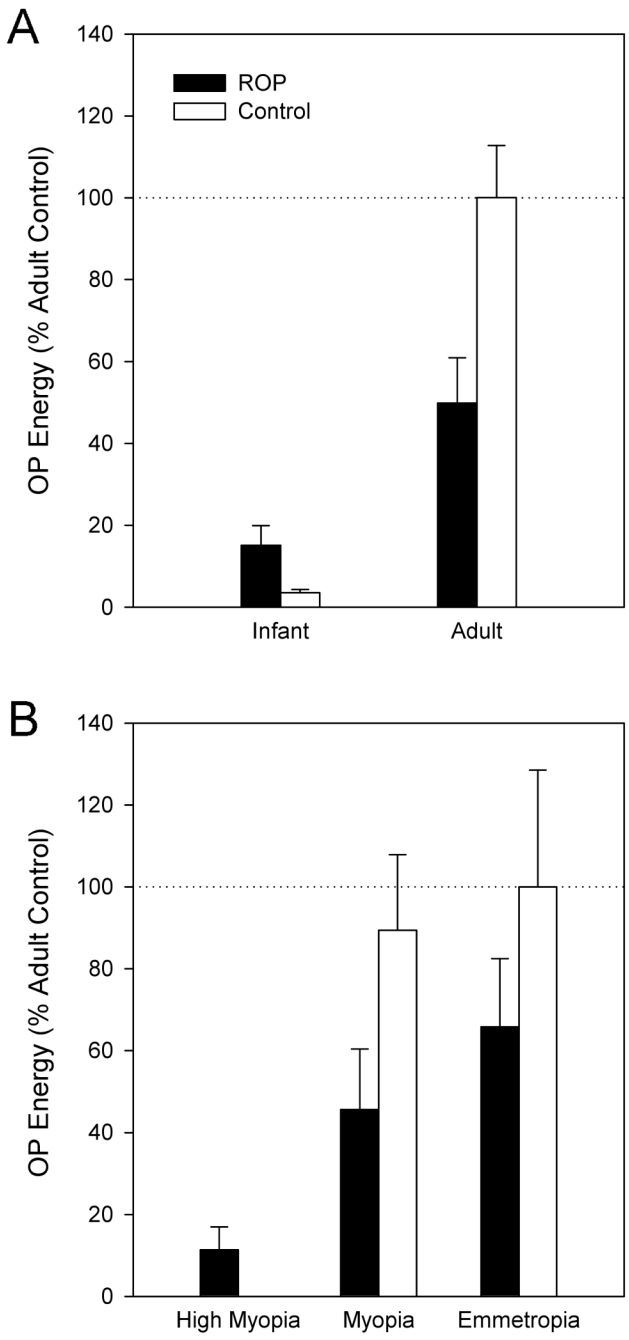

Fig. 9.

Oscillatory potentials. (A) OP energy in term born infants, ROP infants, and older ROP subjects plotted as percent of the normal adult mean (±SEM). Energy is the area under the Gaussian fit to the power spectrum and is related to the square of the summed OP amplitude (Akula et al., 2007b). (B) OP energy in older ROP subjects and mature normal controls stratified by spherical equivalent. Among the ROP subjects, high myopia ranged from -8.40 D through -14.00 D (N = 4); myopia ranged from -0.37 D through -5.75 D (N = 11); and emmetropia ranged from plano through +2.44 D. Data from 14 myopic and five emmetropic controls are shown; there were no controls with high myopia. A subset of the OP data was reported by Akula et al., 2007b.

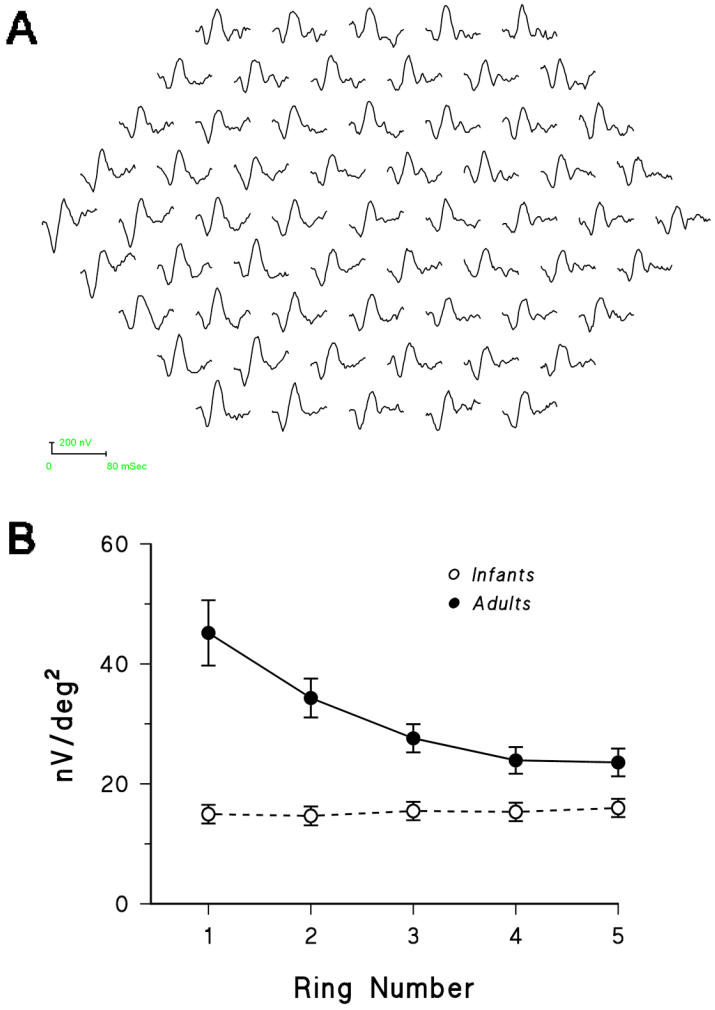

Fig. 10.

Multifocal ERG responses in term born infants. (A) The traces represent the response from each of the 61 hexagons in the unscaled array from an infant. (B) The mean (±SEM) amplitude of the positive component of the wave, P1, in term born infants (N = 18) and adults (N = 6) is plotted as a function of ring number. Data in panel B re-plotted from Hansen et al., 2009.

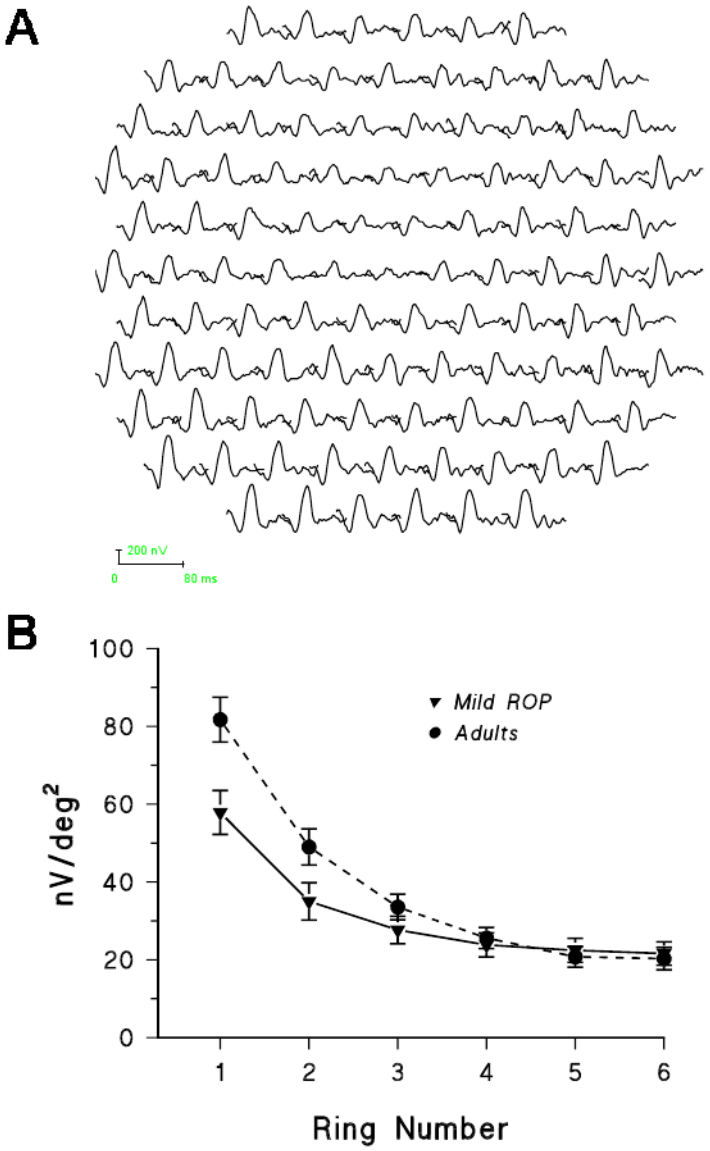

Fig. 11.

Multifocal ERG responses in subjects with a history of ***Mild ROP***. (A) The traces represent the response from each of the 103 hexagons in the scaled array from a 13 year old subject. (B) The mean (±SEM) amplitude of the positive component of the wave, P1, is plotted as a function of ring number for ***Mild ROP*** subjects (N = 11) and healthy controls (N = 9). Data in panel B re-plotted from Fulton et al., 2005.

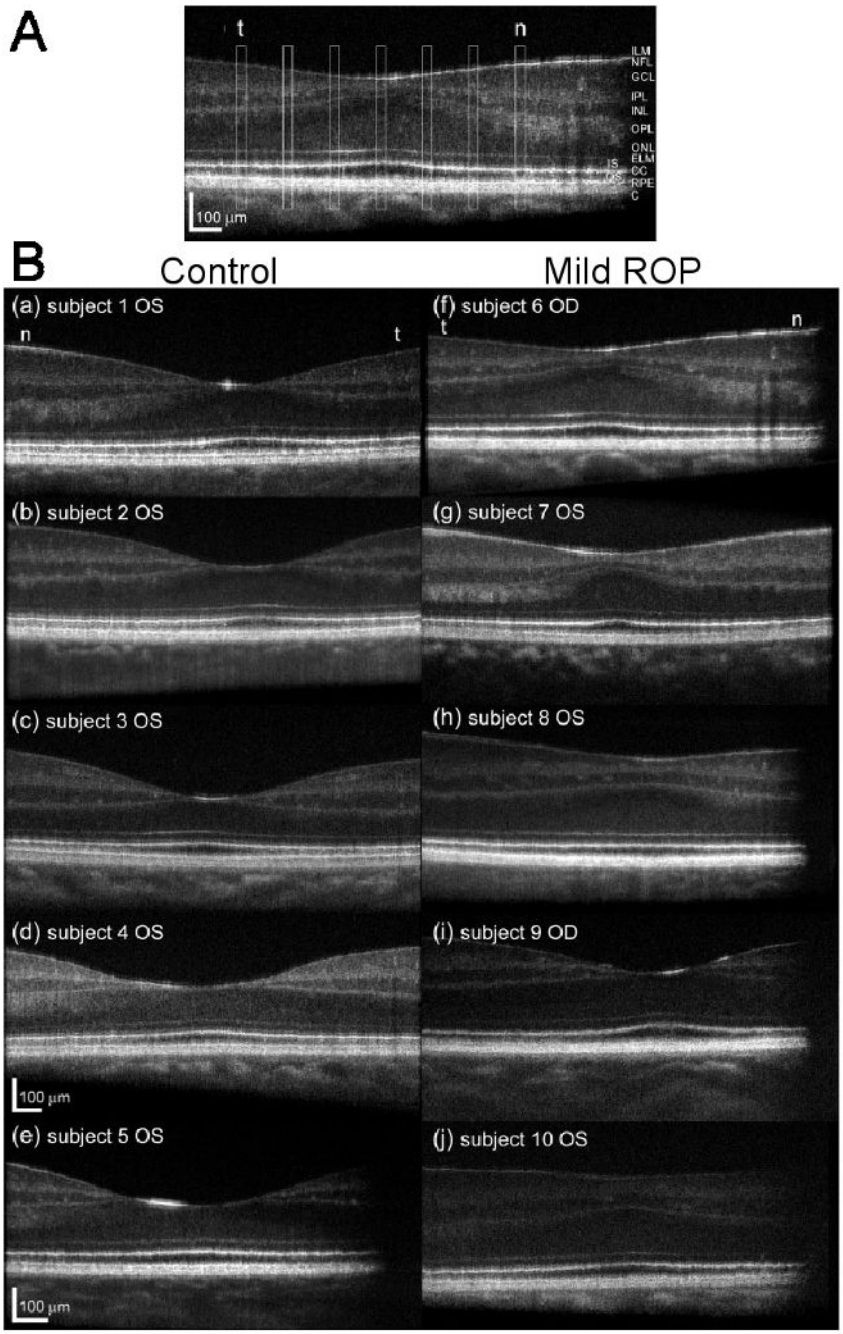

Fig. 12.

Optical coherence tomography (OCT) images. (A) The retinal lamina are as indicated: ILM, inner limiting membrane; NFL, nerve fiber layer; GCL, ganglion cell layer; IPL, inner plexiform layer; INL, inner nuclear layer; OPL, outer plexiform layer; ONL, outer nuclear layer; ELM, external limiting membrane; CC, connecting cilium; RPE, retinal pigment epithelium; C, choroid; IS, inner segment layer; OS, outer segment layer; t, temporal; n, nasal. (B) Cross-sectional images from one eye of five control subjects (left) and five subjects with a history of ***Mild ROP*** (right). In ROP subjects, the fovea was shallower and broader than in controls. Adapted from Hammer et al., 2008; copyright Association for Research in Vision and Ophthalmology.

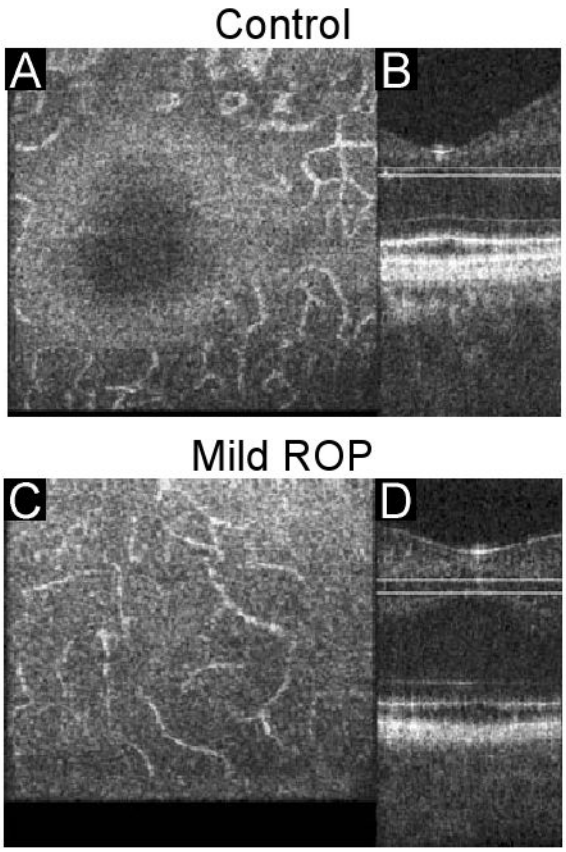

Fig. 13.

Retinal vasculature in OCT images in a control subject (top) and a subject with ***Mild ROP*** (bottom). En face views showing vessels in the outer plexiform layer (A, C) were created by averaging the axial slices shown between the horizontal lines in the corresponding cross-sectional images (B, D). Adapted from Hammer et al., 2008; copyright Association for Research in Vision and Ophthalmology.

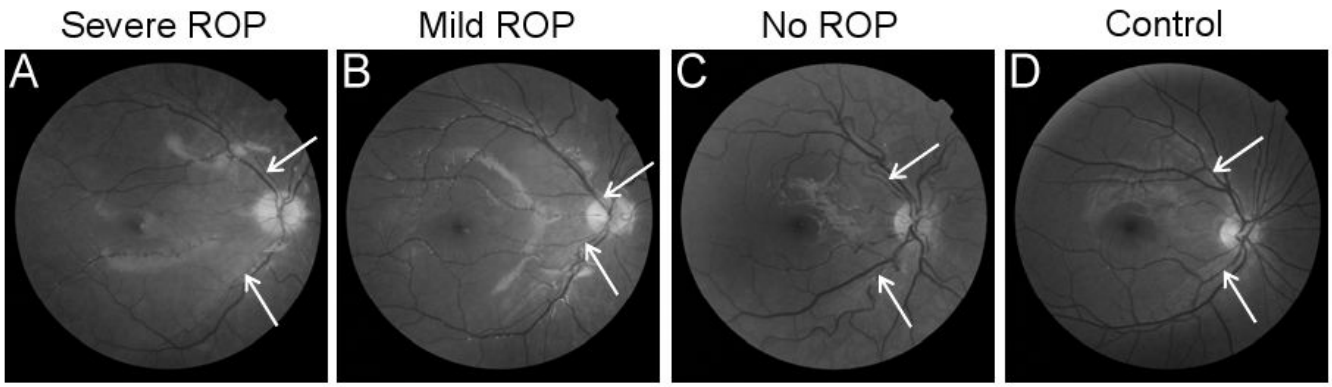

Fig. 14.

Fundus photographs of children (4 to 8 years old) representing each of the ROP categories, ***Severe*** (A), ***Mild*** (B), ***None*** (C) and a term born control (D). The caliber of the retinal arterioles (arrows) was similar in the ***Mild, None***, and term born control eyes. The ***Severe ROP*** eye had attenuated arterioles. Also, consistent with the OCT results (Ecsedy et al., 2007; Hammer et al., 2008), the foveal dimple appeared blunted in eyes with ROP, suggesting a shallower foveal pit.

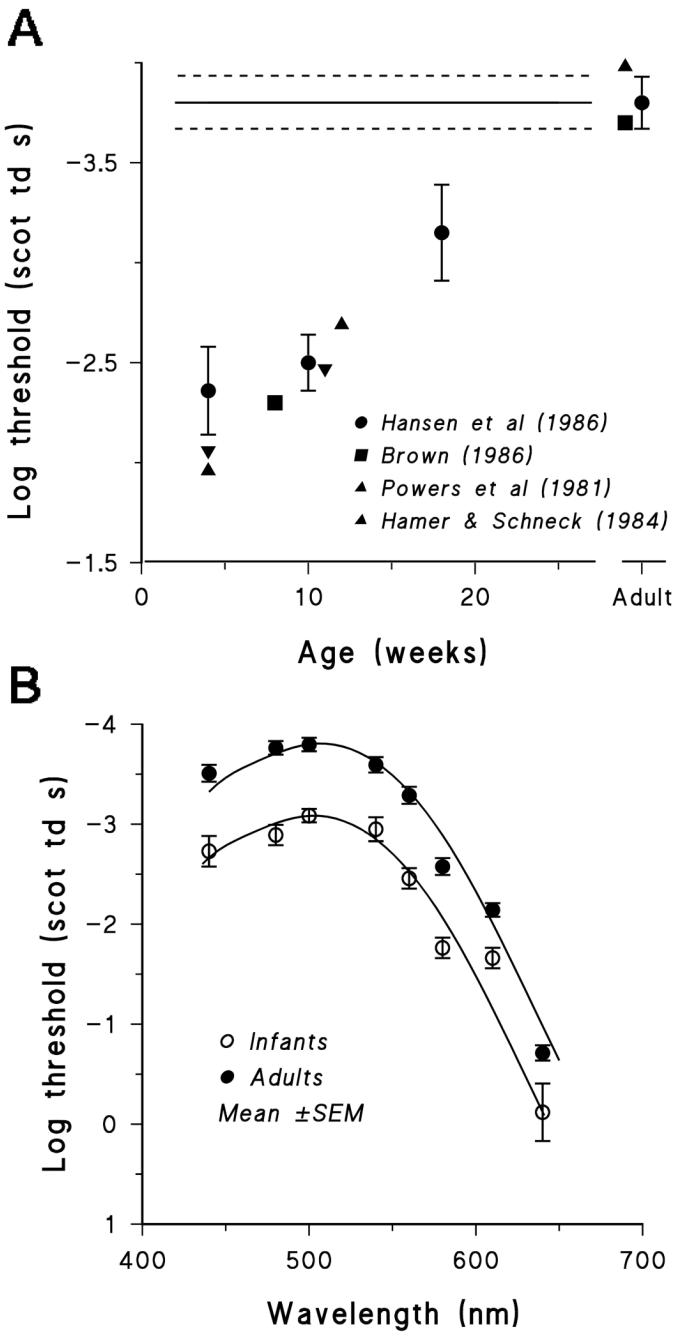

Fig. 15.

Dark adapted scotopic thresholds in young infants. (A) Dark adapted thresholds (scot td s) of young infants plotted as a function of age. Results from several studies are summarized (Hansen and Fulton, 1981; Powers et al., 1981; Hamer and Schneck, 1984; Brown, 1986). The average adult threshold is represented by the solid horizontal line; the dashed lines show ±SD. (B) Spectral sensitivity functions of dark adapted 10 week old infants and adults. Thresholds were measured at eight wavelengths in each subject. Mean (±SEM) threshold is plotted as a function of wavelength for infants and adults. The smooth waves are V_{λ}' (Wyszecki and Stiles, 1982). Re-plotted from Hansen and Fulton, 1993.

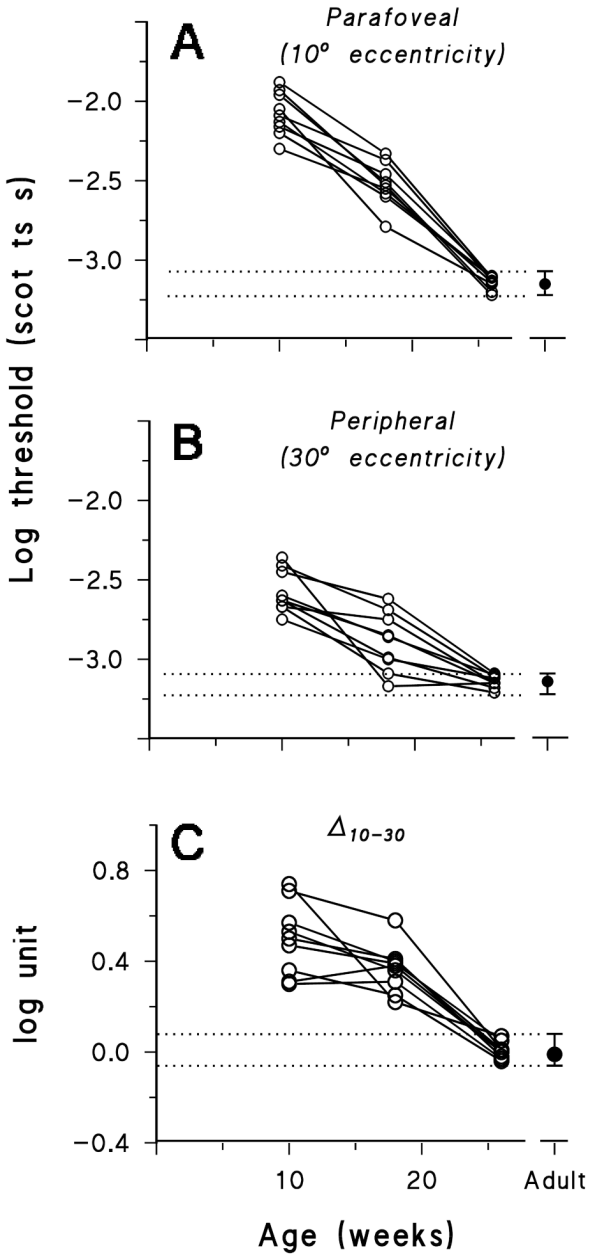

Fig. 16.

Threshold development at parafoveal and peripheral sites in term born infants. Each infant (N = 9) was tested at both sites at age 10, 18, and 26 weeks. The longitudinal data from each individual are connected by line segments. (A) Threshold at 10° eccentricity as a function of age. (B) Threshold at 30° eccentricity as a function of age. (C) Difference between parafoveal and peripheral thresholds ($\Delta_{10\text{-}30}$). The mean adult value (triangle) and its range (dotted lines) are shown in each panel. Re-plotted from Hansen and Fulton, 1999.

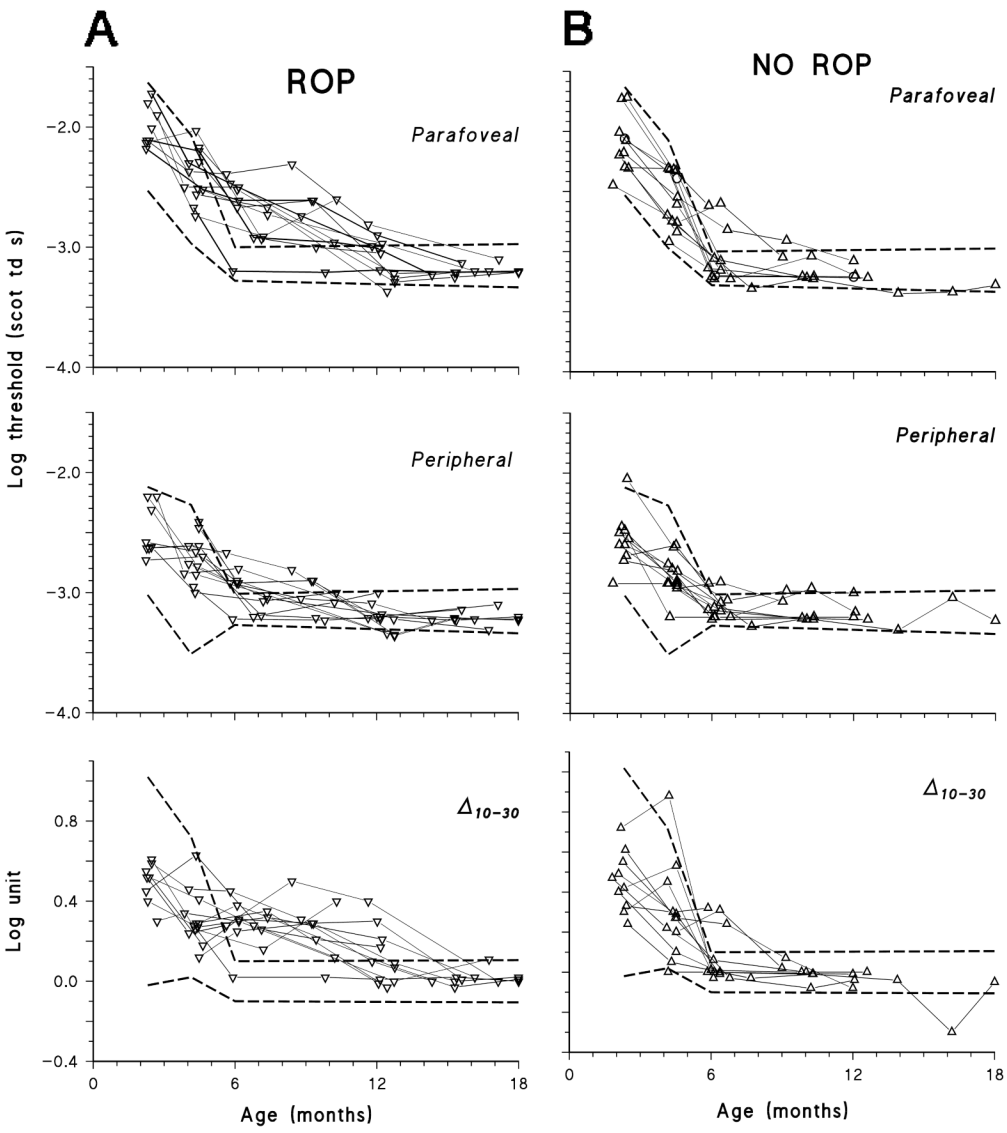

Fig. 17.

Threshold development in subjects with ***Mild ROP*** (A) and ***No ROP*** (B). Thresholds were measured longitudinally at parafoveal (10° eccentric) and peripheral (30° eccentric) sites. Results for individual infants are connected by line segments. Each infant was tested at both sites at every visit. The difference between parafoveal and peripheral thresholds ($\Delta_{10\text{-}30}$) is plotted in the lower panels. In every panel, the dashed lines represent the 99% prediction interval for normal threshold development derived from the results in Fig. 16. Adapted from Barnaby et al., 2007; copyright Association for Research in Vision and Ophthalmology.

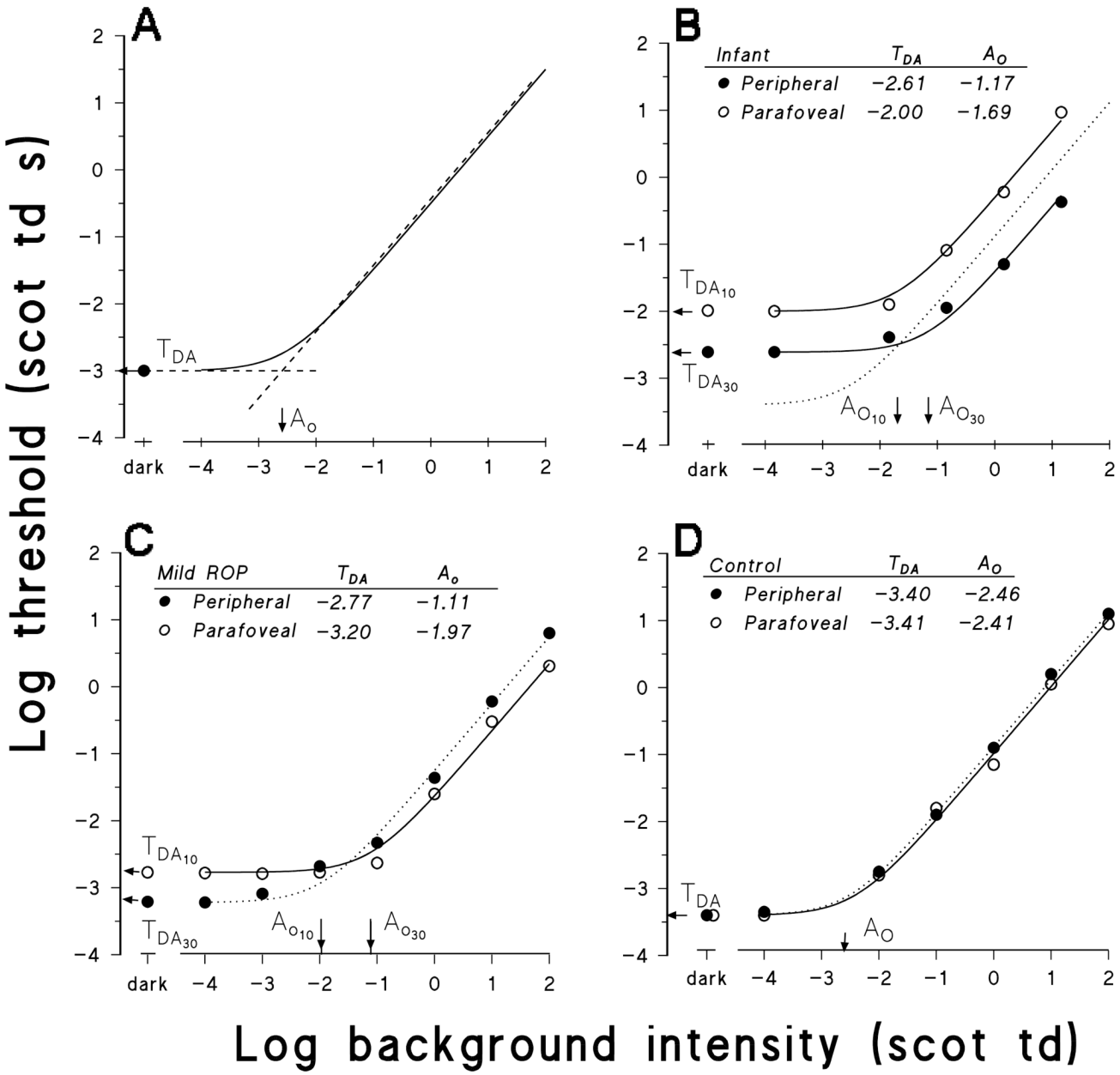

Fig. 18.

Background adaptation. Threshold is plotted as a function of background intensity on log-log axes. (A) The smooth curve plots the equation log T = log T_{DA} + log [(A_o + I)/ A_o] (Eq. 6). The model parameters, dark adapted threshold (T_{DA}) and the *eigengrau* (A_O), are indicated by the arrows. The horizontal dashed line asymptotes the curve at T_{DA}; the oblique dashed line intersects the horizontal line at A_O. Values of T_{DA} and A_O were determined for each subject at the parafoveal (10° eccentric) and peripheral (30° eccentric) sites. Increment threshold functions from (B) a 10 week old term born infant, (C) a 13 year old ***Mild ROP*** subject, and (D) a 14 year old control are shown. The values of T_{DA} (log scot td s) and A_O (log scot td) at the peripheral and parafoveal sites are shown in each panel. Panels B, C, and D re-plotted from Hansen and Fulton, 2000a,b.

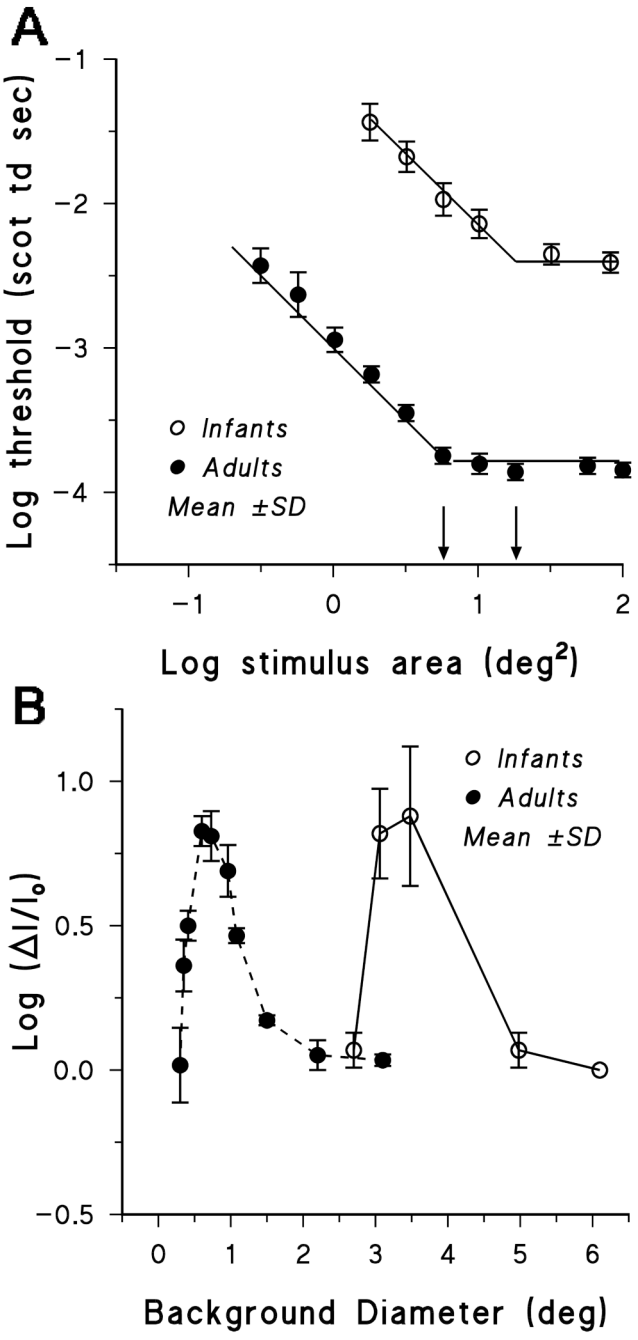

Fig. 19.

Scotopic spatial summation and interaction. (A) Dark adapted spatial summation in term born 10 week old infants and adult controls. Threshold in scot td s is plotted as a function of stimulus area. Points represent the mean ±SEM. The oblique and horizontal lines intersect at the critical areas for complete summation. The average critical area for summation in infants and adults are indicated by the arrows. The corresponding critical diameters are 4.42° and 2.32°, respectively. (B) Average Westheimer functions for infants and adults. Infants were tested using 2°, 20 ms stimuli presented on backgrounds of 2.7 to 6.1° diameter. Adults were tested with 10′, 10 ms stimuli on backgrounds of 0.3 to 3.1° diameter. The background diameters

which produced the maximum threshold elevation are about four times larger in infants (3 to 3.5°) than in adults (0.64 to 0.75°). Panel B re-plotted from Hansen and Fulton, 1994.

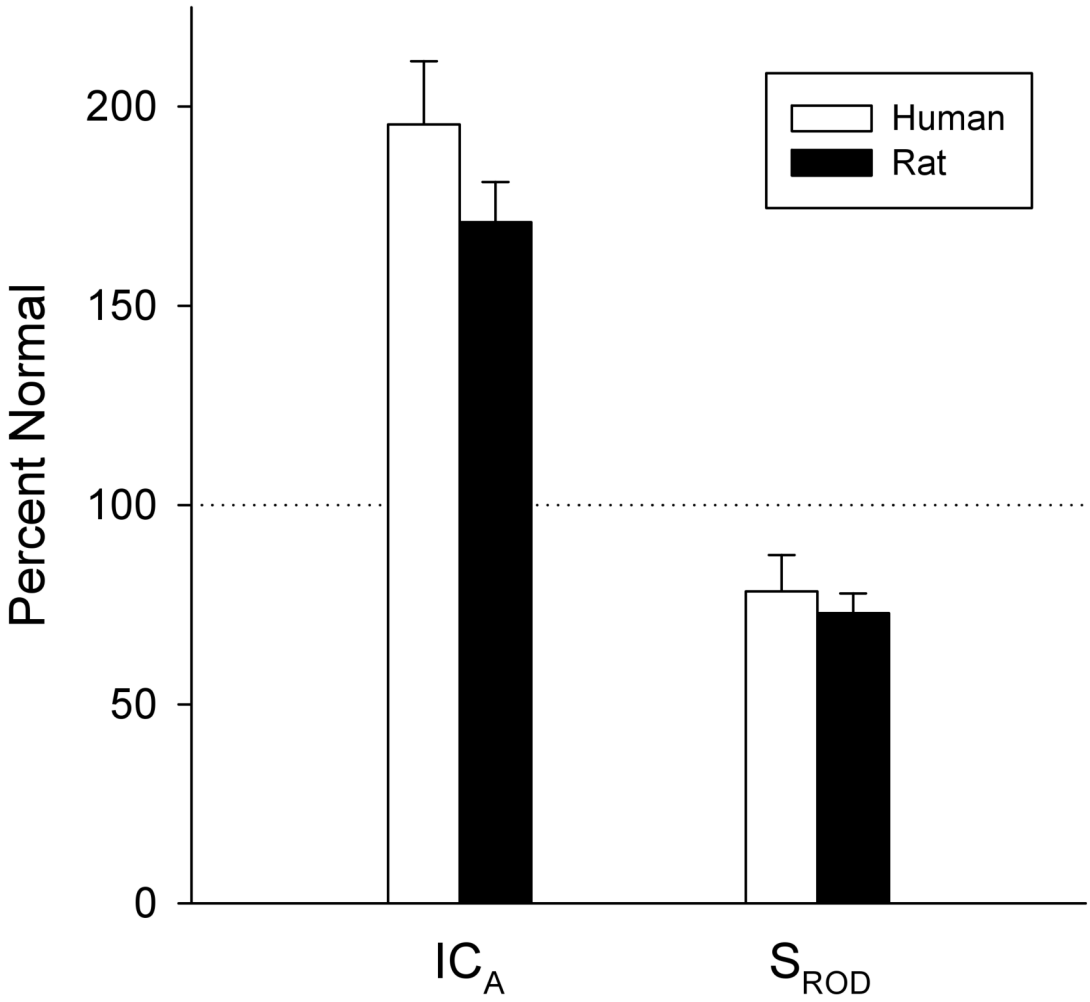

Fig. 20.

Mean (+SEM) arteriolar integrated curvature, IC_A (left), and rod photoreceptor sensitivity, S_{ROD} (right), in infants with a history of ROP and in rat models, plotted as percent of normal for age (dotted line). In both the human and animal subjects, mean IC_A is nearly two times higher in ROP and rod sensitivity (S_{ROD}) is reduced by ~25%. Data re-plotted from Fulton et al., 2001; Gelman et al., 2005; Moskowitz et al., 2005a; Fulton and Hansen, 2006; and Akula et al., 2007a.

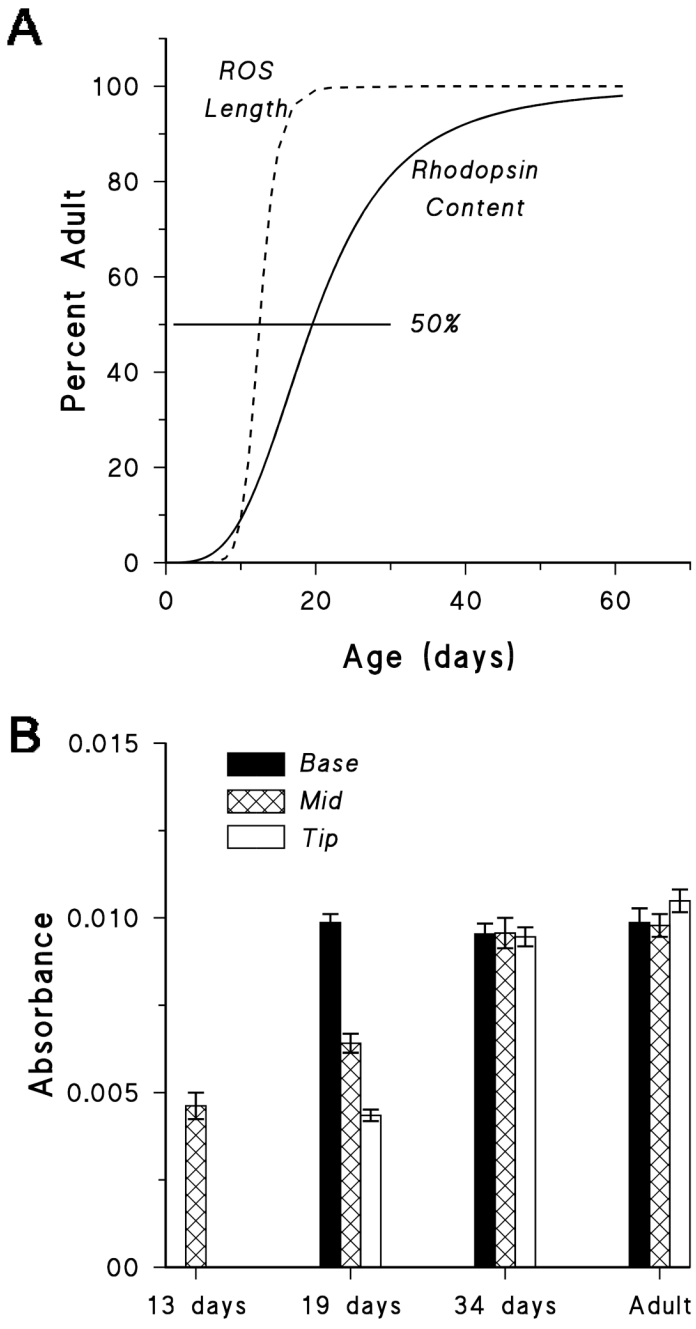

Fig. 21.

Development of rat rod photoreceptor outer segments. (A) Dashed curve: Developmental elongation of rod outer segments (ROS) follows a logistic growth function (Fulton et al., 1995). The ROS are 50% of the adult length at P12.5 (95% CI: P12.1–P12.8). Rhodopsin concentration (weight of rhodopsin per dry weight of retina) follows a similar course (Timmers et al., 1999), reaching half the adult value at P13.4 (95% CI: P12.1–P14.7). Solid curve: The amount of rhodopsin extracted from the whole retina is approximately 50% of that in adults at age P18.7 (95% CI: P18.2–P19.2 days). (B) Rhodopsin absorbances in rat ROS determined by microspectrophotometry (Dodge et al., 1996). Mean (±SEM) of absorbances in dark adapted ROS are shown at four ages: 13, 19, and 34 days and adult. In 19 day old rats, there is a gradient

of absorbance along ROS length. The oldest, least mature disks at the tip have absorbance similar to that found in the 13-day-old ROS. The newest, most mature disks at the base have absorbance similar to that found in adult ROS. In the adult ROS, absorbance is similar along the entire length of the ROS. Adapted from Dodge et al., 1996; copyright Association for Research in Vision and Ophthalmology.

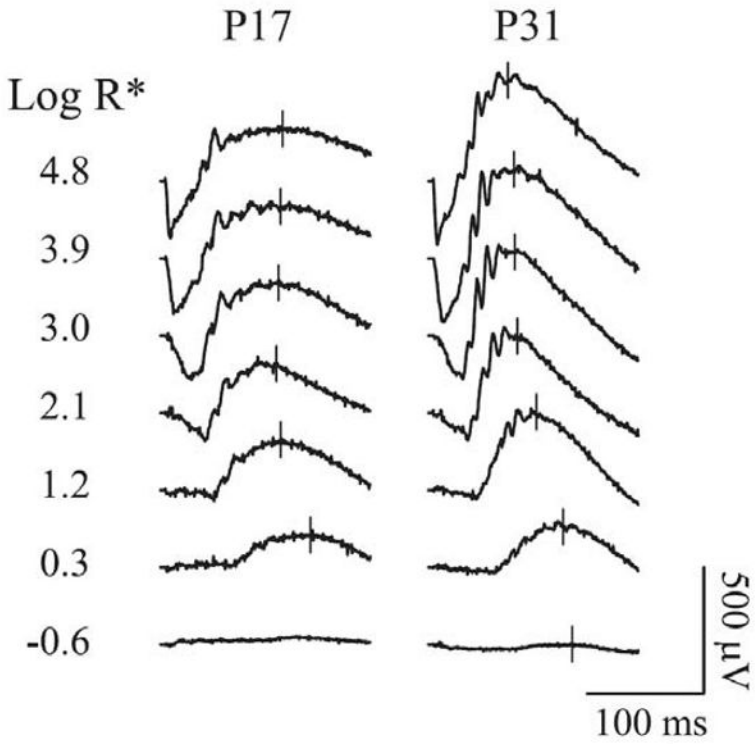

Fig. 22.

Rat control sample records. Sample ERG records of a control rat tested at P17 and P31. ERG responses to a range of brief (<1ms), full-field strobe flashes were recorded. The stimuli were controlled in intensity by calibrated neutral density filters and were increased in 0.3 log unit steps. The unattenuated flash (5.2 log $\mu W/cm^2$) produced approximately $10^{4.8}$ isomerizations per rod per flash. The numbers to the left of each row of traces indicate the stimulus intensity (log R*). For clarity, only every third record is shown. The start of each trace coincides with stimulus onset. Adapted from Liu et al, 2006a; copyright Association for Research in Vision and Ophthalmology.

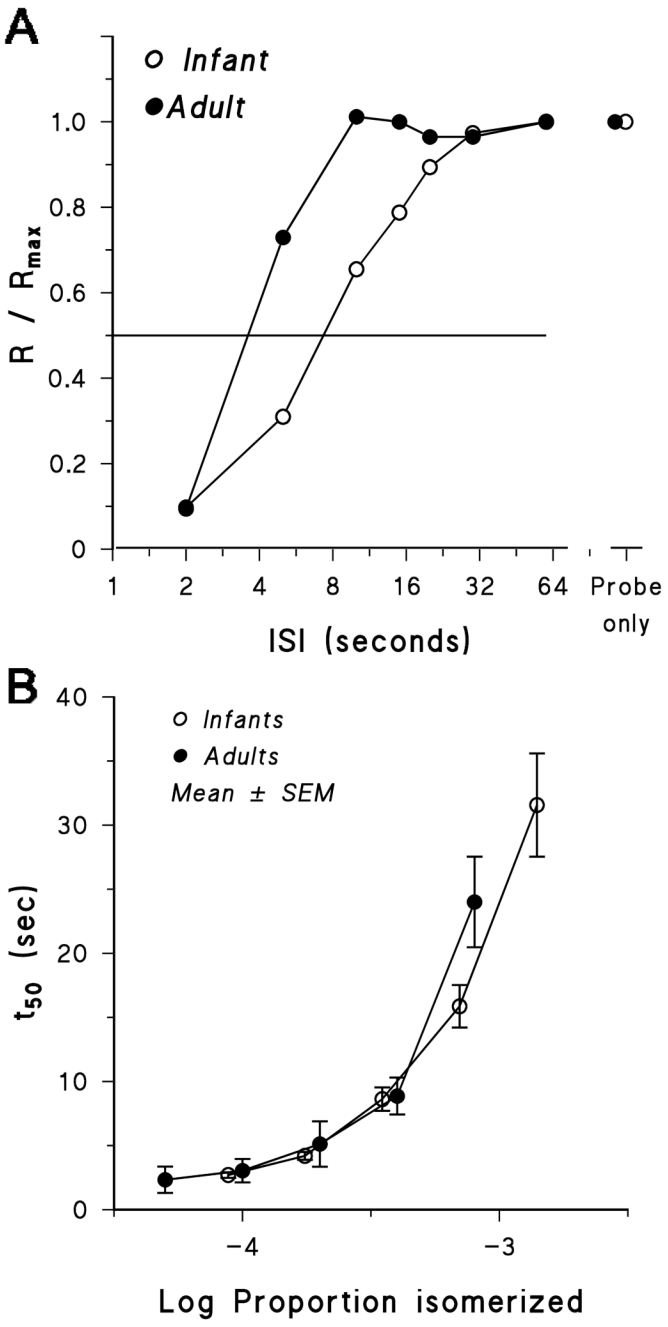

Fig. 23.

Deactivation of the rat rod photoresponse. (A) The amplitude of the a-wave response to the probe flash, expressed as proportion of the amplitude of the response to the test flash alone, plotted as a function of ISI. The data are from the infant and the adult who had the median t_{50} for the 4.0 log $\mu W/cm^2$ flash. (B) Mean t_{50} plotted as a function of stimulus strength, expressed as estimated proportion of rhodopsin molecules isomerized/rod/flash. The infants' and adults' functions do not differ significantly. Data re-plotted from Fulton and Hansen, 2003.

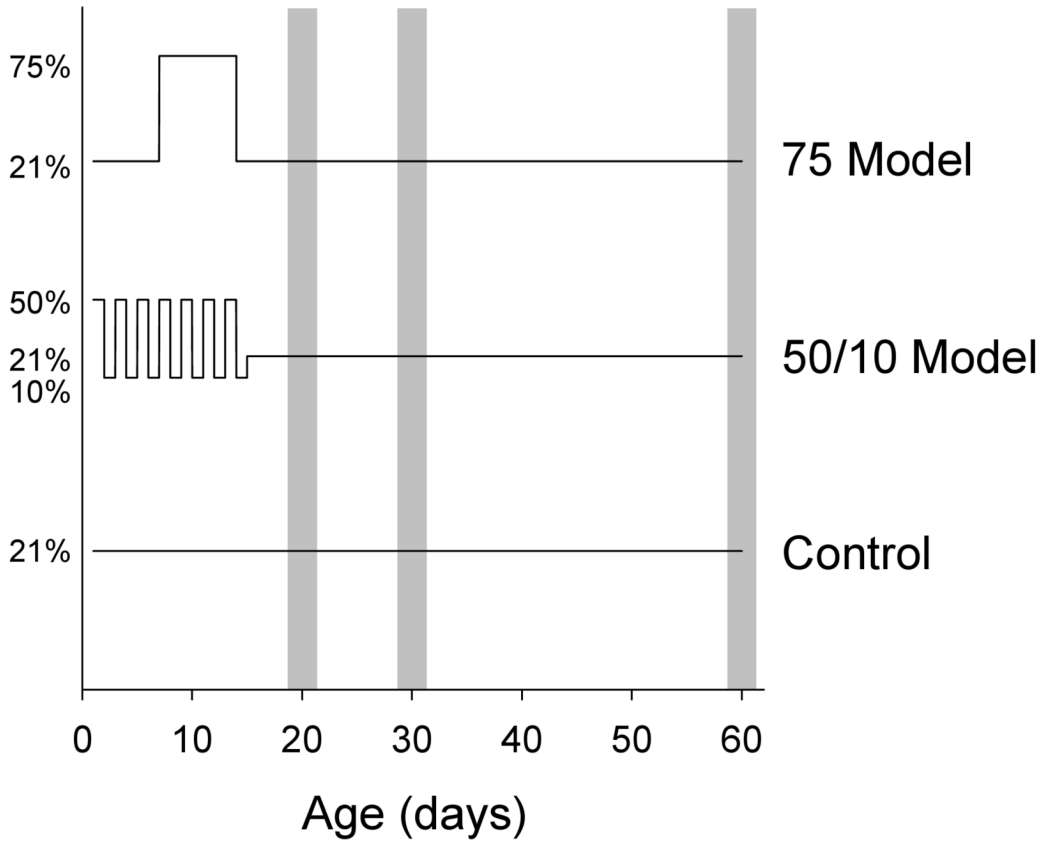

Fig. 24.

Induction of retinopathy. Two models of ROP were created by exposing rat pups to different ambient oxygen environments during the ages when the retina was immature and rhodopsin content increasing. ERG responses and fundus photographs were obtained at P20, P30, and P60 (*gray bars*). Top: The 75 model: oxygen was maintained at 75% from P7 to P14. Middle: The 50/10 model: starting on the day of birth, ambient oxygen concentrations were alternated every 24 hours between 50% and 10% for 14 days. Bottom: Room air is 21% oxygen. Adapted from Akula et al., 2007a; copyright Association for Research in Vision and Ophthalmology.

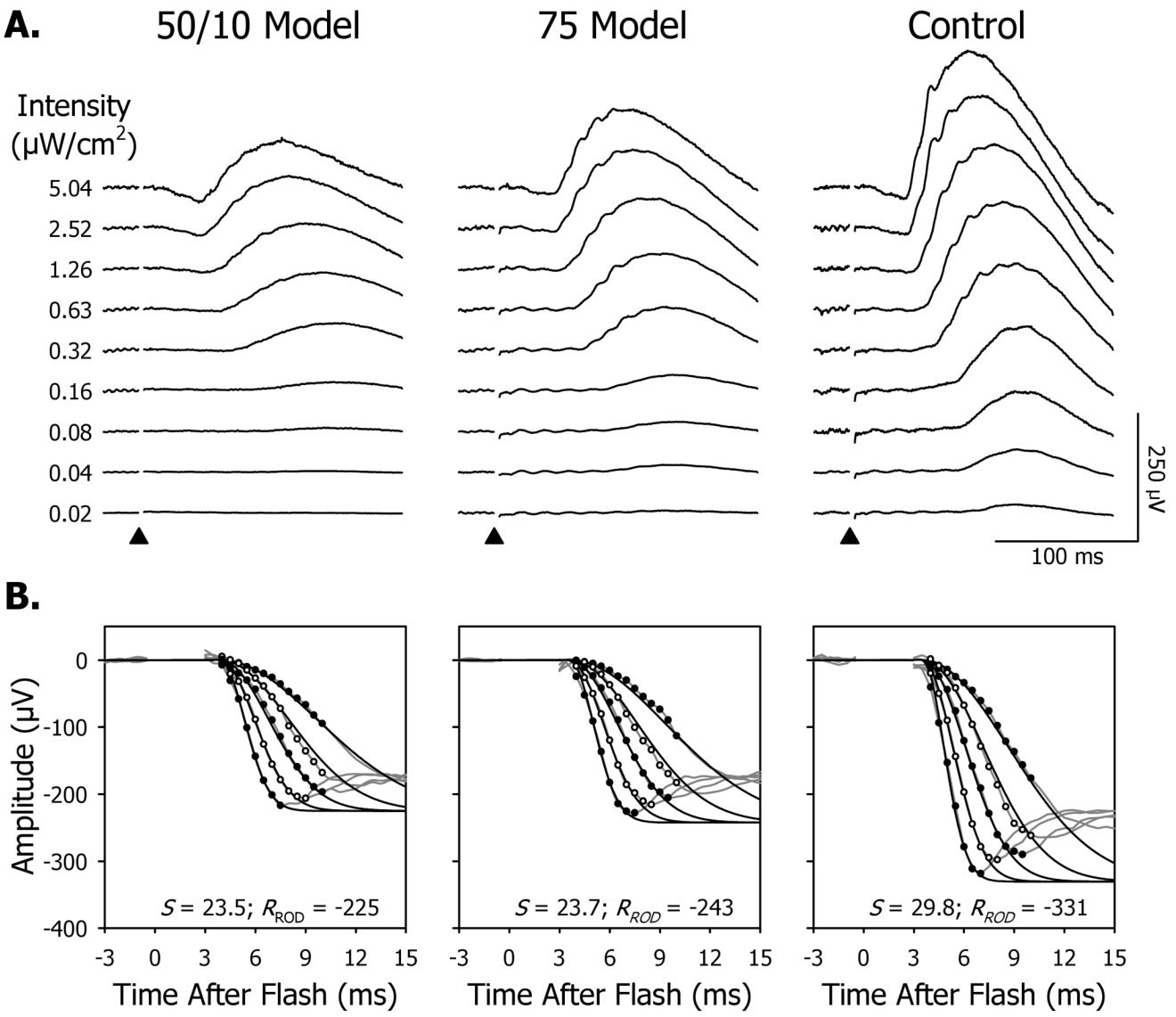

Fig. 25.

Sample records from P20 rats and a-wave model fits. (A) Responses from 50/10 model, 75 model, and control rats. Flash intensity in μW/cm^2 is shown to the left of the traces. Arrows indicate stimulus delivery. (B) Fits (black lines) of a model of the activation of phototransduction (Eq. 2) to the a-waves (gray lines with dots). Fitting was restricted to the leading edge of the a-wave to a maximum of 10 ms after the flash. S_{ROD} and R_{ROD} are indicated in each panel. Adapted from Akula et al., 2007a; copyright Association for Research in Vision and Ophthalmology.

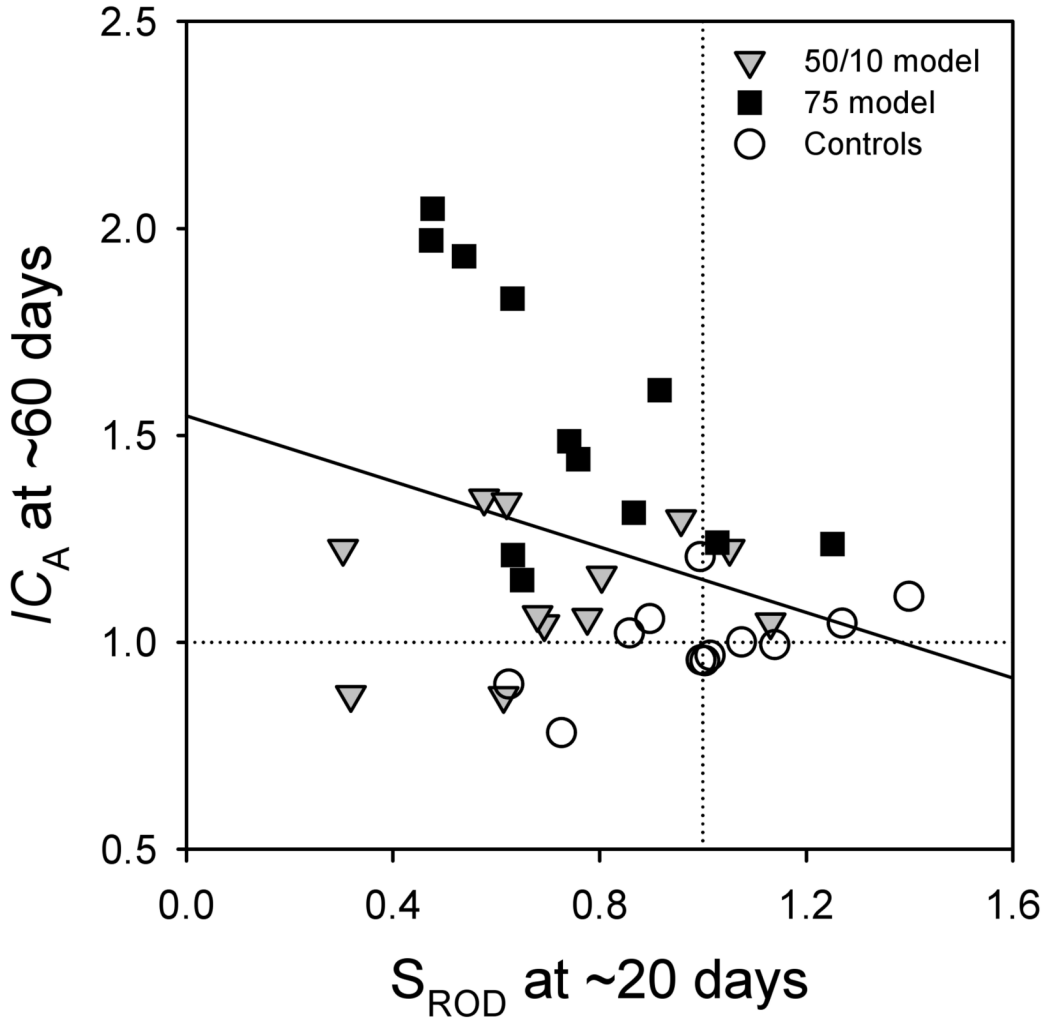

Fig. 26.

Integrated curvature of retinal arterioles (IC_A) and rod photoreceptor sensitivity (S_{ROD}) as proportion of the control mean in 50/10 model, 75 model, and control rats. S_{ROD} at P20 is plotted on the abscissa and IC_A at P60 on the ordinate. The dotted horizontal and vertical lines indicating the control means intersect at $IC_A = 1.0$ and $S = 1.0$. The solid line is a linear regression through the data. Rod sensitivity at P20 predicted vascular abnormality at P60. Re-plotted from Akula et al., 2007a.

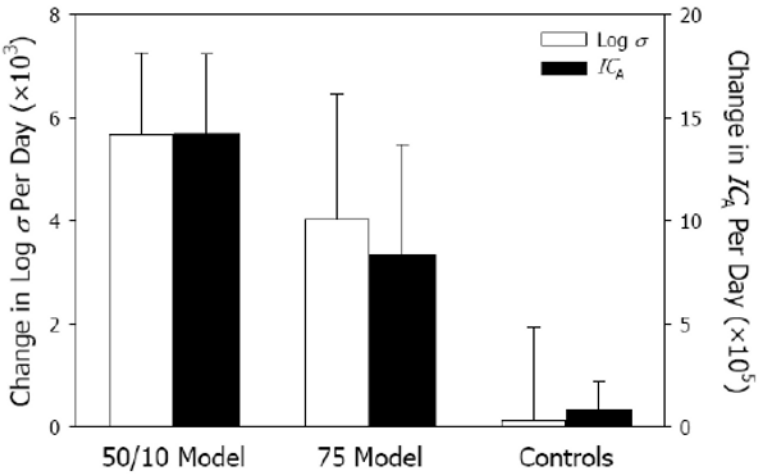

Fig. 27.

Mean (±SEM) rates of change in post-receptor b-wave sensitivity (log σ) and integrated curvature of the retinal arterioles (IC_A) for 50/10 model, 75 model, and control rats. Reprinted from Akula et al., 2007a; copyright Association for Research in Vision and Ophthalmology.

Table 1

Categories of ROP subjects.

Category	Clinical Features
No ROP	No ROP ever
Mild ROP	Stage 1 or 2, Zone II or III*; resolved spontaneously
Severe ROP	Stage 3*; treated

* International Committee for the Classification of Retinopathy of Prematurity, 2005